Project no.: **101022587**

Project full title: **Sustainable energy system for achieving novel carbon neutral energy communities**

Project Acronym: **SUSTENANCE**

Deliverable number:	**D2.2**
Deliverable title:	Models and controls for electric to heat systems
Work package:	WP2
Due date of deliverable:	M20
Actual submission date:	M20 - 28/02/2023
Start date of project:	01/07/2021
Duration:	42 months
Reviewer(s):	Richard van Leeuwen (SAX), Morten Veis Donnerup (NEOGRID), Zakir Rather (IITB)
Author/editor:	Gerwin Hoogsteen (UT)
Contributing partners:	Aalborg University (AAU), AURA Energi (AURA), Neogrid (NEOGRID), Universiteit Twente (UT), Saxion University of Applied Sciences (SAX), Instytut Maszyn Przeplywowych IM Roberta SZEwalskiego Polskiej Akademii Nauk (IMP), Stay-On Storage Engineering (STAY)

Dissemination level of this deliverable	**PU**
Nature of deliverable	R

This project has received funding from the European Union's Horizon 2020 research and innovation programme under grant agreement No 101022587, and the Department of Science and Technology (DST), Government of India under the SUSTENANCE project. Any results of this project reflect only this consortium's view and the funding agencies and the European Commission are not responsible for any use that may be made of the information it contains.

Document history

Version no.	Date	Authors	Changes
0.1	30-8-2022	Gerwin Hoogsteen	Initial skeleton with envisioned chapters and sections
0.8	19-1-2023	Gerwin Hoogsteen	Near final draft
1.0	16-2-2023	Gerwin Hoogsteen	Final version for delivery

Contributors

Partner no.	Partner short name	Name of the Contributor	E-mail
1	AAU	Rakesh Sinha Birgitte Bak Jensen Jayakrishnan Radhakrishna Pillai Pavani Ponnaganti	rsi@energy.aau.dk bbj@energy.aau.dk jrp@energy.aau.dk pap@energy.aau.dk
4	NEOGRID	Morten Veis Donnerup Pierre Vogler-Finck	mvd@neogrid.dk pvf@neogrid.dk
7	UT	Gerwin Hoogsteen Aditya Pappu Bahman Ahmadi	g.hoogsteen@utwente.nl a.pappu@utwente.nl b.ahmadi@utwente.nl
8	SAX	Richard van Leeuwen Cihan Gercek Javier Ferreira Gonzalez	r.p.vanleeuwen@saxion.nl c.gercek@saxion.nl j.ferreiragonzalez@saxion.nl
9	IMP	Patryk Chaja Weronika Radziszewska Sebastian Bykuć	patryk.chaja@imp.gda.pl wradziszewska@imp.gda.pl sbykuc@imp.gda.pl
11	STAY	Pawel Grabowski Krzysztof Rafal Hubert Biedka	pawel.grabowski@stay-on.pl krzysztof.rafal@stay-on.pl hubert.biedka@stay-on.pl
	IITB	Zakir Rather	zakir.rather@iitb.ac.in

Table of Contents

1 Executive Summary

The purpose of this deliverable is to investigate the possibilities for the integration of electricity-to-heat devices within the electricity grid throughout the energy transition. Within SUSTENANCE, the focus is on aggregation of flexibility offered by electricity-to-heat systems to ensure the economic integration and decarbonization of the grid through energy management and market integration.

The opportunities for electricity-to-heat systems within this transition are tremendous. Not only do these devices utilize significant amounts of energy, but they also provide a sheer amount of flexibility through thermal storage, both in buffer vessels as well as by utilizing the thermal mass found in buildings. Value can be created through offering flexibility to the energy markets, in which a shift is observed to more dynamic tariffs and flexibility services by aggregators. An acceleration is observed since the start of the war in Ukraine in Europe. Furthermore, the electrification also leads to more congestion problems in the grid, offering an opportunity for heating systems to add value.

For successful integration it is, however, important to have models and optimization algorithms for optimal control. Various heat models exist for the different possible components and with different levels of accuracy. This leads to a flexible and modular framework that can be tailored to the use-case (e.g., SUSTENANCE's demonstrators) taking into account the local context, technical needs, and demands for market integration. Furthermore, non-linearities within heating systems are a non-negligible aspect when it comes to demand forecasting and planning for operation. Hence utilization of models also depends on the time to delivery of flexibility.

The result of this study is a modular framework for energy management that encompasses the aforementioned points. A flexible framework is created by employing an agent-based system using hierarchical control. As a result, computations can be executed on different levels to ensure privacy, but also to allow for scalability through decentralization of processes. Therefore, clear communication interfaces, such as FlexOffers, should be employed. This approach allows us to also carefully select the right models in terms of accuracy and computation needs with respect to both time and location. A clear definition of 7 (optional) building blocks, with roles and the respective responsible parties, together with timing and location are defined for this in Chapter 5. The main distinction here is a planning-phase for e.g., day-ahead markets, and an operational phase to ensure local grid constraints are satisfied.

The resulting framework and composition of models are tested in simulation. Firstly, through literature and simulation studies the separate building blocks and models are verified for correctness. Next, the composition within the framework is tested, where aggregated flexibility of heat pumps is optimized ahead of time based on cost minimization using day-ahead energy prices. This planning is used as blueprint for operational control, wherein local grid voltages are measured to change control actions whenever needed to assure power quality. Through this simulation case, the working of the proposed framework is validated to work correctly and ensure economic benefits.

2 Introduction

The climate change concerns have resulted in legislation and incentives to transform our energy system to become fully sustainable. Energy usage for (space) heating is, next to transportation, originally a dominating demand in overall energy use within the residential sector of Denmark, Poland and the Netherlands. In contrast, India expects to have a peak demand of 143 GW due to air conditioning systems. As most renewable energy sources directly generate electricity, the electrification of heating systems play a key-role in this transition. Furthermore, the recent geopolitical developments have added another strong driver to increase our energy independency and accelerates the transition to reduce natural gas usage for heating. However, most existing grids have never been designed with the ongoing electrification of demand in mind, resulting in congestion problems. Hence, during the electrification of heating systems, several obstacles need to be tackled. This deliverable explores models, tools, and methods for a sustainable transition and integration of heating systems into the existing electricity infrastructure and its markets.

2.1 Opportunities for the energy transition

Whereas one might see the electrification of heating systems as a threat to the electricity systems, they may as well be a welcome element in the energy transition. Next to high volumes of energy use, the electrification of heat also brings the potential of affordable storage and demand flexibility. For example, households have inherent thermal storage capacity through their construction and hot water buffers and boilers are relative cheap in terms of energy capacity per euro. Coupling of heat systems to the electricity grid comes in the form of converting devices, such as heat pumps (HPs) that convert electricity into heat. Alternatively, combined heat and power (CHP) devices may also convert (sustainable) gas into both heat and electricity. Through these interactions, heat demand can be translated into its equivalent electricity demand. Using technology, such as smart thermostats and control signals, the production of heat, and therefore the use of electricity, can be controlled.

However, there are challenges that need to be tackled to utilize the flexibility that heating systems can bring to the energy system and its markets. One factor is the operation in different time scales, whereas electricity is nearly instantaneous, heating systems react slow. Furthermore, heat usage in the residential sector is tightly coupled with user behaviour and weather conditions, making forecast and control prone to errors when looking at individual households. From a physics perspective, the complexity comes from the interaction that all components have on the heating demand such as, windows, open doors and ventilation. Therefore, heating systems likely will play a key-role on longer term energy balance rather than instantaneous system stability.

Another complexity is defining the flexibility of a building. Different regulations and requirements concerning insulation of new buildings lead to vastly different thermal performance of buildings and therefore their inherent flexibility. Often these parameters can be estimated based on construction year of a building, but intermediate and undocumented upgrades may result in large errors. Furthermore, some parameters have a significant impact on the perceived comfort and hence may require different requirements on both the heating system and control by an energy management system (EMS). As a result, coupling heating systems to the electricity infrastructure is most likely not possible using a one-solution-fits-all approach. This is already observed in the physical domain where distinctions can be made between low- and high-temperature heating systems. Furthermore, large buildings such as, apartments and flats, often have a shared heating system. But also, in residential areas with normal houses, a new district heating system can sometimes be the most cost-efficient solution and hence we see more new district heating systems being developed in the Netherlands and Denmark.

In this context, hybrid setups also exist, where multiple heat source can be coupled to one (district heating) system. For individual households, this can be in the form of a hybrid heat pump, which combines a heat pump with a gas boiler. This adds the option to relieve the electricity grid during congestion by switching back to conventional gas heating. Similarly, district heating networks may have different sources such as waste heat, but also local heat pumps and combined heat and power. With the latter, electricity can also be generated and sustainable options with short-term carbon cycles, e.g. biogas, could be available [Hom19]. Such solutions add complexity to the control system as the heat sources become a heterogenous set of devices. On the other hand, these systems may play a key role in overcoming seasonal aspects to heating, especially when the demand for heat is high in winter when renewable energy from solar is at its lowest.

It must be noted that some of the aforementioned complex interactions in heating systems can be mitigated during operation using thermal storage. Due to the lower thermal output of heat pumps, buffers for hot tap water are necessary to meet domestic demand. These buffers are a source of flexibility, but utilizing energy to fill up such buffers needs to be considered with due diligence to avoid massive energy losses over time. New insulation technologies and the application of phase changing materials (PCM) makes it possible to reduce the losses and significantly increase the capacity per litre. Also here, large scale thermal storage district heating systems is an option. Large projects, such as Ecovat [Goe19] make it even possible to locally store enough heat to balance out seasons.

Based on these observed trends, the most promising opportunity for electricity-to-heat integration lays within community-based heating systems. With this, thermal flexibility can be integrated from an aggregated scale, which allows energy management solutions to utilize group behaviour and therefore avoid large errors that individual systems can impose to the control system. Additionally, this allows an EMS to coordinate the flexibility in both *time and space*, meaning that it can avoid aggregated peaks in time while also balancing the instantaneous load within the grid to avoid power quality issues and grid congestion problems.

This community scope imposes two critical requirements on the technical foundation for the success of electricity-to-heat integration within electricity systems and markets:

1. Acting on different timescales requires advanced predictive and self-learning models, potentially with machine learning techniques. Such models are essential to model-predictive based optimization frameworks to establish market interaction.
2. Controlling multiple heating assets requires a scalable solution that can integrate new assets in the future with ease. Furthermore, this set of devices is likely to be a heterogenous set, meaning that the devised models and algorithms for the EMS need to be generic enough to adequately optimize a wide variety of devices, sizes and technologies, which all belong to a specific heating system.

Yet, the local scope of individual households must not be neglected. We are speaking here of a human-machine interaction, where the technical (machine) component must ensure comfort constraints of individuals are met. Hence, a direct link to user behaviour is made, but thereby also the thermal properties (e.g., insulation) of a building. Thus, from a modelling perspective, the individual details cannot be neglected when controlling flexibility on an aggregated level.

2.2 Research Scope

Given this context, the research scope within this deliverable is on the potential of aggregated flexibility of electricity-to-heat systems within the electricity system. Given the requirements, the following challenges and research questions need to be investigated to allow for a successful implementation within demonstrators and their replication:

- How to accurately model heat demand profiles and comfort constraints on a building level and derive its flexibility on an aggregated level?
- How to translate complex non-linear thermal models from their long-term time-scales into accurate discrete flexibility models for optimal control in short-term electricity systems?
- How to efficiently coordinate a heterogeneous set of thermal devices within a community?
- What is the added value and accuracy of thermal control on an aggregated community level over existing “business-as-usual” individual control?

2.3 Method and Outline

This deliverable first surveys existing literature on modelling of heating systems in Chapter 3. Next, the trends and local context of SUSTENANCE’s demonstration sites with respect to electricity-to-heating systems is presented in Chapter 4. Based on this, control concepts and structures are surveyed in Chapter 5. Eventually, this leads to a modular energy management framework that can be tailored to different use-cases to integrate within the local context, both from market as technical perspective. The presented models and approach are validated through a simulation study in Chapter 6. Chapter 7 concludes the deliverable.

3 Theoretical modelling framework

This chapter details the theoretical foundation in terms of models and equations that allow us to describe thermal demand in domestic settings, energy use by devices, and behaviour of storage assets. Furthermore, we outline how user preferences and comfort constraints can be taken into account. The models presented in this chapter form the underlaying basis for control and optimization methods, presented in Chapter 5. The theory is independent of location and hence ensures that developed methods within the SUSTENANCE project can be reused and replicated elsewhere.

3.1 Thermal demand models

Modelling heat demand starts with maintaining the indoor temperature of a house or building at a predefined temperature, the setpoint. Based on physical phenomena, energy will be both added and withdrawn from a building. This section elaborates on models of a building envelope and all aspects that contribute to the temperature. Figure 3.1 shows a model of a household and the different sources that contribute to the indoor temperature, as well as a control system with a thermostat that activates the heating system (here a heat pump) based on the observed zone temperature. The models presented in this section are based on the work by Van Leeuwen [vLe17] and ASHRAE [ASH13]. Demand profiles that can be obtained with these models serve as a lower bound constraint to device operation and hence also flexibility usage.

Heat demand for space heating

Figure 3.1. below depicts the basis of a household with floor heating system (q_h) and all other sources that influence the indoor temperature. Based on this drawing, we first introduce the main components that influence the temperature and therefore the stored energy within a building that results in a certain temperature.

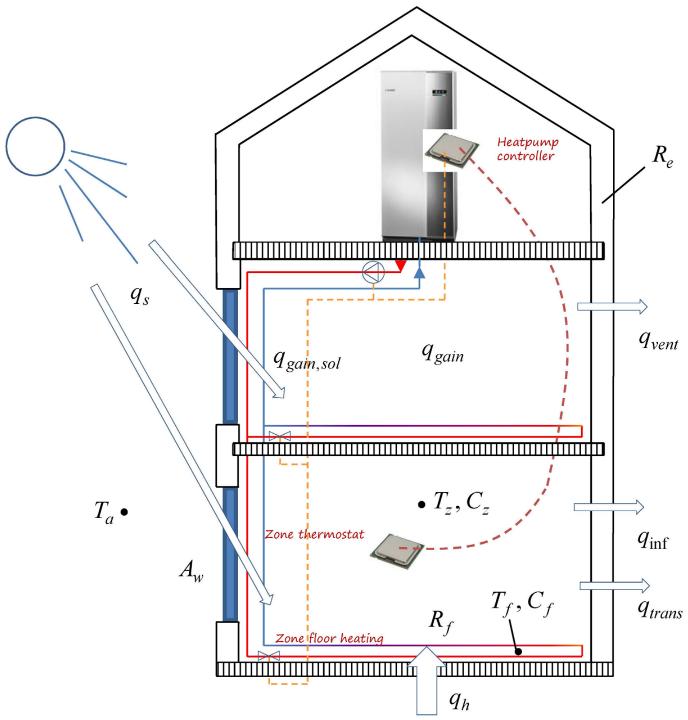

Figure 3.1: Thermal model of a house [vLe17]

The heating system adds heat to the *zone* the living room in this case where the thermostat controller is located. Through the windows, additional heat can be added by solar irradiation, which depends on the window size. Also other sources, e.g. humans and devices emit heat energy heating up the room. When the ambient (outdoor) temperature is lower than the indoor temperature, heat energy will leak through the walls, depending on insulation and the temperature difference. Furthermore, heat will also be removed through active ventilation, open doors, and open windows.

The used symbols in Figure 1 are as follows [vLe17]:

- T_z the interior zone temperature
- T_f the average floor heating surface temperature
- R_f the resistance between the floor heating and interior zone thermal mass
- C_f the capacitance of the floor heating thermal mass
- C_z the capacitance of the zone thermal mass
- R_e the thermal resistance between the zone thermal mass and the ambient
- A_w the effective window area on the south side of the building
- q_s incident total solar energy on the southern vertical building plane
- $q_{\text{gain,sol}}$ the solar energy gain of the interior zone, i.e. $q_{\text{gain,sol}} = A_w \cdot q_s$
- q_h heating energy from an external source (e.g. heat pump) to the floor heating
- q_{trans} heat loss by transmission through the exterior walls and windows
- q_{gain} thermal gains by people and appliances
- q_{vent} , q_{inf} heat loss by ventilation and infiltration air streams.

The aforementioned model can be translated into an equivalent electrical circuit with resistances and capacitors to study the interactions. Herein, the voltage is replaced by temperature and the current by heat flow. The resistances represent the physical elements that prevent heat transfer, whereas the capacitors model heat storage. The latter can be in the form of air, building materials, furniture, etc. Typically, it is assumed that static building parameters can be obtained from building documents and/or learning models based on observations. These are the following parameters: Resistances R_*, capacitances C_*, and window areas A_*. Furthermore, ambient temperature T_a can be obtained from historical meteorological measurements and weather forecasts.

A heating system often comprises of at least one heat source (Section 3.2), often piping, and elements to transfer heat to the air. The latter often happens using radiators or a floor heating system. But alternative heating systems also exist, such as electric heaters or infrared panels, which do not need piping and hot water flows to transfer the heat form the source to the zone. Also, for these heating elements, the capacity and resistance values can often be obtained directly or through calculations of the specifications of technology used.

Creating an equivalent circuit model results in a white-box model, in which all interactions are described. This allows the model to be easily modelled in simulation tools like TRNSYS, SIMULINK, or DEMKit [Hoo19]. Yet, different degrees of freedom concerning complexity is possible. Van Leeuwen surveyed six different of these white box models, depicted in Figure 3.2.

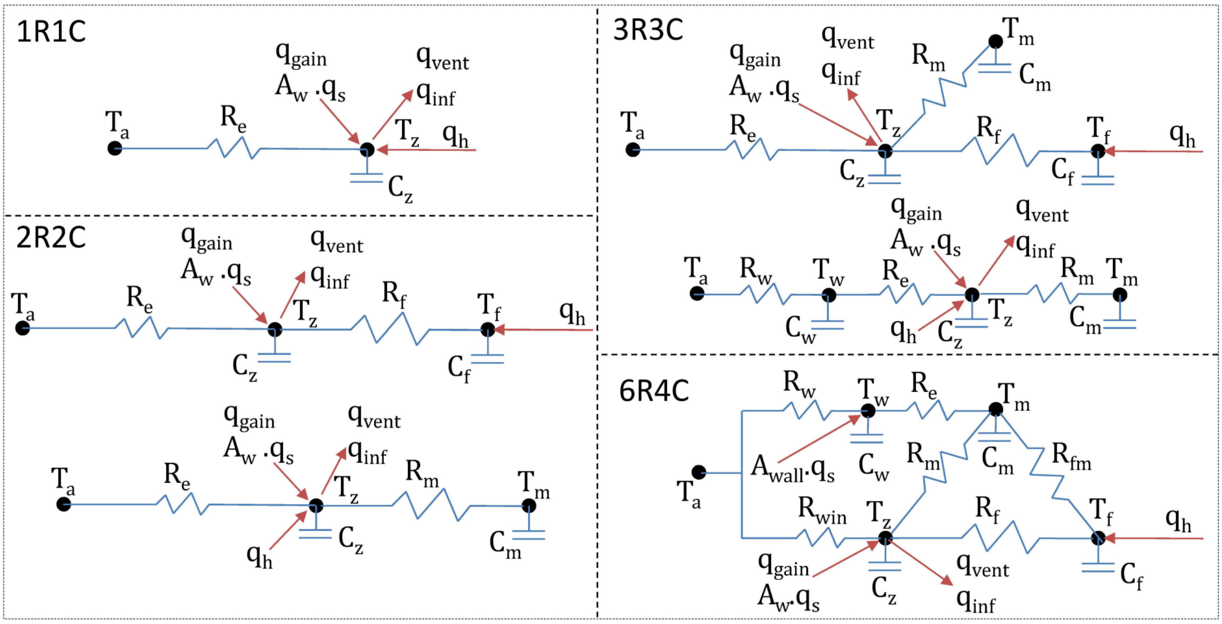

Figure 3.2: Thermal network representations [vLe17]

Based on various simulation and use-case studies, the first 2R2C model displayed in Figure 3.2 seems to provide a rather good accuracy for practical usage [vLe17]. Its limited complexity reduces the simulation times, making it useful for model predictive control. Furthermore, the more complex models have many parameters that need to be either calculated or learned. With various sources of unpredicted disturbances in real life, e.g. open doors and windows, the theoretical benefits of these more accurate models may also be nullified when applied in practice.

Van Leeuwen has performed extensive validation of the top 2R2C model in comparison to more sophisticated TRNSYS models. Here, the parameters of the model are estimated using a minimization optimization formulation using only the measured indoor temperature (T_z) as a reference. The results in Figure 3.3 show that the output of the model ($T_{z\_prediction}$) is accurately following the outcomes of the TRNSYS model. Furthermore, Van Leeuwen finds that the 3R3C model is the most accurate overall, but for the 2R2C model parameters can be obtained directly from physical properties [vLe17]. Furthermore, building parameters for various types of Dutch houses are provided by [vLe17].

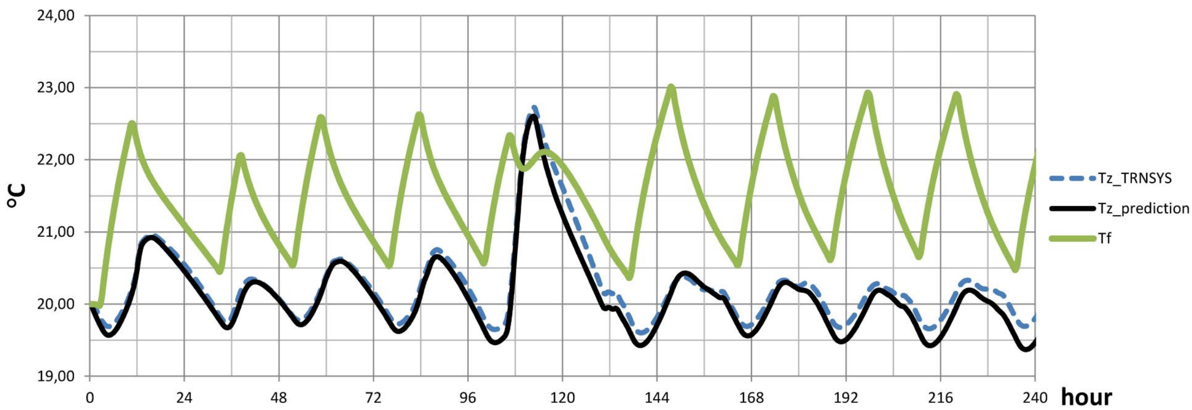

Figure 3.3: Thermal model validation [vLe17]

Furthermore, for practice, data may not be available for all parameters and therefore need to be estimated automatically by e.g., machine learning methods. In such a setting, the interaction that parameters have on each other may lead to ill-fitting and tuning of parameters when used in grey-box models or hybrid models. Hence, The 2R2C-model is seen as a workable and sensible trade-off in the context of both studying and implementing benefits of utilizing electricity-to-heat flexibility within the energy transition.

Modelling heat gain and loss components

As specified, many sources add and subtract heat energy from a room. These are the parameters indicated by q_*. This subsection outlines all these sources, except for the heat energy added by a heating device and/or system, which is be explained in Section 3.2. Furthermore, many gains depend on human presence and behaviour and follow from their comfort constraints. Models to obtain these required profiles and input with regards to user interaction will be outlined in Section 3.4.

Ventilation:

Air within a house needs to be refreshed over time to keep the indoor CO_2 levels at acceptable levels. The rate at which air is refreshed is expressed by the air change rate (ACR), which is defined as the ratio of entire interior volume that is refreshed per hour. Different variants of ventilation exist, such as passive ventilation and active ventilation, of which different sub-types exist. With passive ventilation the ACR depends on human behaviour of opening vents, wind force and direction and air pressure differences. This adds many unknowns and complexity to the model. Therefore, we limit the scope to active ventilation methods in this section, as they are common in newer houses and allow for more exact control over ventilation modelling. The heat loss due to ventilation can be calculated as follows:

$$q_{\text{vent}} = ACR \cdot V_{air,i} \cdot \frac{p}{Ta \cdot Rs} \cdot c_{p,air} \cdot (T_a - T_z)$$

Herein, $V_{air,i}$ is the interior air volume, p is the ambient air pressure, R_s the specific gas constant of air, and $c_{p,air} = 1.005\ [kJ/kg\ K]$ the specific heat of air. However, another model exists with less parameters:

$$q_{\text{vent}} = \phi_v \cdot \rho_{air} \cdot c_{p,air} \cdot (T_a - T_z)$$

Where φ_v is the ventilation air flow schedule in $[m^3/h]$ and $\rho_{air} = 1.25\ [kg/m^3]$ is the air density. It is important to note here that the ventilation air schedule depends on the persons in a house and also their activities. We will elaborate on how to obtain good schedules in Section 3.4. Note that the losses due to ventilation are heavily dependent on the system used, where heat recovery systems require a substitution of T_a with an efficiency factor.

Solar gains:

Heat gain through solar q_s depends on the solar irradiation multiplied by the area of a window $A_w\ [m^2]$:

$$q_{gain,s} = q_s A_w$$

Here, q_s $[W/m^3]$ can be obtained from the solar irradiation (measured, historical or forecasts) on a plane considering the orientation of the window, given by the inclination and azimuth. This can be calculated using equations presented by Duffie [Duf80] and Erbs [Erb82].

The window surface can be obtained from building properties. However, different windows have different shading coefficients, blocking some of the sun irradiance. Typical shading coefficients (SC) are provided by ASHRAE [ASH13] and window manufacturers. However, window manufacturers have shifted towards the use of the Solar Heat Gain Coefficient ($SHGC$), and therefore an approximate 0.87 multiplication conversion must be applied [ASH13]. Hence for the solar gains, the following equation is used:

$$q_{gain,s} = q_s \cdot A_w \cdot SHGC \cdot 0.87$$

Note that the contribution of each window can be considered individually. South-faced facades of windows, such as used at the Dutch demonstrator Vriendenerf, have a significant contribution to the heat demand. In these buildings, the design and architecture is optimized to cleverly utilize the free heat provided by the sun in winter and often also block sunlight in summer to avoid overheating.

Other heat gains:

Two sources of heat gains remain: Those of active devices that convert another energy carrier (e.g., electricity) into heat and the contribution by humans in a room. The former can be obtained by applying a constant efficiency factor to the energy usage of a device [ASH13]. Next to this, each adult body contributes approximately 120W when being idle, and children approximate to 97W. To ease the model, we do not consider other activities, that raise the heat emissions. Although these gains can be modelled, they heavily depend on human behaviour.

Domestic hot water usage

Another significant portion of demand for heat is domestic hot water (DHW) usage. Often, hot water is also provided by the same devices that perform space heating, and so the interaction of electricity-to-heat devices also depends on DHW. Similarly to subsection 3.1.2, DHW usage also depends on human behaviour. Hence, here we presented the theoretical model, whereas Section 3.4 will provide the necessary input derived from human presence and activities.

Dominant factors in DHW usage are tap water usage for washing, showering, bathing and cleaning. However, in some cases it can also be used by whitegoods machines, such as hot fill washing machines. Differently than heating demand for space heating, DHW usage does not so much depend on the season and therefore remains rather constant throughout the year. However, the exact timing of DHW use is much harder due to human behaviour and the fact that DHW requests are often short in time duration, typically a couple of minutes. Hence, intermediate buffering is advised for flexibility applications.

Generally speaking, DHW demand $\dot{Q}_{dhw,h}$ can be modelled as follows:

$$\dot{Q}_{dhw,h} = \phi_i \cdot \rho_w \cdot c_w \cdot (T_{hw} - T_{cw})$$

Where ϕ_i is the flow of demand in $[L/s]$, ρ_w the specific density of water, c_w the specific heat of water, T_{hw} the hot water supply temperature, and T_{cw} the cold water supply temperature. It is important to notice that the flow can be obtained through measurements. Van Leeuwen [vLe17] shows that this can also be approximated for an aggregation of multiple houses using a set of Gaussian distribution functions. This approach results in the DHW demand shown in Figure 3.4. The overall shape (green) follows actual measurements (blue) and trends accurately. Section 3.4 presents an alternative approach to generating the DHW demand based on occupancy profiles.

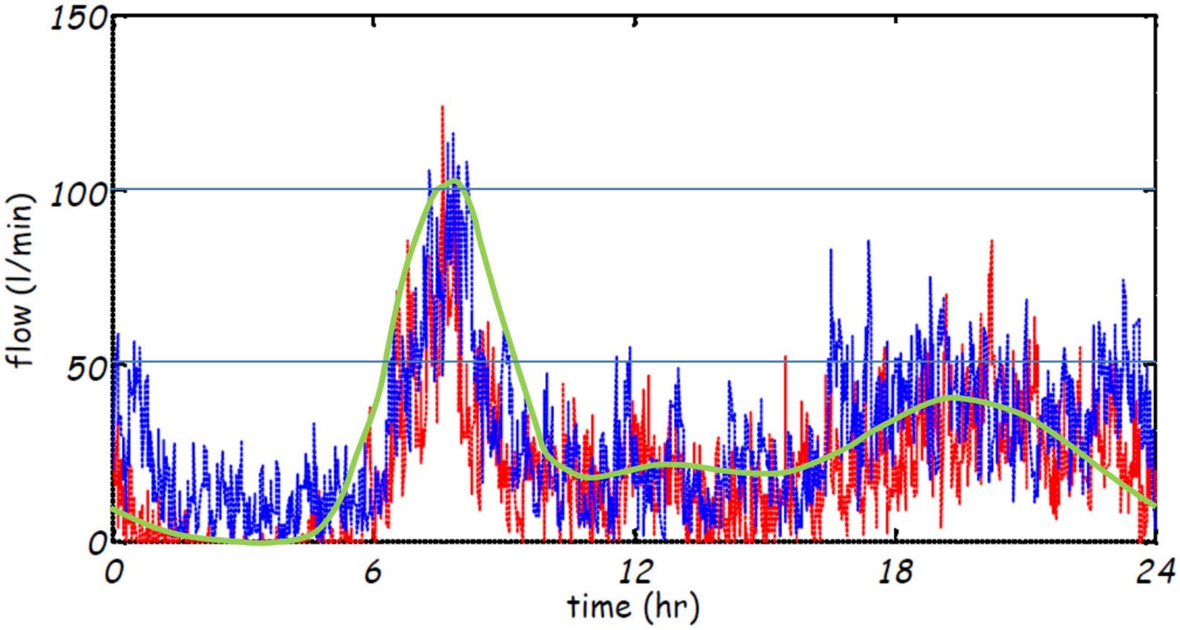

Figure 3.4: Approximated DHW demand [vLe17] compared to other literature [Blo07], source [vLe17]

3.2 Heat generation device models

Heat pumps

The mathematical modelling of heat pumps (HPs) is generalised, despite of various existing technologies for heat sources and sinks. The thermal power delivered by the HP is defined by eq. (1). The temperature of the heat transfer fluid (HTF) flowing out of the HP (T_{out}) depends upon the temperature of the HTF into the heat exchanger of HP (T_{in}), nominal flow rate of HTF ($\dot{m}_s$) and operating power of the HP (P_{HP}) (eq. (2)). To maintain constant flow rate of HTF ($\dot{m}_s$), ΔT is maintained constant during the operation of the HP. The HP will stop operating automatically when ΔT is less than its operational limit.

$$\dot{Q}_{heat} = COP \cdot P_{HP} \qquad \text{[W]} \qquad \text{eq.(1)}$$

$$T_{out} - T_{in} = \Delta T = \frac{\dot{Q}_{heat}}{\dot{m}_s C_w} \qquad \text{[kg/s]} \qquad \text{eq.(2)}$$

$\dot{m}_s$ = flow rate of heat transfer fluid through HP for thermal power delivery [kg/s]
$\dot{Q}_{heat}$ = rate of heat energy delivered by HP [J/s]
COP = coefficient of performance of HP
P_{HP}= electrical power of HP [J/s]

Herein, it is important to mention that the COP depends also on the temperature of the source. Especially with air source heat pumps the ambient temperature ($T_{ambient}$) has an important impact, together with the efficiency of the Carnot cycle (η_{carnot}):

$$COP = \eta_{carnot} \cdot \frac{T_{supply}}{T_{supply} - T_{ambient}}$$

Using TRNSYS (version 17), a thermal and fluid flow simulation model was constructed utilizing the specifications and weather data from the Gdańsk, Poland (see Figure 3.5). Within this model, an air-source heat pump with a 1 cubic metre water tank for domestic hot water was modelled with a usage profile obtained from a multifamily building. The model is a single-stage air-to-water heat pump is based on user-supplied data files containing catalogue data for the capacity (for the water), and power, based on the entering water and air temperature to the heat pump. Performance data for the Air-Water Heat Pump (type 941) are listed in Table 3.1 below and depicted in Figure 3.6:

Table 3.1: Heat pump model performance

Fraction of Capacity	Fraction of Power	T_air_in	T_water_in
0.759	0.787	2.2	25
1.080	0.868	7.2	25
1.137	0.843	12.2	25
1.233	0.843	15	25
1.403	0.844	20	25
0.737	0.860	2.2	30
1.048	0.938	7.2	30
1.106	0.923	12.2	30
1.199	0.924	15	30
1.359	0.924	20	30
0.714	0.944	2.2	35
1.017	1.044	7.2	35
1.075	1.016	12.2	35
1.165	1.017	15	35
1.314	1.018	20	35
0.692	1.027	2.2	40
0.986	1.136	7.2	40
1.043	1.108	12.2	40
1.131	1.109	15	40
1.269	1.112	20	40
0.670	1.132	2.2	45
0.955	1.255	7.2	45
1.012	1.224	12.2	45
1.097	1.226	15	45
1.224	1.229	20	45
0.648	1.249	2.2	50
0.923	1.385	7.2	50
0.981	1.352	12.2	50
1.062	1.355	15	50
1.180	1.359	20	50

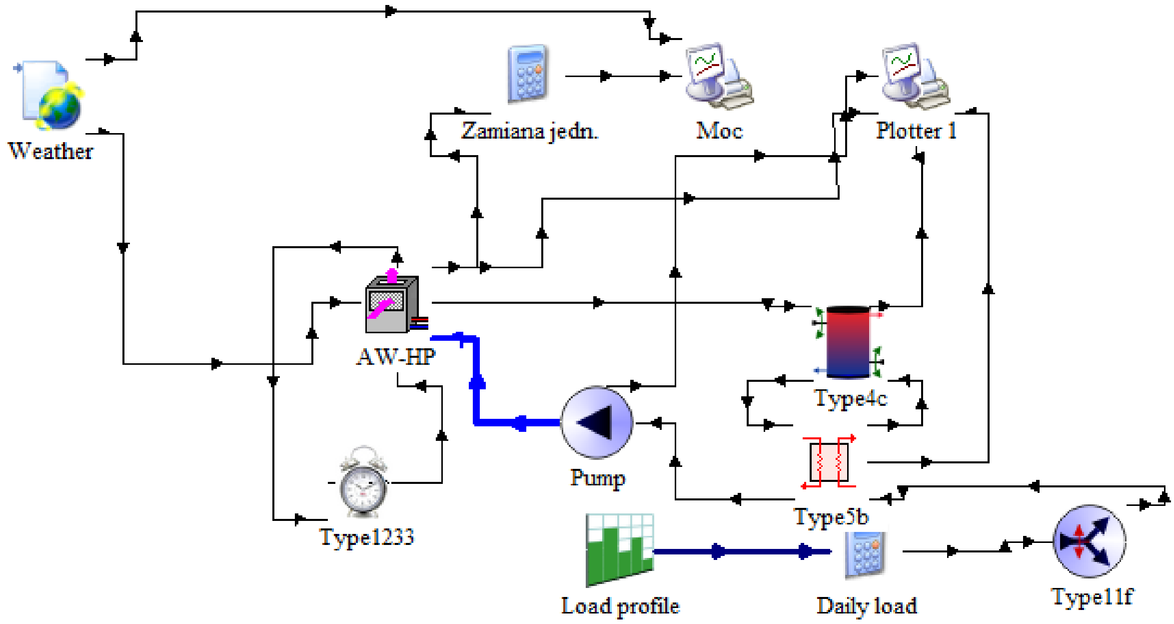

Figure 3.5: Layout of TRNSYS 17 with Air-Water Heat Pump and tank

Figure 3.6: Results of simulation in TRNSYS 17. Chart of temperatures and flows in hydronics cycle

Electric boilers

Electric boilers (EB) can be modelled as the resistive heating element with constant impedance load [Sin17]. Heat delivered by EB is given by eq.(3).

$$\dot{Q}_{heat,EB} = \frac{\eta}{100}\frac{V_{poc}^2}{V_{r,b}^2}P_{eb} \qquad [W] \qquad eq.(3)$$

$\dot{Q}_{heat,EB}$= rate of heat delivered from EB
η= Efficiency of EB [%]
V_{poc}= voltage at point of coupling of EB
$V_{r,b}$= rated operating voltage of EB
P_{eb}= operating power of EB [W]

3.3 Thermal storage models

Heating system's storage capabilities can be a promising source of flexibility to the electricity grid through power-to-heat options. Different methods exist, with a dominant separation between sensible heat storage and latent heat storage methods.

The amount of heat stored is based on the thermal capacitance of the material, overall heat transfer coefficient of material, and temperature difference between the material as shown in eq. (4)

$$Q_{stored} = mC_p\Delta T \qquad \text{eq.(4)}$$

Q_{stored}= heat energy stored as sensible heat [J]
m= mass of material [Kg]
C_p= specific heat capacity of the material [J/kg.K]
ΔT= change in temperature of the material [K]

Storage of thermal energy in terms of sensible heat requires a large storage size. However, higher temperature storage is possible with sensible heat storage.

Sensible heat storage

Hot water buffer vessels are often used to store sensible heat for DHW usage, but sometimes also for space heating purposes. These systems often consist of a large insulated buffer tank that contains hot water and an inlet and outlet. The outlet allows hot water to flow out on demand, which is useful for especially DHW usage. The inlet allows the water volume to be topped up. Two methods are possible, either the buffer is refilled using hot water from e.g., a heat pump, or cold water is added and subsequently heated in the buffer. Figure 3.7 below shows a schematic drawing of the latter system [vLe17].

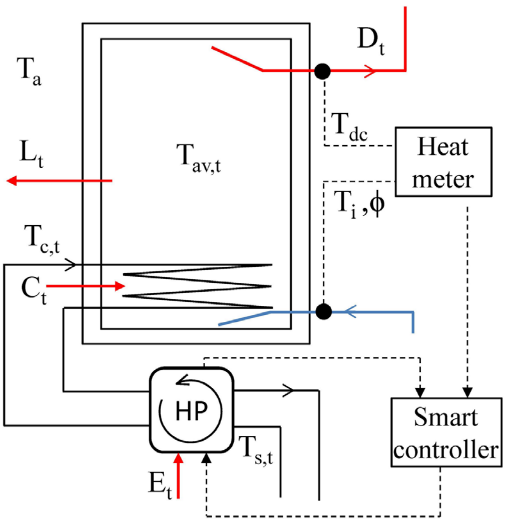

Figure 3.7: Schematic overview of a thermal storage [vLe17]

Herein, C_t is the thermal energy charged to the buffer from a heat source as described in Section 3.2, D_t is the discharge of thermal energy, L_t the loss of energy to the environment in time interval t. Various temperatures are included, of which the average temperature of the water in the tank $T_{av,t}$ is the most important one, and the others denoting observable temperatures related to the heat system. In this example, the direct electricity-to-heat coupling is also visible with the heat pump (HP) taking electricity E_t to produce thermal energy C_t.

Different models exist in literature, ranging from white-box models, to black-box models and includes also machine learning methods [Goe19, Lee17, Rid14, Spil21]. For sake of understanding, we first introduce a simple linear model and subsequently briefly introduce two simple alternative models that allow the model stratification and mixing behaviour of water in the buffer.

Linear model:
Using a simple linear model, the following relations concerning the operation of the buffer can be described [vLe17]:

$$\Delta S_t = C_t - D_t - L_t$$
$$S_t = S_{t-1} + \Delta S_t$$

Here ΔS_t is the change of stored energy within a time interval t, and S_t the stored energy at time t. The maximum energy that can be stored (S_{max}) can be obtained using the following equation:

$$S_{max} = V \cdot \rho \cdot c_p \cdot (T_{max} - T_i)$$

Where V is the volume in $[L]$, ρ the specific density of water, c_p the specific heat of water in [J/kg K], T_{max} the maximum temperature, and T_i the inlet temperature. The latter we assume to be constant over time. As a result, the state of charge SoC_t at time t of a buffer can also be defined:

$$S_{oC_t} = \frac{S_t}{S_{max}}, 0 \leq S_o C_t \leq 1$$

Based on the heat demand D_t the thermal energy withdrawn from the buffer can be obtained as follows:

$$D_t = \Delta t \cdot \phi_t \cdot \rho \cdot c_p \cdot \left(T_{dc,t} - T_{i,t}\right)$$

Where ϕ_t is the flow of water, $T_{dc,t}$ the observed temperature at the outlet, and $T_{i,t}$ the inlet temperature at time t.

Multi-layered stratified model:
The linear model is very simple, however. In practice, stratification occurs, resulting in multiple layers of heat, of which only a limited number of levels have enough heat. Modelling stratification behaviour is important to maximize the heat usage [Ros01]. An overview of stratification models is reported by [Han12]. However, heat losses due to stratification are just as important, which is a topic surveyed by

[Fan12]. Experiments by [vLe17] also show the stratification effect when discharging a buffer at constant flow rate, see Figure 3.8.

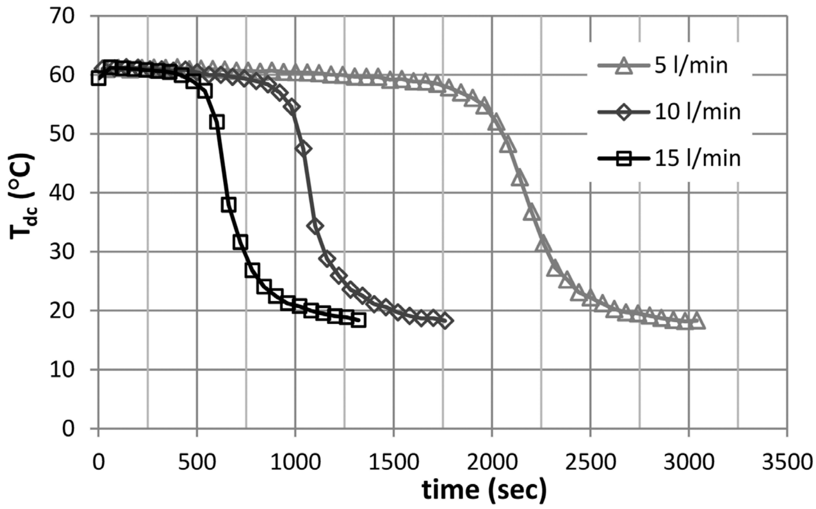

Figure 3.8: Observed outflow temperature over time when discharging a buffer at constant rate [vLe17]

Here, three layers or zones can be observed. A hot layer, a cold layer and an intermediate mixed layer. Each of these layers has a time variable volume and temperature. Since only the hot layer is of interest as it contains the usable thermal energy, a simplification is presented by [vLe17] which includes only two layers. Here, the hot layer is denoted by volume $V_{h,t}$ and temperature T_{max}. The other layer is a mixed layer with the remaining volume $V - V_{h,t}$ and average temperature $T_{w,t}$. A schematic drawing of such a model is depicted in Figure 3.9.

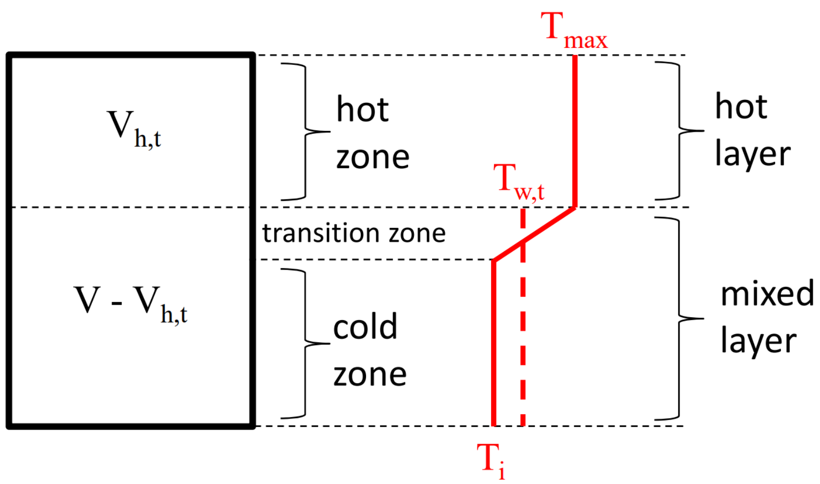

Figure 3.9: Multi-layer buffer model [vLe17]

With this model, $V_{h,t}$ becomes dependent on the SoC and hence can be obtained as follows:

$$V_{h,t} = V \cdot SoC_t$$

The stored thermal energy S_t at time t can be obtained as follows:

$$S_t = \rho \cdot c_p \cdot \left[V_{h,t} \cdot (T_{max} - T_i) + \left(V - V_{h,t}\right) \cdot \left(T_{w,t} - T_i\right)\right]$$

Further details for this model can be found in Section 4.3 of [vLe17]. Next to this simplified model, it may be useful to introduce more layers for large storage systems as applied in district heating systems. A novel approach is presented by De Goeijen [Goe19], where an Integer Linear Programming model is created to operate an EcoVat, a large seasonal underground vessel. Here, multiple heat sources are attached to a large underground water tank using heat exchangers, allowing for maximum efficiency and electricity-to-heat integration, coupled with seasonal storage.

Diffusion Buffer (DiBu) model:

One observation of the experiments by [vLe17] is that the behaviour of a buffer is similar to that of other storage devices, such as electrical storage. Homan et al. [Hom18] have developed a novel model based on diffusion of energy within a buffer. It consists of 4 separate stages and equations, see Figure 3.10:

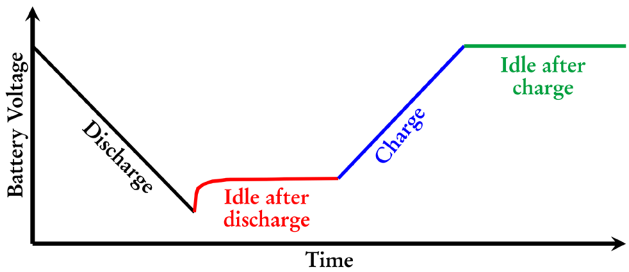

Figure 3.10: Four stages of the DiBu model. Source [Hom20]

Except for the *Idle after discharge* state, the behaviour of the stages can be modelled using the linear equations as presented before. Homan does however present more advanced models based on external observations in [Hom20]. The idle after discharge state adds the possibility to model the mixing of water. This is modelled using the following equation using the observed temperature T_t:

$$T_t = T_{t'} + T_{max'} - T_{t'} \cdot (1 - e^{-\frac{t-t'}{\beta(t-t')+\gamma}})$$

Here $T_{t'}$ is the observed temperature at the start of the *idle after discharge* state at time t', $T_{max'}$ the maximum observed temperature during the discharge state, β and γ are storage specific parameters. We refer to Homan [Hom20] for more details on this model. Therein it is also explained how the necessary parameters for this model can be obtained from measurements for electrical storage systems. It is expected that thermal buffers can be characterized in a similar way and perhaps online using data analytics and machine learning.

PCM storage devices

Latent thermal storage (LTS) technologies can be an interesting alternative to sensible heat type storages due to the former's higher energy storage densities, which are better suitable for demand response (DR) applications in distribution grids for capacity relief, or on the electricity market for balancing. However, the existing energy models are not capable of representing the rate of energy exchange inside the storage tank due to interdependencies of heat transfer coefficient and temperature difference between heat transfer fluid and phase change material (PCM), which is an important factor for finding the energy stored and transferred at any point in time. This work presents detailed modelling using average and discretized methods for PCM based storage systems. The proposed models can capture the heat system dynamics which can further enhance energy flexibility. In addition, the deployment of LTS can consequently reduce the heat pump's size and thereby costs.

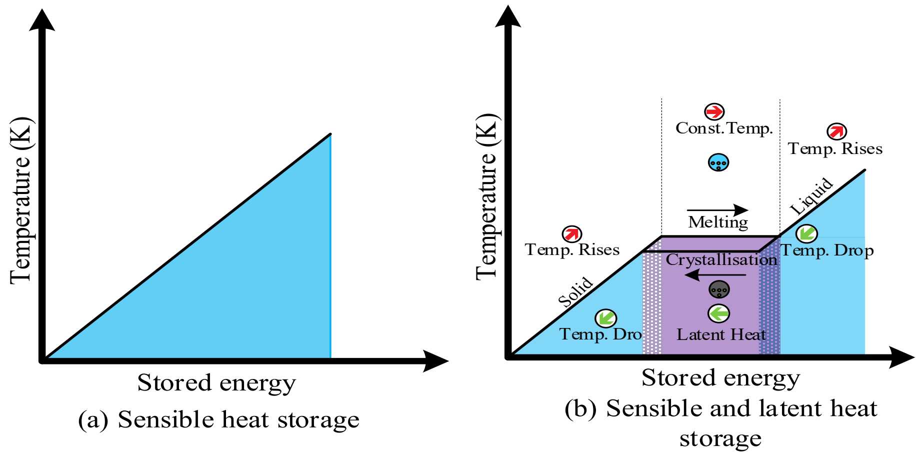

Figure 3.11: Methods of thermal energy storage as sensible and latent heat

Latent heat storage stores thermal energy without significant temperature changes in the storage material. However, it involves the phase change of the material. The capacity of latent heat storage is determined using eq. (5). Heat storage in the form of latent requires smaller volume as the latent heat is much greater than the specific heat of the same substance. In some of the material with added impurities, the temperature of liquification and crystallization during latent heat process is different as seen in Figure 3.11 (b)

$$Q_{lhs} = mL \qquad \text{eq.(5)}$$

L= latent heat [J/kg]
m= mass of the material [kg]
Q_{lhs}= capacity of latent heat storage [J]

The amount of energy store in the phase change material (PCM) can be derived from the eq.(6)

$$Q_{pcm} = m_{pcm}[C_{ps}(T_m - T_{pcm,i}) + \beta\Delta q + C_{pl}(T_{pcm,f} - T_m)] \qquad \text{eq.(6)}$$

β= melt fraction
C_{pl}= specific heat of PCM in liquid phase [J/kg.K]
C_{ps}= specific heat of PCM in solid phase [J/kg.K]
Δq= latent heat of fusion of material [J]
m_{pcm}= mass of PCM material [kg]
Q_{pcm}= storage capacity of PCM [J]
T_m= melting temperature of PCM [K]
$T_{pcm,f}$= final temperature of the PCM material [K]
$T_{pcm,i}$= initial temperature of the PCM material [K]

The energy balance inside the PCM based thermal storage tank is shown in Figure 3.12.

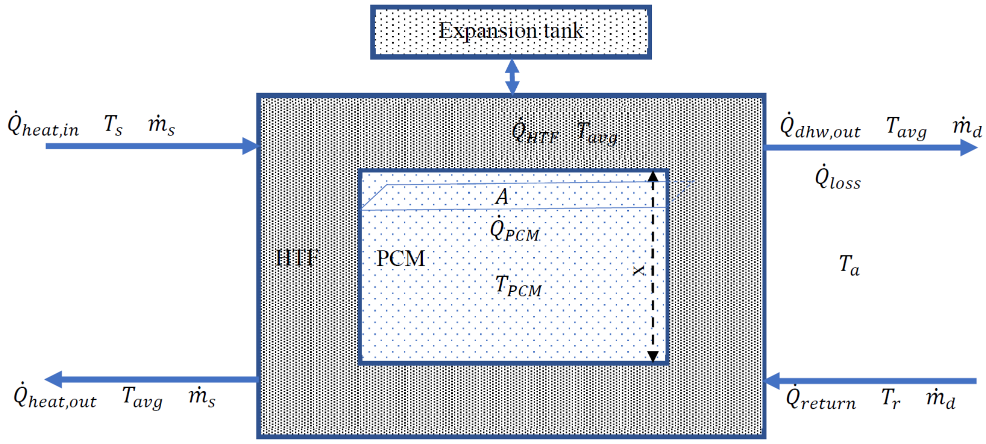

Figure 3.12: Schematic of PCM storage tank with energy flow

$\dot{m}_d$ = flow rate of heat transfer fluid for discharging storage tank [kg/s]
$\dot{m}_s$ = flow rate of heat transfer fluid from source for charging storage tank [kg/s]
$\dot{Q}_{dhw}$ = rate of heat energy exiting tank to district heating [J/s]
$\dot{Q}_{heat,in}$ = rate of heat energy entering storage tank from source [J/s]
$\dot{Q}_{heat,out}$ = rate of heat energy exiting tank to source [J/s]
$\dot{Q}_{HTF}$ = rate of heat energy transfer in HTF [J/s]
$\dot{Q}_{loss}$= rate of heat loss to the environment [J/s]
$\dot{Q}_{PCM}$ = rate of heat energy transferred in PCM [J/s]
$\dot{Q}_{return}$ = rate of heat energy entering tank as return from district heating [J/s]
$\dot{Q}_{tank}$= rate of heat energy stored in tank [J/s]
T_a= ambient temperature [K]
T_{avg} = average temperature of HTF in storage tank [K]
T_{PCM} = temperature of HTF in storage tank [K]
T_s = temperature of HTF from heat source for charging storage tank [K]
T_r = Temperature of return HTF from heat sink [K]

Based in energy balance as shown in Figure 3.12, eq.(7) is derived.

$$\dot{Q}_{tank} = \left[\left(\dot{Q}_{heat,in} - \dot{Q}_{heat,out}\right) - \left(\dot{Q}_{dhw} - \dot{Q}_{return}\right) - \dot{Q}_{loss}\right]$$
$$= \dot{Q}_{PCM} + \dot{Q}_{HTF} \qquad \text{eq.(7)}$$

The detailed modelling using average and discretized methods for PCM based storage tank is presented in Annex A (9.1 and 9.2 respectively)

3.3.1.1 Modelling of HP and PCM Storage in DigSILENT PowerFactory

The implementation of user-defined dynamic models of HP, Control, and PCM Storage, in DigSILENT PowerFactory, is developed using DigSILENT Simulation Language (DSL). DigSILENT PowerFactory is a power systems simulation tool. DSL is a platform to design and simulate dynamic models used in electric power systems. The implementation of various dynamic systems in a single simulation tool has the advantage of reducing simulation time while investigating demand response over a period.

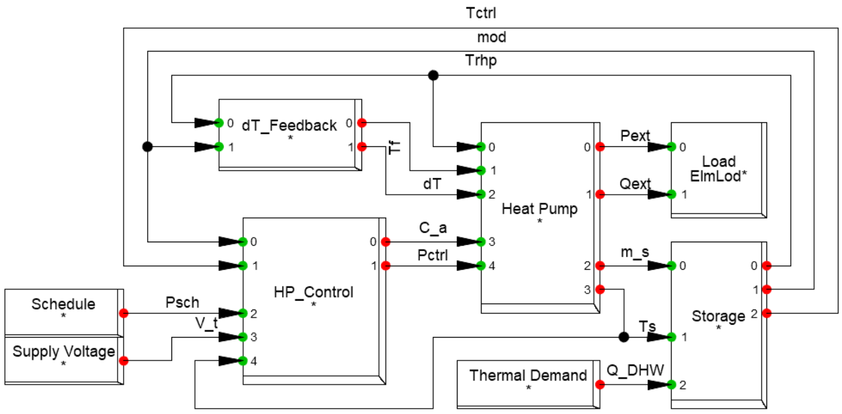

Figure 3.13: Block frame diagram of thermal system developed in PowerFactory

The diagram of the complete thermal system developed in DSL - PowerFactory is shown in Figure 3.13. The thermal system consists of measurement units (supply voltage), schedule unit, thermal demand profile (thermal demand), PCM based storage system, heat pump unit, control unit for HP activation, feedback unit to maintain the temperature of HTF from HP and finally the electrical load to power system. These components are elaborated in more detail below.

Measurement unit: Power system voltage at the point of coupling of HP (V_t) of HP is measured using the 'supply voltage' block. The 'HP_control' unit utilizes (V_t) as a part of demand response to regulate distribution system by allowing connecting or forced disconnection of the HP. The HP is allowed to connect only if the system voltage is greater than 0.95 pu (per unit voltage equivalent) and will be forced disconnect below 0.92 pu.

Thermal demand profile: This block provides the characteristic profile of thermal energy supplied to the consumer (Q_DHW).

Schedule unit: This unit provides the optimized schedule for thermal power delivery (Psch) from HP based on estimated demand and electricity price. The optimization is based on Chapter 5.

Control unit: The control unit block (HP_Control) is an output block. It performs logical evaluation of temperature and voltage at the point of common coupling of the HP (V_t) to determine the On/Off operational status of HP (C_a) and thermal power generation (Pctrl). The control scheme of the heat pump is based on two control levels. The first level of control comes from the scheduling block and the output of this block is based on forecasts of the generation and demand through gathering of energy price information. The second level of control will manage the operation of HP with respect to state of energy of storage, HP dynamics, supply voltage and user's priority. This two-level control ensures the reduction of forecasting errors through a feedback to first level from the second level control, and supports local node voltage regulation.

Heat pump: This unit represents the HP dynamics as described in Section 3.2.1.

Operating temperature of HP: The output temperature of HP is maintained by the block 'dT_Feedback' unit. This is an inbuilt function of the HP which maintains the temperature difference between incoming and outgoing HTF. This unit continuously monitors the temperature of HTF from the bottom of the storage tank to the HP and sends the feedback (Tf) signal to determine the output temperature of HTF to the storage. This temperature difference helps to maintain the constant flow rate of the HTF.

Load: This unit represents the electrical load of HP as active and reactive power to the power system.

Storage: this unit represents the PCM based thermal storage system. Two different model of storage can be selected based on the requirement. One is average model where, temperatures of HTF and PCM are uniform through the storage. The second is stratified model of storage where, temperatures of HTF and PCM are determined for each stratified layered of the storage. Output signal from the storage are: Tctrl- feedback of temperature for control, mod: working mode of storage (average or stratified), and Trhp-return temperature of HTF from bottom of the storage to HP.

3.4 User preferences and constraints

As indicated in Section 3.2, many thermal interactions involve user behaviour and preferences. The most obvious is the direct control a user has over its heating system: the thermostat setpoint. But also DHW usage has a significant influence on thermal energy demand. Next to these direct links, also the perceived comfort of the end-users must be taken into account when controlling heating systems, but also introduce the bandwidth of inherent thermal flexibility to the control system.

Profile generation and occupancy

We first start this Section with a brief introduction of user behaviour and occupancy profiles which form the basis of many energy related usage patterns in residential environments. Pflugradt [Pfl13] describe how psychological behaviour can be modelled and how this contributes to energy usage. This resulted in the Load Profile Generator[1]. However, this extensive model requires a lot of configuration to generate energy usage profiles. A simpler approach is presented by Hoogsteen et al. [Hoo16] that only uses high level input data and statistics to generate demand profiles. The resulting open-source Artificial Load Profile Generator (ALPG)[2] resulted initially in accurate electricity demand figures for residential areas. Later, the work of Van Leeuwen [vLe17] was combined, resulting in a tool that exports files for both simulation of electricity demand and heat [Hoo17]. Therefore, the resulting ALPG output matches with the open variables from Section 3.2 and also ensures that the electricity and heat demand profiles match, whereas the dedicated input files preserve the nonlinear behaviour of heating in simulation studies. We briefly describe the ALPG generation steps with respect to the heat demand.

The overall modelling is based on characteristics of the neighbourhood and its inhabitants. Therefore, the following main inputs are required:

- Physical location of the neighbourhood;
- Historical weather data;
- Types of households including persona types.

[1] Loadprofilegenerator.de
[2] https://github.com/utwente-energy/alpg

Randomization using Gaussian functions is performed within predefined bounds to result in a mixed set of households and persons that follow the general statistics. From the input, a model is generated, in which the modelled persons perform a key role.

The first simulation step is to determine the occupancy of each person in a household. These can be *active* (at home) and *inactive* (e.g., at work or sleeping). Only active persons can change the power consumption and DHW usage in a house. Using a process, power consumption is determined from this occupancy profile. This is done in a couple of distinct device classes. Each profile consists of a vector of values, where each element represents the activity in one discrete time step with a length of 1 minute. We refer to [Hoo16] for more details on this. Based on this occupancy profile and power usage, we can determine the necessary input for the space heating demand:

Ventilation:
The ventilation is directly based on the occupancy profile by multiplying the active persons in a house with a scalar to obtain the desired airflow in the house. Additionally, if a person is cooking, additional airflow is added to the model. This results in the following equation:

$$q_{vent} = \max(300, 30 + N_p \cdot 30 + C \cdot 150)$$

Where q_{vent} is given in $[m^3/h]$, N_p is the active number of persons, and C is a Boolean indicating that cooking equipment is active.

Heat gains:
Two important heat gains are those of human bodies and active equipment as outlined in Section 3.2. The added heat by active persons follows directly from the occupancy profile, where each user also has an age to determine the heat they add to the room. For the different device groups, the added heat to the zone is proportional to the electricity usage based on [ASH13]. The following scalars are used:

Table 3.2: Device groups in the ALPG [Hoo16]

Device group g	Scalar s_g
Fridges	0.5
Electronics	1.0
Lighting	0.8
Standby	1.0
Other	0.3

As a result, the electricity power consumption $P_{g,t}$ at time t for a group of devices g can be translated into a heat gain $q_{gain,g,t}$ given the scalar s_g:

$$q_{gain,g,t} = P_{g,t} s_g$$

Thermostat setpoints
From the occupancy profiles, also the desired thermostat setpoints can be derived. Each person has its own preference, which also depends on the age [vLe17]. The thermostat will be set to the maximum desired setpoint of all active persons in a household. Additionally, random events may be incorporated to test the effect of random behaviour of inhabitants on control systems.

Domestic hot water usage

DHW usage is generated by Gaussian functions, similarly to the electricity use. For showering, each person has preferences (e.g., showering in the morning or evening) and an average shower time. Using randomization based on these Gaussian distributions, we derive moments of hot water usage and generate a profile that resembles the DHW energy usage each discrete time interval.

Perceived comfort

Evaluating thermal comfort mostly depends on how people feel about it. Models [ASH55, ISO7730] have been developed for thermal comfort, which can be evaluated using the Predicted Mean Vote (PMV) and Percentage of People Dissatisfied (PPD). From analysis, it is found that the desired operated temperature depends on the zone temperature and radiation from bodies in a room. This model is however complex, as it involves 6 thermal bodies. Another observation by [ISO7730] is that the perceived comfortable temperature depends on the ambient temperature. In general, a perceived comfortable indoor temperature can be 2 ℃ lower when the outdoor temperature is below 15 ℃. Next to this, fluctuations in indoor temperature should be limited as well according [ISO7730]. Periodic variations should be limited to 1 ℃ and the maximum rate of change should be no higher than 2 ℃ per hour.

Next to the temperature, the relative humidity also impacts the perceived comfort. With respect to humidity, the ASHRAE Standard-55 2017 states that humidity control systems must be able to maintain a dew point temperature of 16.8 °C (62.2 °F) [ASH55]. However, the standard does not state any lower bound to the humidity level.

4 Use-cases

This Chapter presents the practical situation within SUSTENANCE's demonstration sites, the local context, and the possibilities, and the specific goals. This forms the basis to select the models that are required. Furthermore, this chapter provides input for Chapter 5 as the energy management strategy must align with the practical setup and context presented in this chapter.

4.1 Denmark

Local context

Heating in Denmark is divided into 2 categories. Within cities district heating and natural gas is the dominating heating sources. And in the rural areas, outside the distribution areas of natural gas and district heating the dominating heat sources are pellets and oil.

In 2020 it was politically decided that the natural gas grid in Denmark should be focused towards industrial high temperature applications, and as such the domestic heating should be moved to either district heating if applicable, or to heat pumps where district heating is not an option. Throughout Denmark there's a lot of biogas production that is upgraded and fed into the natural gas distribution grid, and it is expected that Denmark within few years will have 100% biogas in the distribution grid.

Currently there are around 100.000 heat pumps installed throughout Denmark, but this number is expected to increase to 500.000 within the next 8 years, and combined with an increasing number of EVs that need charging in the distribution system, local grid congestion is expected.

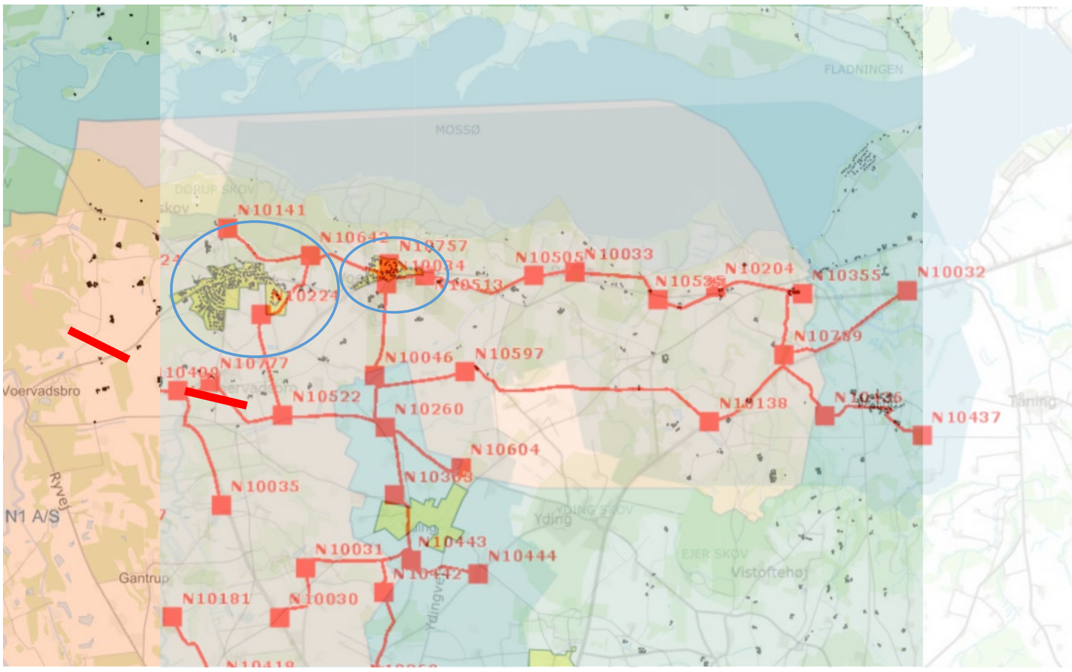

Figure 4.1: Location of the Danish demonstrator site

The location of the Danish demonstrator is depicted in Figure 4.1. Here, the 2 red bars on the map, indicate the supply lines to the area, and the circles mark the location of the 20 demonstration sites in the project.

The test site in the villages of Voerladegaard (Figure 4.2) and Dørup (Figure 4.3) are selected as it is a well-functioning community, far from neighbouring district heating plants and in a closed end of the electrical distribution grid. All the test houses have been selected on the criteria that they have fossil fuel (natural gas or oil) and that they have either PV on their house or own an electric vehicle (or plan to get it during the project).

Figure 4.2: Voerladegaard

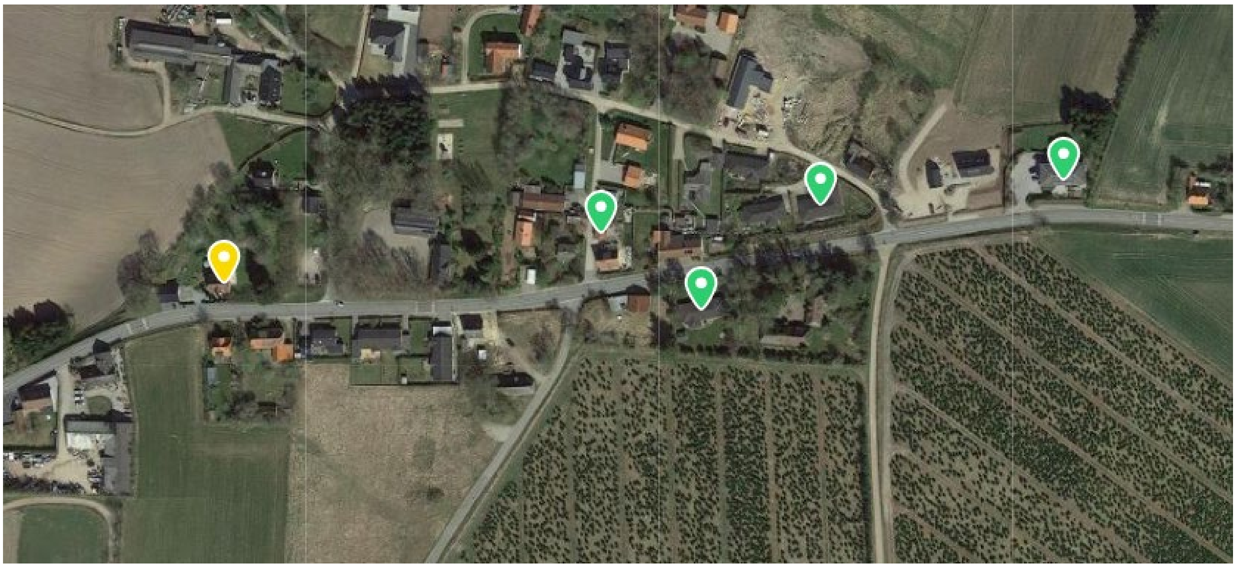

Figure 4.3: Dørup

The Danish demonstrator has a significant variety in the houses used in the demonstration:

- Heated areas from 90 to 250 m^2.
- Construction year from 1930 to 2010
- Heating demand from 10.000 to 30.000 kWh

Opportunities for market integration

Over the recent years the energy market has become much more volatile as the portion of renewable energy increases. Generally the prices have increased during the past 2 years, and the fluctuations within the same day can sometimes be by several factors.

Electricity for heat pumps is tax-free, and therefore are a good incentive for consumers to switch from taxed fuels like oil and gas to electricity. With the community energy management system, we will enable consumers and prosumers to benefit from each other. In a more imaged way, this would mean that the excess production from the Petersen household's PV system can be used by the heat pump from the Hansen household, and they help relieve the stress on the distribution grid. Generally speaking the energy prices give an accurate representation of the grid-load at any given time.

Demonstrator use-case

In the Voerladegaard demonstration we will equip 20 households with a controllable heat pump that is combined with a thermal storage and possibly also a PV system. This will enable us to run an optimization algorithm that optimizes for the lowest operation cost.

4.2 Netherlands

Local context

Heating in the Netherlands has been dominated by the use of natural gas since the discovery of vast deposits in the north of the Netherlands in the sixties. However, the increasing number of earth quakes in the province of Groningen have led to the decision to close down wells by 2024[3], depending on the geopolitical situation. As a result of this, newly build houses do not mandatory need to be built with a natural gas connection since 2018 [Ezk18] and new houses are built without natural gas since 2019 [Kli19].

However, due to the dominance of natural gas usage for heating in the Netherlands, switching to heat pumps in existing areas may lead to severe grid congestion. The Netherlands has been underinvesting in its electricity grid in the last 10 years despite warnings from several experts[4]. To overcome problems, several experiments are conducted in residential areas to transition away from natural gas[5]. Hereby, insulation of in particularly older households may cause problems when shifting away from high temperature heating systems. Data analysis by Tado shows that the insulation of houses is at most mediocre[6]. Next to electrification, also district heating systems are extended to reduce the strain on the electricity grid. However, the monopoly of district heating systems in areas brings its own concerns,

[3] https://www.rijksoverheid.nl/onderwerpen/gaswinning-in-groningen/afbouw-gaswinning-groningen
[4] https://nos.nl/nieuwsuur/artikel/2446932-toezichthouder-negeerde-waarschuwingen-overbelast-elektriciteitsnet
[5] https://www.rijksoverheid.nl/onderwerpen/aardgasvrije-wijken/bestaande-gebouwen-aardgasvrij-maken
[6] https://www.tado.com/gb-en/press/uk-homes-losing-heat-up-to-three-times-faster-than-european-neighbours

especially with respect to the climate agreements and goals. New legislation is being developed with the "wet collectieve warmtevoorziening 2" (English: law on collective heat supply 2). Herein it was recently decided that district heating infrastructure will be taken out of private hands and from 2031 onwards be collectively organized by governmental bodies [Jet22]. This decision is made to ensure that the energy transition can carry on and people are not excluded. More information on the heat transition as a result of the climate agreement can be found in [Kli19].

Use Case 1 – Energy community Vriendenerf in Olst

Vriendenerf is a community of 12 houses and 1 common house located in the municipality of Olst-Wijhe as shown in Figure 4.4. These houses were constructed as per Zero Energy Building (ZEB) standards and have the following properties:

1. 12 houses divided into groups of 3 as shown in Figure 4.5.
2. 69 PV panels for each group of 3 houses.
3. Each house is equipped with a heat pump, domestic hot water storage and ground source.
4. Houses are fully insulated.
5. Equipped with active air ventilation system.
6. Houses are in the process of installing EV charging stations.

Figure 4.4: Location of Vriendenerf, the Dutch demonstration site

Figure 4.5: 4 groups of 3 houses and 1 common house

Current energy system in Vriendenerf:

The PV panels produce 6400 kWh/year and 5600 kWh/year for a single corner house and a single in-between house on average. Of this annual PV yield, it is estimated that annually 3500 kWh is used for heating, cooling, ventilation and domestic hot water production. While the houses in Vriendenerf are designated "Zero-on-the-Meter" (ZOM) or "Zero Energy Building" (ZEB), energy balancing guarantee is dependent on an average thermostat setting of 20 °C and on heating the 150 litres hot water storage tank once every 24 hours. The houses in Vriendenerf have been designed to minimize energy usage for heat generation. This has been achieved by three design decisions.

Design decision 1 – High insulation:

The houses in Vriendenerf are very well-insulated to minimize heat loss. The ground floors, outer walls and roof panels are have a heat resistance of 5 to 6m^2.K/Watt and the windows are of a high quality, namely HR++.

Design decision 2 – Innovative ventilation system

Each house is equipped with a "balanced ventilation with heat recovery" system. This system extracts the heat from the hot air in the house, from spaces such as the kitchen and the bathroom to name a few. Then it uses this heat to pre-heat the incoming fresh air from outside. This results in a 30% reduction in the heat energy demand of each house. This "balanced ventilation with heat recovery" is illustrated in Figure 4.6.

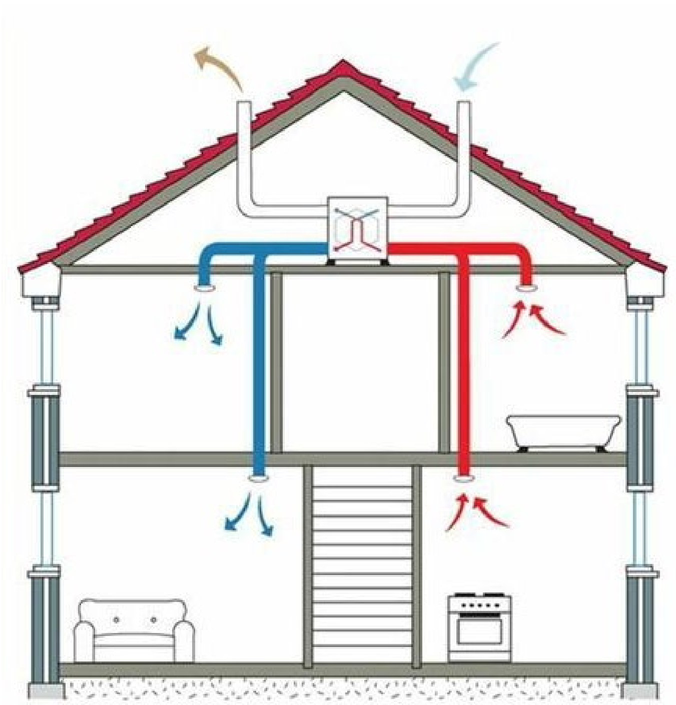

Figure 4.6: The "balanced ventilation with heat recovery" system implemented in each house

Design decision 3 – Heat pump and ground heat exchanger network

All houses have an innovative heat flow system as shown in Figure 4.7. This system consists of a heat pump which is connected on one end to a ground heat exchanger which acts as the heat source. On the other end, the heat pump is connected to an underfloor heating system which acts as the heat output as well as a hot water buffer tank of 150 litres. During the winter, heat is extracted from the ground via the ground heat exchanger and used for underfloor heating. Conversely, in summer, the heat from the underfloor heating is dissipated into the ground via the ground heat exchanger.

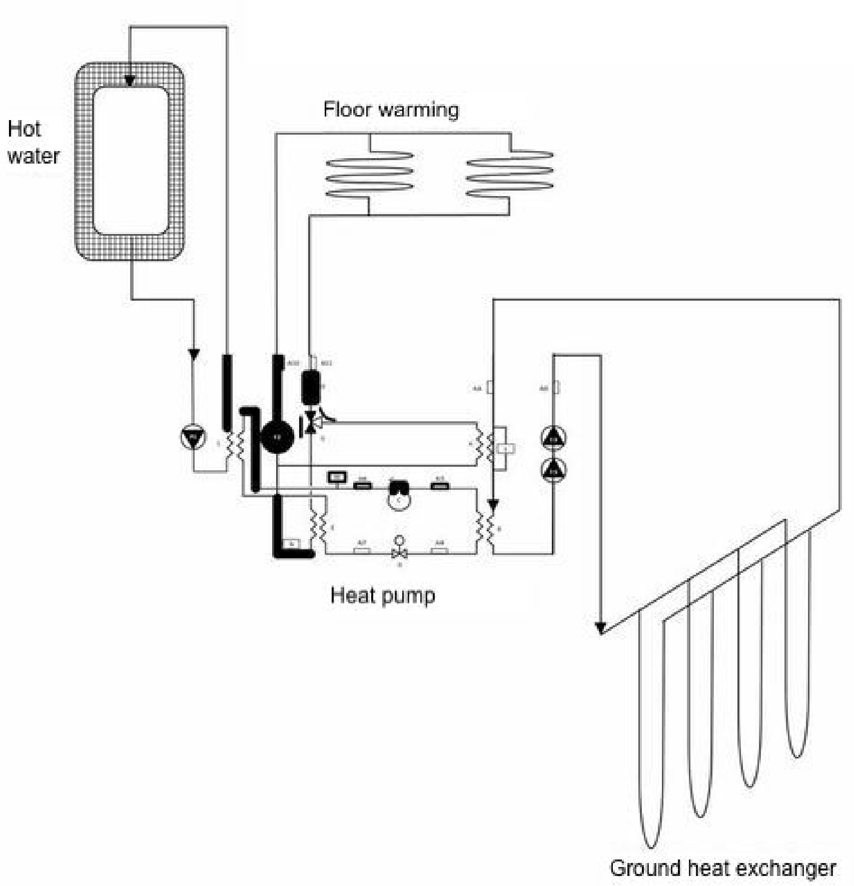

Figure 4.7: The heat pump, ground heat exchanger, warm water buffer tank and underfloor heating

Specific goals of Vriendenerf are as follows:

- Model heat-to-electricity systems and study their flexibility potential.
- Develop and demonstrate the integration of heat-to-electricity systems into a smart Energy Management Systems (EMS).
- Combine heat-to-electricity systems with batteries, electric vehicles and boilers to encourage a high-level of self-consumption within the energy community.

Opportunities for market integration

Peer-to-peer trading between customers and/or energy communities is not yet allowed, due to delayed implementation of the new Energy law in the Netherlands[7] The network operators, which are TenneT (Transmission system operator (TSO)) and local distribution system operators (DSOs) are working in cooperation with policy makers and regulation authorities to design and operate the power grid in several markets. As a result, DSOs are investigating new tariff schemes for residential users (e.g., a bandwidth scheme[8]) and also local congestion markets are expected to emerge soon. Multiple public

[7] https://www.rijksoverheid.nl/documenten/publicaties/2021/11/26/wetsvoorstel-energiewet-uht
[8] https://tweakers.net/reviews/10360/all/betalen-per-kw-vermogen-nettarieven-op-basis-van-bandbreedte.html

bodies (e.g., DSOs and Agentschap Telecom (Telecom Authority)) are investigating solutions to maintain a reliable grid and supply of energy under extreme conditions (e.g., weather, cyber-attacks). As a result, aggregators will not only need to play on the national energy markets, but also within the local domain in the future. Next to the new energy law, also new legislation on collective heat systems will be implemented in 2024, resulting in changes for the electricity-to-heat systems as well [Jet22].

The localized nature provides an opportunity to solve congestion issues regarding electricity-to-heat systems in a communal manner. Therefore, we explore cooperative demand side management methods for energy and flexibility sharing. Opposed to a competitive ecosystem, we bring together stakeholders in an equal playing field. The upcoming energy law, based on EU Directive 2019/944, provides the legal framework for this. Furthermore, with the upcoming law on collective heat systems, new opportunities for energy communities regarding heating systems emerge in the Netherlands. Hence, a trend is seen to more localized solutions where citizens actively support the energy transition through sharing of energy locally within communities.

Demonstrator use-case

The goal for the demonstrator is to actively contribute to the energy transition in the Netherlands and the decarbonization. Hereby, reducing stress on the grid is an important aspect. Given the playfield being in transition as well, a hybrid digital setup is required that can evolve over time, using the existing assets. The emphasis will therefore be on an intelligent EMS that utilizes heat flexibility with three important aspects and drivers:

1. The foreseen bandwidth model requires individual households to reduce their peak load. Hence, thermal flexibility must be used in cooperation with other smart domestic assets, such as electric vehicles and solar PV. Being individually in power is still important to inhabitants as well, regardless of their community efforts.
2. Energy may be traded among the members of community through new legislation and local market frameworks, such as Entrnce[9]. Also market integration could be an option, but has less priority for the community.
3. Congestion problems may arise in the Netherlands given the state of the electricity grid. Hence, it is expected that there may be demanded reduction of electricity use at times as indicated in USEF's red phase [USEF21]. To this end, external requests, so called *energy modii*, will be developed.

In order to execute this, the control system should have a layered structure, where both the individual households can set their own preferences and which can adhere to local (bandwidth) limits. A communal layer is required to coordinate the community efforts on a higher level of the grid and ensure community energy is used to trade on energy markets (be it global or local). On this level, requests from grid operators to temporarily reduce electricity use should also be incorporated. Hence a distributed consensus system seems a logical structure for this demonstrator.

[9] https://www.entrnce.com/communities-trading-energy

4.3 Poland

Local context

Predominantly, the Polish media marked is dominated by relatively low numbers of some local companies that are providing the media for the domestic use. At the Estate, where the demonstrator is located, there are a few city grids available, that provide utilities for the inhabitants. These are:

- Water, operated by Aqua Sopot S.A.
- Sewage, operated by Aqua Sopot S.A.
- Gas, operated by PGNIG
- Heat, operated by GPEC
- Electricity, operated by Energa Operator
- Telecom, operated predominantly by Vectra and UPC

The grid of the utilities is available in the summary scheme in Figure 4.8; separate images are available in Deliverable 7.1. The main goal for this investment and modification is removal of the heating gas from the estates

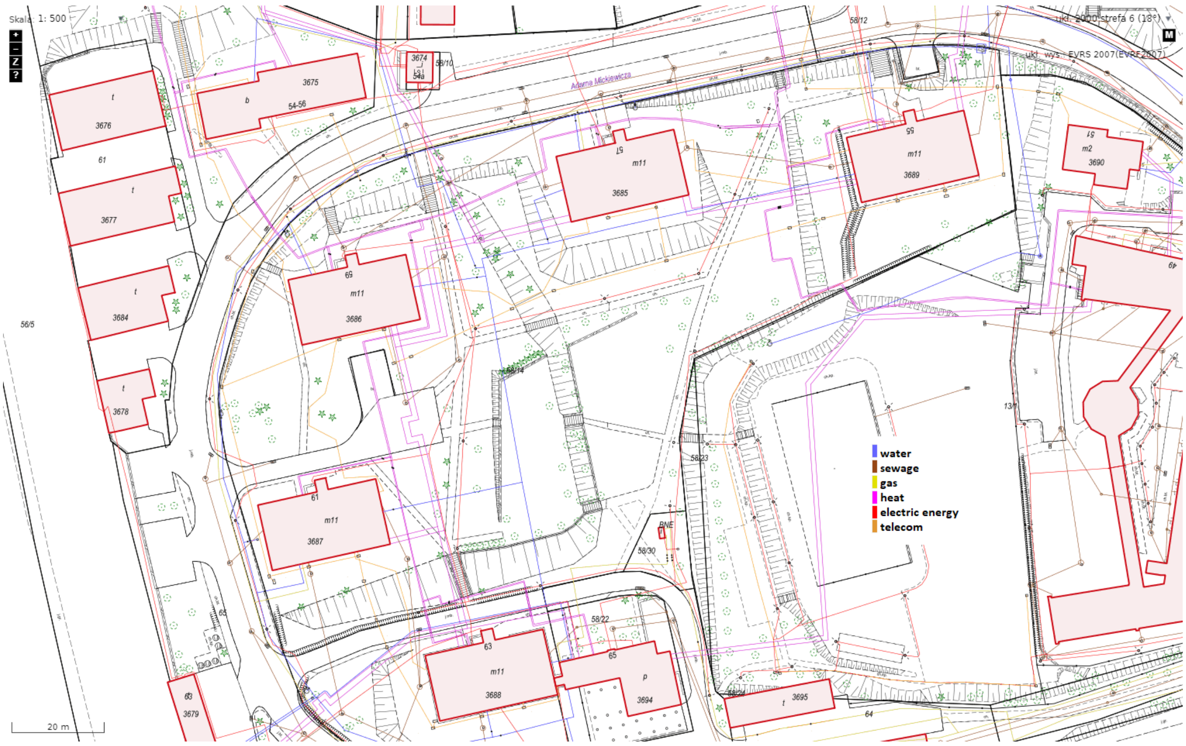

Figure 4.8: Grid of media lines available at the estate; colours according to legend, scale 1 : 500

Opportunities for market integration

There are few possibilities for the energy delivery to the buildings such as the demonstrator: either through the municipal network or by local in-house installations. This is a special case for the heating system, where in Sopot the energy can either be delivered from the municipal network (as in case of the polish demonstrator) or can be provided by local boiler houses belonging to particular estates or boilers that provide heating for particular buildings. In either case, the diversification of the energy sources (e.g natural gas or electricity) as well as having some independence would have become an added value.

Since the heating is outsourced completely, the only possibility to contribute to towards that energy would be on-site electricity production for either power electrical heaters or the natural gas boilers that still require an outsourced gas. It is desired in long term to replace the natural gas completely as it is neither a “green” nor a “safe” energy carrier.

Demonstrator use-case

The demonstration activities in Poland comprise of the following activities and/or objectives:

1. Concept and installation of measurement systems for data gathering of electrical grid, heat systems and water.
2. Development of the local “energy island” concept, with community members engagement, techno-economic analysis and financing structure of such initiative.
3. Installation, demonstration and testing of technologies for local electricity and heat production, EV (electric vehicles), energy storage and management for energy efficiency and increase in share of local RES, visibility and flexibility of the power grid.
4. Development of legal solutions and business models for the proposed technological and organizational solutions enabling their development and dissemination.

The Energy Management System for Polish case is designed to acquire electrical data from distributed energy resources and control energy storage system, V2G charging station and heat pumps. These energy resources and loads are placed in different locations around the housing estate. Because of that, the EMS system is designed as a decentralized, cloud-based system.

Server-site service is the heart of the overall EMS system, performing the vast majority of calculations (prediction, optimization, aggregation, presentation), storing acquired data and provides end-user services, such as dashboards or remote control. Local iEMS controllers and global EMS (gEMS) service are communicated bidirectionally to exchange telemetric data and commands. This approach allows us to provide real-time balancing and overall flexibility for distributed energy nodes and easy expansion of the system as well.

The Global EMS (gEMS), see Figure 4.9, will be integrated with two local iEMS controllers. Every iEMS individually control electrical system integrated behind the meter. In this case systems will consist as follows:

POC 1 (EV):

- Bi-directional EV charging station
- Energy Storage System

POC 2 (Mickiewicza 59):

- Loads: elevator and public lighting
- Heat pumps
- PV installation

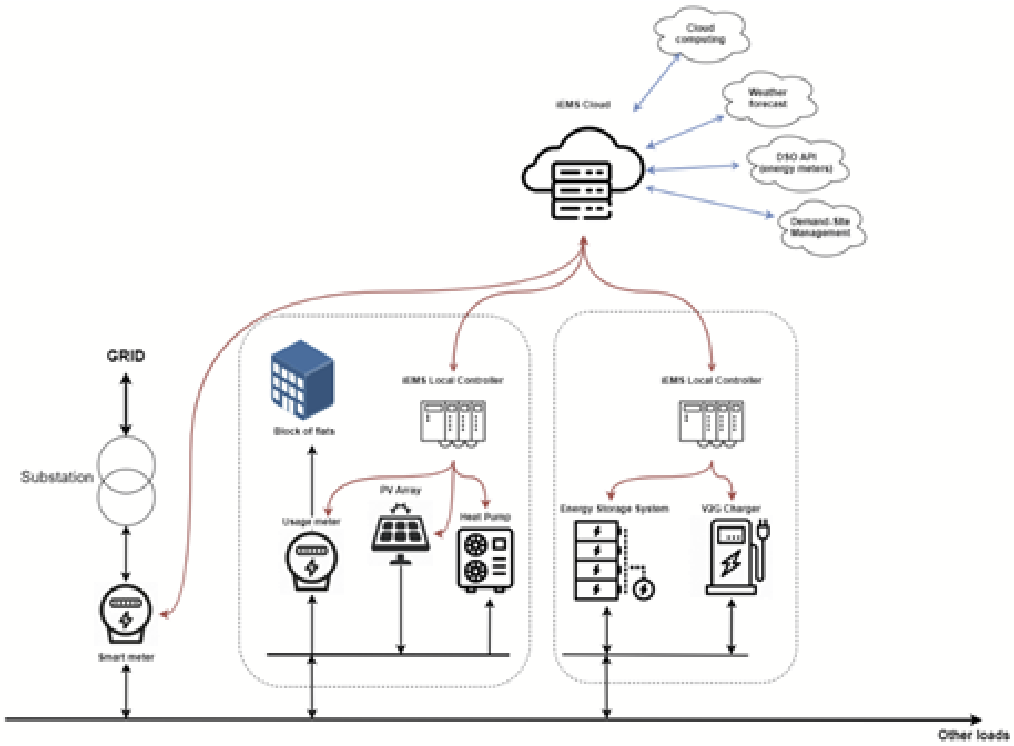

Figure 4.9: Planned topology of electrical and IT system.

Originally the installation of a Vanadium Redox Flow battery was envisioned for the Polish demonstrator, but this was unavailable. Originally an energy storage system with a power of 5kW and capacity of 30kWh was deemed to be sufficient to demonstrate the required features. In this case, since the VRFB battery technology is not available, a switch to a Li-Ion based energy storage system has been made with a higher installed capacity, a similar usable capacity, and comparable lifetime of the energy storage system. In this case it has been assumed the ESS with installed capacity of 50kWh Li-Ion battery working at 80% DoD will reach similar capacity requirement as assumed originally with the VRFB battery. Also, the lifetime of such a battery will meet the project's requirements.

The additional benefit of such a battery selection is the possibility to increase the power of ESS up to 20kW. This will impact the flexibility of the system and add additional demonstration features to the SUSTENANCE project.

The Global EMS system is designed to provide features, such as:

- **Peak shaving**: ESS will be able to store energy produced by PV and discharge during peak demands. The aim is to perform energy flow forecasting to provide optimal charging and discharging scheduling and to reduce time of deep discharge and full charge of the ESS. The algorithm therefore takes battery degradation into account.
- **Peak shifting**: The heat pump working schedule can be fitted into forecasted PV peak production to maximize self-consumption in the microgrid.
- **Minimization of energy costs:** Through this feature the EMS can store energy during the energy price valleys to minimize energy consumption when energy is expensive.
- **EV charging support** – ESS can be used as a support to provide EV fast charging even if AC grid power will be not sufficient to supply the charger.

- **Taking part in global DSM**: Thanks to the global iEMS, the whole system can be part of DSO Demand-Site Management and deliver services such as energy demand reduction.
- **Island mode**: (on local iEMS level) The system could be set up as an energy island to provide off-grid power supply for selected loads. These loads could be supplied from energy storage and EV battery, thanks to the V2G possibilities.

4.4 India

Grid management in India started in the sixties and was done on a regional basis. Each state's electric grid was inter-connected to that of the neighbouring states thus forming a regional grid [10]. 5 separate regional grids existed, namely, Northern, Eastern, Western, North-eastern and Southern regions. In 1991, the first efforts were made to connect these regional grids to one single national grid. By 2013, all the 5 regions were connected and a single synchronous national grid operating at 50Hz (tolerance band 49.5Hz - 50.5Hz) emerged. India has a total installed capacity of 411.6 GW (January 2023) with around 106 GW from wind and solar power. In India, air-conditioners (ACs) are responsible for a major share of the load. Letschert et al. [Let12] estimate that by 2030, the total electricity demand from ACs would increase to 239 TWh/year, translating into a peak demand of around 143 GW. The construction of nearly 300 new coal fired plants for 500 MW each would be required to meet his huge demand if the additional AC load is to be met from coal-based sources only. With an increasing number of heatwaves pushing the temperature to and above 40 °C, the International Energy Agency expects India to account for one third of total worldwide AC sales by 2050[11]. Phadke et al. [Pha13] state that by focusing efforts on improving AC efficiency, this electricity demand can be reduced by up to 40%, equivalent to avoiding the construction of 100 new power plants. Therefore, there is a critical need for research into efficient HVAC systems and the implementation of demand side management approaches to reduce the share of ACs in the residential and industrial load in India. While AC load forms a significant proportion of heat heating/cooling load, heat demand by industrial load also constitutes a reasonable share of the overall heating load.

4.4.1 Indian Demonstration:

In the Indian demonstrations under the SUSTENANCE project, multi-Utility Heat Pumps for rural applications will be capable of flexibly handling multiple utilities. The cooling requirement can be decoupled with the heating or drying requirements with respect to time by suitably integrating thermal storage on cold and/or hot sites. Multi-Utility Heat Pumps for Rural Applications can make the local processing of agricultural produce economically attractive, because of the high overall coefficient of performance (COP), while cogenerating cold and hot utilities. It can also add value by drying the excess produce when the market realization is low. These small capacity units can be deployed in rural households and can serve many applications. They can help reduce post-harvest losses and contribute to the improved cold chain. They will also enhance the livelihood of small and marginal farmers.

IITB is developing a customised multi-utility heat pump for various applications in Barubeda site in Jharkhand state. The villagers have a reasonable number of cows, however, due to a lack of adequate storage/chilling facility, cow milk is largely underutilised and limited to only household consumption,

[10] https://www.powergrid.in/one-nation-one-grid
[11] https://www.iea.org/data-and-statistics/charts/global-air-conditioner-stock-1990-2050

despite having the potential to supply milk to the local market. Further, vegetables grown locally cannot be fully utilised due to their low shelf life and lack of storage. The multi-utility heat pump being developed by IITB for Barubeda site is expected to help the village inhabitants in drying and storing the vegetables, see Fig. 4.1. Based on the applications of multi-utility heat pump in Barubeda site, it is expected to act as a flexible load to the local Sustainable RE based energy system, and hence help in better and effective utilisation of renewable energy.

Fig. 4.1 Multi utility heat pump for agro produce drying

5 Control and optimization methods

The focus of this chapter is on the model and methods for optimization and control over heating devices. First on individual level, then on community level.

5.1 State of the art control methods

This section outlines control methods applied in both practice and those studied in scientific literature. These control methods range from reactive control, i.e. react on observations, to model-predictive based type of controllers. In this context, it is important to estimate the state of the system as often not variables required for control can be assessed directly though sensors. For model-predictive control, it is important to also estimate and forecast the future. Furthermore, (a collective of) controllers can work stand-alone or jointly coordinated. To this end we first describe agent-based control concepts to provide a theoretical framework in which we can place other concepts.

Agent-based control

Within control theory, agent-based control is a well-established concept. As control systems may become quite large, especially in the field of smart grids, it is important to add structure to the system such that subsystems can be developed stand-alone but be integrated in the larger system. An agent represents a control algorithm that optimizes the behaviour of a set of actuators. It does so based on external inputs, which could be information through ICT systems, but also preference of the end user. Based on this input, and the current state, it controls the actuator(s) accordingly. The advantage of this concept is that models are created locally and also information is stored and processed locally.

In a local setting, in which there is no communication with external systems, the system works fully autonomously and only within the local context. This is typically the case for a house thermostat system, in which the thermostat controls the heating system and sometimes the generation of domestic hot tap water based on predefined setpoints by the end-user. However, for electricity-to-heat integration, these systems need to evolve into an agent-based system that takes external *stimuli* into account, such as electricity market prices. Hence, systems need to make trade-offs between comfort for the end-user and overall system efficiency.

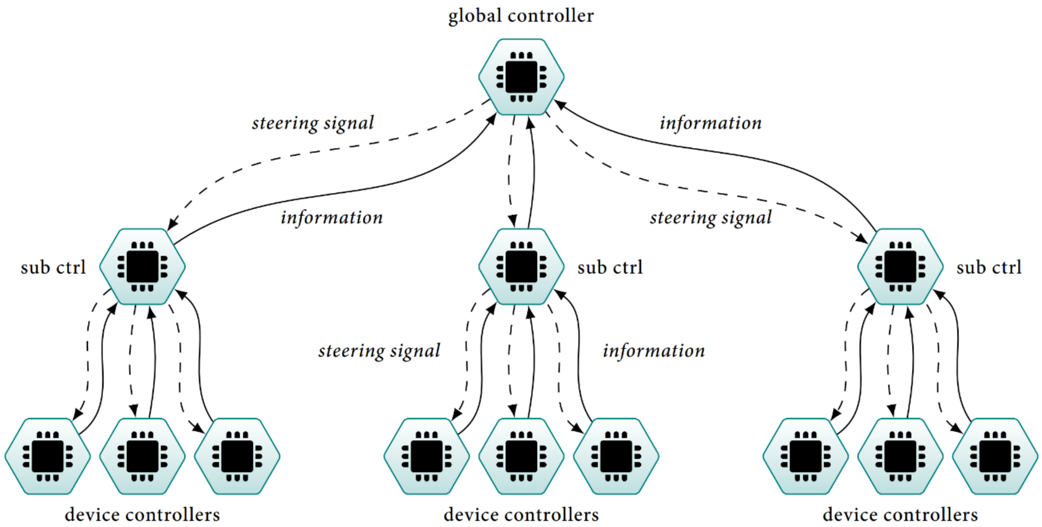

Figure 5.1. A multi-level agent-based system with bi-directional communication [Hoo17].

Herein one can see the external stimuli or steering signals as coming from another agent (see Figure 5.1), namely a higher-level steering agent that indirectly controls by influencing the lower-level decisions. Hence there is no direct control over actuators as such, but rather device agnostic signals are used to change the behaviour of lower-level agents. This level of abstraction with generic flows of information allows the system to become scalable and allows to easily integrate new technologies. Furthermore, information and models of the actual assets can remain within the low-level agents, hence complexity is limited as higher-level agents are not required to know and process this information.

Next to only sending out steering signals, a higher-level agent could also be coordinating its children. Likewise reading of sensors, lower-level agents may also provide information back, such that the higher-level agent can make informed decisions or perform coordinating tasks. Within this context, Transactive Energy [Gri15] is well known, in which bi-directional communication is leveraged to ensure that the response of lower-level agents is known to certain stimuli. This can be implemented using e.g. an auction model, and allows for the coordination among agents to ensure that steering signals do not lead to overreaction and system instability. This concept works for both reactive observation-based control as model-predictive and optimization based methods. Essential in both cases is to clearly define how and what information has to be exchanged, i.e. an interface definition is required. Note that these agents not necessarily need to be executed on a specific location and computer system. Instead, they may also be centralized in separate processes, yet they define a structure that is easy to extend.

Dynamical model fitting

This section discusses literature on models and methods to accurately estimate the state of a system when certain model inputs are not known due to lack of sensors. Furthermore, it describes literature to forecast energy demand based on e.g., historical data and weather forecasts.

One of the important aspects of predicting what will be the load is the need for forecasts on the weather. The heat demand for the upcoming period can in theory be determined using weather forecasts, a sufficient model of the thermal envelope of buildings, and aspects of user behaviour and their desires. Many meteorological institutes provide weather forecasts and often here is not the bottleneck to predicting the heat demand. However, solar irradiation is an aspect that may be more problematic. Solar irradiance has a large impact on the heating of households through the windows. Solar irradiation forecasting approaches fall in one of two categories; Dataset based approaches and Structure & Operation based approaches [Sing22]. Forecasting approaches based on datasets can be 1) time series dataset based or 2) meteorological/geographical dataset based or 3) a combination of these two approaches (hybrid dataset). With advancements in computing infrastructure, approaches based on structure and operation are finding frequent implementation as well. This category includes regression models, Markov chains, deep learning artificial neural networks (ANN) and support vector machines (SVM) based approaches. Specific examples of PV forecasting approaches are discussed in the next paragraph.

Prediction services such as Solcast[12] and Forecast.Solar[13] do provide data based on satellite images. In practical experiences [Nij22] they seem to be quite unreliable on cloudy days, however. There has been an increased application of machine learning and neural network models towards the problem of solar irradiation prediction, especially long short-term memory (LSTM) models. For example, Lee et al. [Lee18] propose a solar forecasting technique based on convolutional neural networks (CNN) and LSTM networks. Their approach can make accurate predictions with roughly estimated weather data and without requiring sophisticated pre-processing of the input data. The authors show that their CNN+LSTM approach out-performs traditional regression-based approaches for solar power forecasting. Simeunović et al. [Sim22] put forward two graph neural network models to achieve deterministic multi-site PV forecasting called the graph convolutional long short-term memory (GCLSTM) and the graph convolutional transformer (GCTrafo) for a forecasting horizon of 6 hours ahead. Both models outperform traditional regression-based forecasting methods, showing promise for deep learning approaches in the field of PV forecasting. Utilizing live data from solar panels seems to open the possibilities to improve the predictions [Len22].

The thermal envelope of a household is just as important. Van Leeuwen [vLe17] has researched methods to learn the thermal envelope by using a grey-box model and applying linear regression methods. This seems to be a quite acceptable method, but so far is only tested in simulation. Other grey-box learned models are considered by Sonderegger [Son78], who determined parameters using measurements of a single room together with electric heaters. On a similar vein, Saurav and Chandan [Sau17] put forward a grey-box approach for modelling a building. Their approach categorises building components as either those connecting the building to the thermal grid (“primary-side” components) or those contained inside the building (“secondary-side” components). Thereafter, the authors take a bottom-up approach by first, developing the models for each component, then estimating the physics-based parameters appearing in the component models using data and lastly, integrating these completed models together to form a model for the overarching “building’ system. As mentioned in the previous paragraph, LSTM networks are also being used to achieve accurate thermal models. For example, Elmaz et al. [Elm22] propose a data-driven hybrid approach wherein a CNN-LSTM model is trained on simulation data (white-box model) and thereafter, the physical parameters of the model are refined using real-world data. The proposed model has a lower root mean square error (RMSE) in comparison with a black-box model. A very simple 3R1C model seems to be learnable and quite acceptable. Another method is applied by Madsen [Mad95] who uses a stochastic system identification technique. Here a 2R2C model is trained using a limited dataset.

These methods specifically look at the modelling the thermal envelope, but do not necessarily reflect the user behaviour. Instead of modelling the thermal behaviour itself, it could also be inferred from the reaction of control systems to heating devices. This however demands the control of a larger cluster of devices. Fink et al. put forward a time model a community with multiple heat pumps as a mixed-integer linear programming (MILP) problem and propose a global MILP approach and a timescale MILP approach to solve the problem [Fin15]. The global MILP approach creates a single large instance of the problem and calculates an optimal solution, it is impractical for real-world usage and not sensitive of future changes or alterations in the profile. In the timescale MILP approach, the authors address these

[12] https://solcast.com/

[13] http://forecast.solar/

problems, by proposing an offline approach wherein the *strictness* of the constraints is adjusted for future intervals. For example, the current interval *i=1* had the highest optimality requirement, while the next 2 intervals *i=2* and *i=3* have lower optimality requirements and the intervals *i=4*, *i=5* and *i=6* have even more relaxed constraints than *i=3* and *i=4* intervals. Fink *et al.* compare the 2 MILP approaches with a reference case of no control and show a peak reduction of 98% and 96% for global MILP and timescale MILP respectively.

Claessens et al. show that [Cla12, Cla13] cluster flexibility can be learned using reinforcement learning techniques under the assumption of repetitiveness. Urieli and Stone [Uri13] put forward a heat pump control agent based on adaptive reinforcement learning (RL) that aims to reduce energy savings while maintaining occupant comfort. Another approach is to track and learn from only a subset of devices, which are called tracer devices [Iac17]. It has also been shown that such models can also be utilized to forecast a flexibility trajectory [Sae22]. Ana David et al. [Dav22] show that optimal control can be achieved using a fully data-driven approach. This makes such machine learning models, based on grey- or black-box models also suitable for Model-Predictive control strategies.

Another way to overcome model errors regarding human behaviour is by making the control algorithm itself more robust to such errors instead of looking for better models [Kla16]. Fischer et al. [Fis17, Fis18,] have studied the control of heat pumps using the Smart Grid Ready interface. They conclude that with a large pool of heat pumps, it is not necessary to have insight in the state of a room and/or heat pump. Instead, controlling a random heat pump within the system seems to be just as effective. Lastly, an overview of heat pump control strategies as found in literature is shown in Figure 5.2.

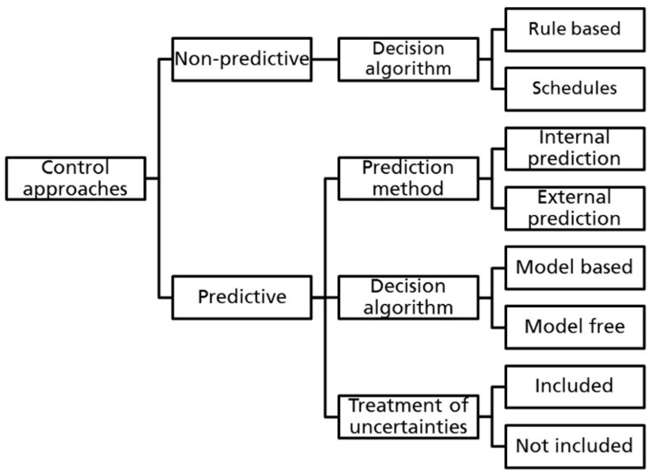

Figure 5.2: Heat pump control strategies as found in literature [Fis17a]

Twomes: real-world thermal envelope learning in practice

Real-world experiments with learning thermal envelopes by applying machine learning are conducted in the Twomes[14] project, in which we will zoom in in the next part. Twomes is a research project spearheaded by the Energy Transition research group of the Windesheim University of Applied Sciences in Zwolle. Estimating the heating parameters of any dwelling by conventional means, such as with a manual inspection by a heating consultant, is a time consuming, expensive and non-scalable approach.

[14] https://techforfuture.nl/project/twomes-digital-twins-voor-de-warmtetransitie/

The Twomes project aims to calculate the same parameters by acquiring weeks of data from the smart meter and the thermostat or central heating buffer of the dwelling by using open-source hardware-based data-sniffers attached at the aforementioned appliances [15]. For each dwelling, the Twomes hardware aims to use the acquired data to understand the characteristic heating factors of that dwelling. Each dwelling is defined by four characteristic factors, namely, the dwelling type, installation type, the thermostat settings and the comfort needs of the dwelling's residents[16].

Figure 5.3 shows the working of the Twomes project. Firstly, open-source hardware records weeks of information from the smart meter and the boiler. Secondly, this data is combined with meteorological data from KNMI and publicly available information about the dwelling. Lastly, analysis of all this data from the dwelling results in useful insight regarding the optimal thermostat settings or the possible (if any) advantages of installing a (hybrid) heat pump in that specific dwelling, to name a few. To summarize, the Twomes project aims to compile a digital heat-specific twin of a specific dwelling and analyse the same to optimize the heat demand and production of that dwelling.

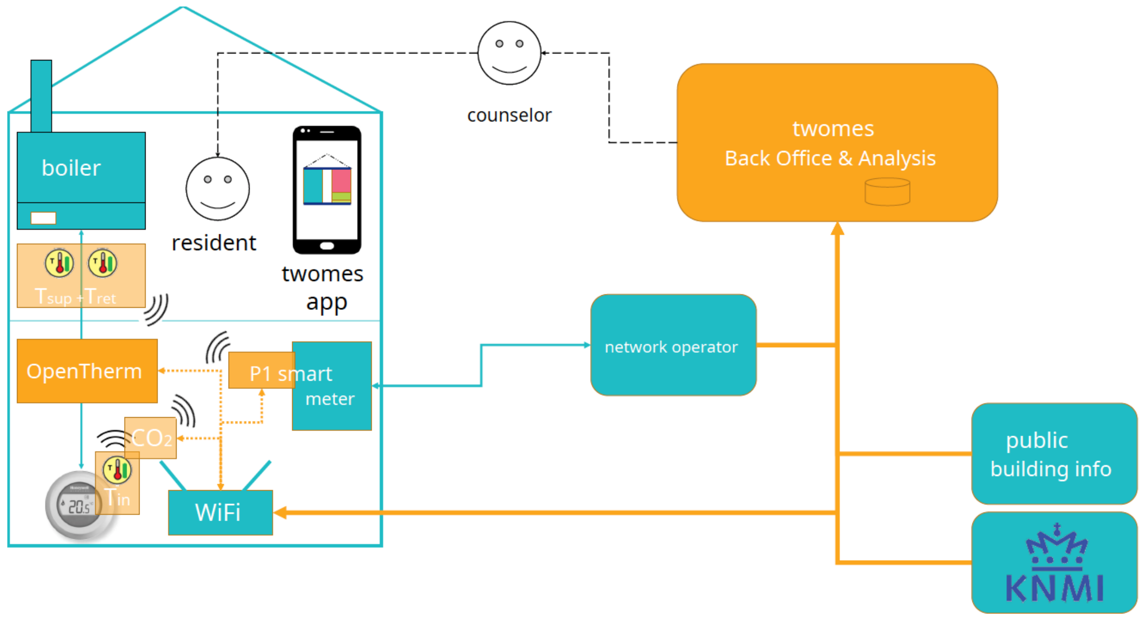

Figure 5.3: General structure of the data flow in the Twomes project

Existing optimization and control methods

This section describes existing control systems and standards found within households and heating systems. These can be seen as stand-alone agents that do generally not take into account external stimuli. Furthermore agent-based systems that react to external stimuli are discussed to the extent where it is done so without coordination and therefore only perform local optimization, but no global system optimization is performed. These systems currently exist and will remain to exist. In the scope of SUSTENANCE it is therefore also important to investigate how these systems can be integrated into aggregated and coordinated control schemes. From here on we move into the multi-level agent systems, leveraging the benefits of coordinated control by employing Transactive Energy through bi-directional communication.

[15] https://github.com/energietransitie
[16] https://www.windesheim.nl/onderzoekspublicaties/twomes-digital-twins-voor-de-warmtetransitie

For a long time we have had thermostats in our rooms to regulate the central heating system. Originally this system would open or close contacts depending on the indoor temperature and the setpoint. By closing the contacts, the heating system would turn on (e.g., a gas boiler). With the introduction of condensing boilers, boosting the efficiency over 100%, it became important to more intelligently control the heating system by reducing the supply temperature to the heating system, such that the boiler can operate withing its most efficient operating range. To this end, the OpenTherm protocol was invented. Currently, thermostats also implement self-learning methods to be able to optimally control the supply temperature, thereby minimizing the energy needs, while maximizing comfort by reducing indoor temperature fluctuations. It is shown that a 16.7% reduction of energy demand can be obtained when using an optimal control policy based on building models compared to a simple rule-based solution [Zha19].

With the advent of energy markets, external signals may intervene with this operation. However, unlocking flexibility still needs to go hand in hand with user comfort. A good source of flexibility for local systems is the use of hot water boilers together with a heat buffer. This buffer makes sure that user comfort is not compromised by the optimization. Machine Learning techniques can be used to learn from historical data. Research by [Mbu20] shows that double Q-learning can be used for local control of electric water boilers to minimize the operation costs and/or maximize the self-consumption of local PV generation. Real-world experiments using Q-learning to control domestic hot water boilers have been executed in [Som17]. Significant increases in self-consumption of PV-energy have been obtained.

Aggregated optimal control of heating devices

Unlocking flexibility seems to be more promising on an aggregated scale. This however requires some cooperation among the assets. This is possible with transactive energy, in which feedback is provided. One of the first solutions is the HeatMatcher [Boo13], which extended the PowerMatcher to control heat pumps in an on-line fashion using 3D bid-functions, more about that is explained in the following section. Coordination of heating devices using a similar auction based structure is considered in [Iac17], where tracer devices are used to infer the cluster flexibility. This makes the system more privacy friendly, as bi-directional communication is not required for each and every heating device to be able to adequately control the heating system. Another way is direct control, in which one system decides which heating device should change its state. An example of this are the Smart Grid Ready interface experiments by Fischer [Fis18].

Another method is by utilizing generic mathematical solvers to solve e.g., (Mixed) Integer Linear Programming problems. Van Leeuwen et al. [Fin16] have employed a Mixed Integer Linear Program (MILP) model to optimally schedule heat pumps 24 hours ahead in time. However, this system is found to be quite computational expensive. Therefore, they came up with a different approach based on earliest dead-line scheduling first, based on user comfort [Fin15]. This latter heuristic seems to perform nearly as good, at a significant lower computational cost. Combined optimal operation of HVAC systems across multiple microgrids is investigated in [Hus17], resulting in over 40% cost reduction compared to the situation without coordination.

Overall, it seems that just utilizing general solvers for mathematical formulations do not yield the desired scalability. Therefore, [Vay14] uses dual composition methods in energy management to spread the workload and achieve scalability. Another method that has gained recent attraction is the Alternate Direction of Multiplier Methods (ADMM) [Boy11], which allows optimization problems to be split up and distributed, whilst maintaining strong mathematical proofs. ADMM is also tested in practice with batteries, which provide similar buffer-type flexibility, by Reijnders et al. [Rij20]. A distributed method based on Dynamic Programming is presented by Bosman [Bos12], called Iterative Distributed Dynamic Programming (IDDP). However further analysis. Toersche [Toe16] has applied this model and compared it to another well-known method, namely Danzig-Wolfe decomposition [Dan16] and Profile Steering [Ger15], of which the latter shows to give good results, albeit with a longer computation time.

Profile Steering [Ger15] is a heuristic that is especially useful when the objective is to schedule the aggregated power profile ahead in time rather than directly optimizing for prices. It sends out a desired profile spanning multiple time intervals into the future, to lower-level agents, which respond with the profile that they can attain. Iteratively new profiles are generated and accepted based on their improvement, measured as the Euclidean distance between the proposed solution and the desired profiles. Iteratively devices react and improve the overall profiles, while the highest-level coordinating node ensures that grid capacity constraints are being met. Originally the scalability was limited, but this has been lifted by Hoogsteen et al. [Hoo18] in later work. Furthermore, by replacing the steering vectors by matrices, it is possible to simultaneously optimize for multiple energy carriers [Sch17], [Hoo20] in hybrid-energy systems. The methods can be used for offline scheduling, but also for online control by utilizing partial optimization whenever significant events happen to the system [Hoo17a].

Van der Klauw et al. [Kla16] have used the Profile Steering method to efficiently coordinate the operation of HVAC systems. Similar observations were obtained with a simulated neighbourhood consisting of 16 houses that try to minimize their electricity import. De Goeijen [Goe19] used a hybrid approach in which a MILP model is used to optimally control multiple heating assets linked to a large seasonal heat buffer. Since the model was too complex to be solved at once, the seasonal patterns were captured first, and subsequently used as blueprint to optimally control the heating assets on the shorter timescale, which was solvable.

Real-world experiments with aggregated flexibility of heat pumps are conducted in the Houthaven HeatMatcher project, in which we will zoom in in the next subsection. Herein, flexibility is aggregated through demand functions. Another concept, called FlexOffers, also communicates aggregated flexibility in a more sophisticated way, which will be presented afterwards.

Houthaven: HeatMatcher real-world heat pump control experiments

The increasing number of device options has led to an increasing control space of variables which cannot all be optimized by the custom (and device-specific) climate control systems of Honeywell or Itho Daaldedrop. TNO attempted to fulfill the need for a general distributed energy management approach with a hierarchical multi-agent system called Heatmatcher (HM) [Boo13, Put18]. Based upon the methodology of the Powermatcher [Kok13], Heatmatcher was built on three principles. Firstly, openness, which is the ability to integrate all distributed energy resources into the control algorithm. Secondly, scalability, which is the ability to connect an ever-increasing number of devices, representative of an increasing residential heating network. Lastly, privacy, which is the ability of the device owner to retain full ownership over the working of their devices.

In HM hierarchy, at the lowest level, each device such as a solar panel, gas boiler or heat pump, to name a few, has its designated *device agent* which proposes a bidding curve on its behalf. The agent's bidding curve represents how much money that specific device is willing to pay for how much energy. Some examples of bidding curves are shown in Figure 5.4.

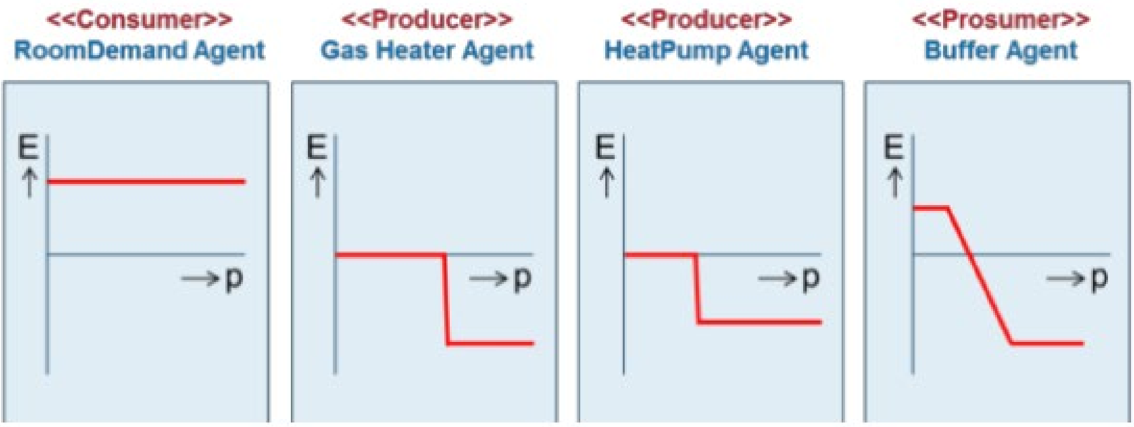

Figure 5.4: Example heat bidding curves for some agents. Heat supply is shown as negative demand in these curves [Put18]

After the device agents come up with the bids for their respective devices, a *concentrator agent* does its job of aggregating the bids of physically closely located device agents [Kok13]. The concentrator agent then sends the aggregated bidding curve upwards to the *auctioneer agent*. The auctioneer agent receives the bidding curve from each concentrator agent cluster, determines the market clearing price and returns this to the concentrator agents, who in turn, pass it down the hierarchy to their respective device agents. The market clearing price is determined using linear programming (LP) as the point of minimal mismatch between the demand and supply of energy while conforming to grid constraints. It is important to note that the bidding curves act as an abstraction, keeping the device-specific details hidden from agents. This retains full ownership of the device's working with the device controller and ensures privacy.

Flex-offers aggregation framework

As part of the MIRABEL project, Bach Pederson et al. [Ped18] put forward an efficient and scalable format that approximately represents flexibility information per device called Flex Offers (FO). There are many advantages in using FOs. Firstly, they are capable of handling state-dependent loads such as heat pumps and grid constraints such as congestion bottlenecks. Secondly, FOs can be applied to convey flexibility information about a number of devices (are device agnostic) and also support aggregation and disaggregation operations (scalability). Lastly, a price component can also be encoded into FOs.

Figure 5.5 shows how a FO for a single device (for example an electric vehicle) looks. Each FO consists of two types of flexibility. The first is *amount/energy flexibility*. This flexibility is encoded on the y-axis. Each bar represents a time slice of energy consumption for that device. a_{min} represents the minimum amount of energy the device needs in that specific time slice to be able to provide its service. The variable a_{max} *creates an interval* within which the device can adjust its energy consumption while fulfilling working constraints (such as the maintenance of a comfort temperature for a heat pump). The second type of flexibility information is *time flexibility*. This flexibility is encoded on the x-axis as the time interval within which the device can operate. The earliest possible start time for the device is represented by t_{es} and the latest possible start time by which the device must start is represented by t_{ls}. Lastly the latest possible end time for the device is represented by the variable t_{le}.

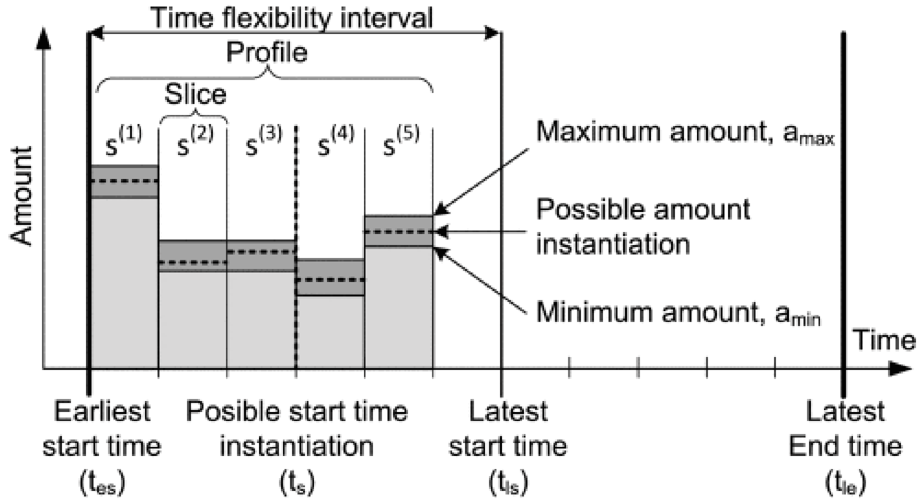

Figure 5.5: Representation of a simple FO for a device. Energy (flexibility) is represented on the y-axis and time (flexibility) is represented on the x-axis

Definition of a Flex Offer (FO):

A *FlexOffer f* is a tuple *f*=([*tes*,*tls*],*p*) , where [*tes*,*tls*] is the start time flexibility interval and *p* is the amount profile. The time is discretized into equal-sized units, e.g., 15-minute intervals. Thus, we use *tes*∈*N* to specify the earliest start time and *tls*∈*N* to specify the latest start time. The *p* is a sequence of slices ⟨*s*1,…,*sd*⟩ , where a slice *st* is a continuous range [*emin*,*emax*] defined by the minimum *emin* and maximum *emax* energy bounds, and *d* is the number of slices in *p* .

$$Total\ energy\ flexibility\ for\ device\ d_i = \sum_{t=1}^{t=d} (a_{max} - a_{min})_t$$

$$Total\ time\ flexibility\ for\ device\ d_i = \ t_{ls} - t_{es}$$

There are 7 stages in the life cycle of FOs explained in Figure 5.6 [Ped18].

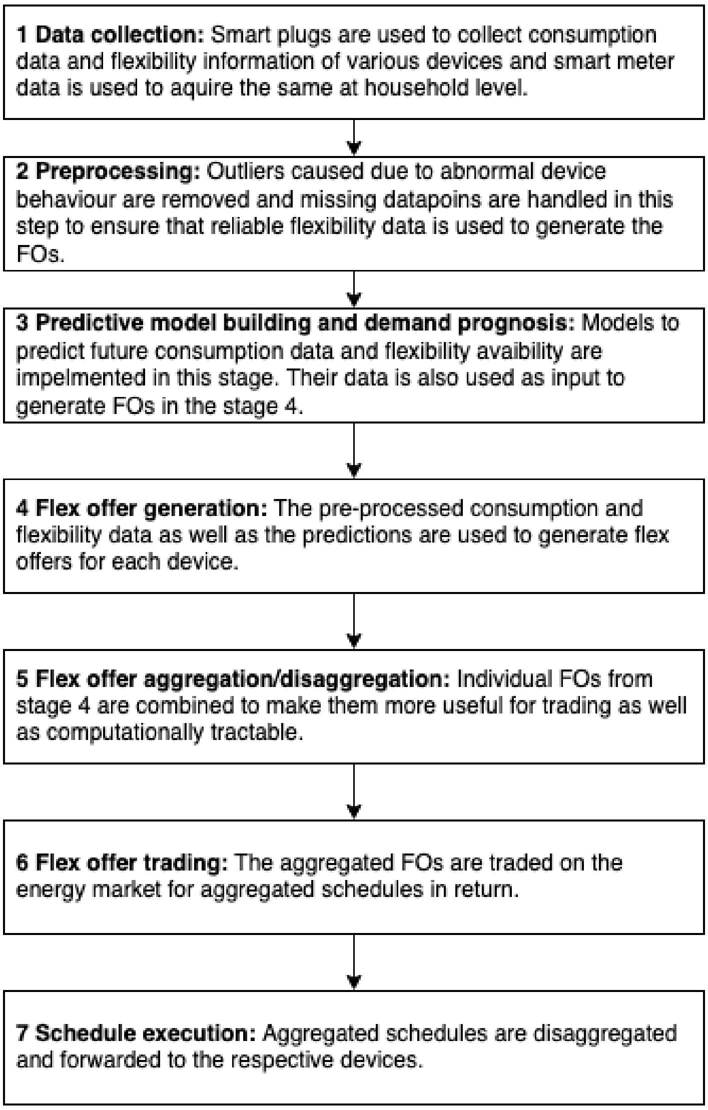

Figure 5.6: The 7 stages in the life cycle of an FO. The cycle starts with data measurement at device and house level and ends with the assignment of a schedule to the same

Existing electricity system integration

Currently, DSOs are aware of the potential power quality and congestion problems within local distribution that result from the electrification. This has led to an increase in efforts, lobbying and literature on potential technical solutions that also require a legal framework. In this light, both USEF [USEF21] and the traffic-light concept proposed by BDEW [BDEW15] serve as a possible techno-legal framework in which DSOs have the opportunity to influence the market and/or directly change the power consumption of assets to avoid grid problems and to ensure a safe and reliable operation.

Within the context of electricity-to-heat systems, the so-called "Smart Grid Ready"-standard [Fis17] for heat pumps is developed. Herein, a signal can be sent by the DSO to reduce the power consumption by maintaining a lower temperature. Also, an increase in power consumption is possible in times of local (over)generation of electricity through pre-heating, generating and buffering hot tap water. Currently, Germany is looking into adapting the law to legally allow DSOs to intervene and change the power consumption of heat pumps [Bar22]. Potential integration of the OpenADR [OADR17] communication standard in Europe is also envisioned.

Within the Netherlands, initiatives to locally control heat pumps in an aggregrated way are limited to pilot sites. An example is *Houthaven* [Boo13], where the HeatMatcher was tested in practice to reduce the load of an apartment building. The USEF framework is tested in the neighbourhood *HoogDalem*[17] in Gorinchem. More recently, a collective floating house, Schoonschip[18], in Amsterdam is connected using one grid connection and its heat pumps are controlled using a smart grid.

Also, more and more utilities and aggregators are starting to see the benefits of offering smart domestic hot tap water boiler systems for their customers. Essent started with experimenting in the Netherlands with the introduction of smart boilers in 2017[19]. Other utilities followed later, such as Eneco in 2019[20]. A study with potential of utilizing residential flexibility in the Nordic countries has been executed, yet many barriers still arise[21].

Outside Europe, direct control of HVAC systems is already employed for more than a decade. Especially in the United States, control over air conditioners, but also HVAC systems through smart plugs or direct control through smart thermostats is already used. In some states, e.g. California and Texas, there are markets in which aggregators and utilities help in balancing the electricity grid using aggregated control of HVAC systems, such as Leap[22].

5.2 Communal coordination of smart integrated heating systems

Based on the previously introduced literature on energy management and control strategies, together with the modelling and the situational context within SUSTENANCE's demonstrators, we can draw out a system architecture. This section merges all aspects and sketches a modular integrated system, utilizing aforementioned models and algorithms, that can be used as basis for the demonstration sites and market integration, both within the current markets, as well as an outlook for potential emerging markets.

Context and objectives

The communal context is central to the SUSTENANCE project. We find common grounds for the different demonstrator sites and their respective countries based on the findings and market outlooks. With regard to market opportunities and integration of flexibility of electricity-to-heat system, we see 3 major opportunities:

1. Both Denmark and the Netherlands have seen an adoption of dynamic prices within the energy sector as stimuli for consumers to change their behaviour on an individual level. This necessitates the inclusion of smart control for electricity-to-heat devices, such as heat pumps as their electricity consumption forms a major part of the energy bill.

[17] https://www.usef.energy/app/uploads/2017/07/Publieksbrochure-Hoog-Dalem-2017.pdf
[18] https://greenprint.schoonschipamsterdam.org/impactgebieden/energie
[19] https://www.installatie.nl/nieuws/proef-met-slimme-boiler/
[20] https://nieuws.eneco.nl/slim-apparaatje-bij-boiler-vangt-pieken-wind--en-zonnestroom-op/
[21] https://www.nordicenergy.org/wp-content/uploads/2017/12/Demand-side-flexability_-DSO-perspective.pdf
[22] https://www.leap.energy/

2. Moreover, we see the emergence of potential congestion problems in the electricity grid in all four countries. Hence, it is expected that the local state of the grid will form a factor to which control systems also must react. The exact implementation is yet highly uncertain, whether it is a time-varying capacity tariff, locational marginal pricing, or a (dynamic) bandwidth model. Nevertheless, local congestion markets are necessary to safeguard the security of supply to customers within the electrification and as such market opportunities are expected to arise. Ideas and concepts have been proposed previously in USEF and experiments with Smart Grid Ready interfaces to avoid congestion are already conducted in Germany. For this, next to market integration, it is important to monitor the grid state and intervene accordingly.
3. Lastly more imbalance is expected in the market due to volatile production of renewables. A supplier might be able to further reduce electricity bills if it can utilize flexibility to perform portfolio balancing utilizing the (passive) imbalance market. Progressive suppliers in the Netherlands, especially those with dynamic tariff energy plans, are already looking into possibilities to do so with their customers as they see market opportunities. This field, however, is new and it is not clear how this will take shape.

These highlight the potential markets for electricity-to-heat flexibility to be integrated, to create value, and to deliver cost savings to customers, while ensuring security of supply with increased shares of carbon-free sources. Overall, it is observed that the price of energy, and even more so fuelled by the war in Ukraine, is the main driving factor for the communities in SUSTENANCE, as well as in broader perspective. In essence, this boils down to the following objective:

Minimising the net cost of importing energy for the community

Herein, community is an important factor as customers are jointly connected to a section of the grid. Hence there is a collective interest in avoiding high grid loads, which could lead to congestion and additional price spikes in one of the (future) energy price components. Thus, next to only an individual driver (e.g., dynamic tariffs), there will be a communal component as well.

Next to this more economic objective, the SUSTENANCE project also aims predominantly on maximizing the utilization of carbon neutral sustainable energy by utilizing the inherent flexibility of devices, including electricity-to-heat systems. This is key for all the four demonstrators and can be achieved on different levels, with their own respective priorities and local context and (economic feasible) possibilities. These are, from high priority to low:

- Strive for a 100% autarkic operation of the local grid, where all energy is sourced locally from RES in combination with (seasonal) storage;
- Maximize the utilization of locally generated electricity within the premises of a customer, or on the community level (or both);
- Utilize energy from the main grid when the carbon emissions are low.

All of these can be fit in the original objective. In fact, in many cases they are (or will be) reflected in the cost of energy. Low day-ahead prices to some extent already coincide with low carbon emissions from the national grid's energy mix (but not always completely [Hoo22]). Feed-in-tariffs are plummeting and subsidies are reduced for PV, resulting in the urgency to utilize self-produced electricity directly for cost efficiency. Furthermore, dynamic capacity tariffs may arise, steering towards local (autarkic) use of energy. Even if markets are not (yet) in place, they may still be inserted in the cost function, allowing to dynamically add these factors per demonstrator and hence keeping the framework flexible enough to fit all needs.

Lastly, these goals are overarching for SUSTENANCE, hence the electricity-to-heat systems must integrate with an overarching control structure in which other devices also play a role. These systems must be integrated in a coordinated energy management system where electricity-to-heat systems form a symbiosis with other devices, such as electric vehicles and battery storage assets, to achieve the general objective for SUSTENANCE.

System architecture and system integration

Given this context, it immediately becomes clear that there are at least two layers upon which must be acted: Global perspective(s) and local perspective(s). This forms a cornerstone for the system architecture for electricity-to-heat integration. Furthermore, there are different data streams and interfaces upon which an energy management system can act or interact. As observed, interactions are expected to be predominantly coming from the electricity market. An important interface is that with other devices within the energy system and the energy management system as a whole, which is topic of other SUSTENANCE deliverables.

In this regard, we envision a modular system where the electricity-to-heat systems are integrated in a decentralized energy management framework and co-exist with other flexible devices in parallel. This section presents the local and global perspectives, their roles, and interactions.

Local perspective

Given the perspectives, it is then logical to have a local Home Energy Management System (EMS) controller that allows for local coordination among the devices within the local domain (see Figure 5.6). This domain could be for instance a household, building or community. Similarly, to the hierarchical structure as presented with the Profile Steering approach, different local levels are an option here too. This allows us to maintain flexibility across different implementations and nuances. A generic method and/or framework to exchange flexibility, such as FlexOffers, profiles (such as in profile Steering), EF-Pi or USEF is required here to ensure interoperability and the flexibility to integrate other devices in the future.

The local level therefore also includes the devices embedded in devices and had access to the local information. This information may be privacy sensitive, such as personal preferences (e.g. thermostat setpoints and operation schedules). The local level by design adds a layer upon which local processing and anonymization can be achieved. External data, such as weather forecasts and electricity market data can be retrieved. Combined with local models and machine learning techniques, local optimization of local assets can be achieved according to the models presented in Chapter 3 and the optimization methods from this chapter. Within this context we assume that all information and data communicated within the system is valid as robustness and cyber security is not a topic of this deliverable.

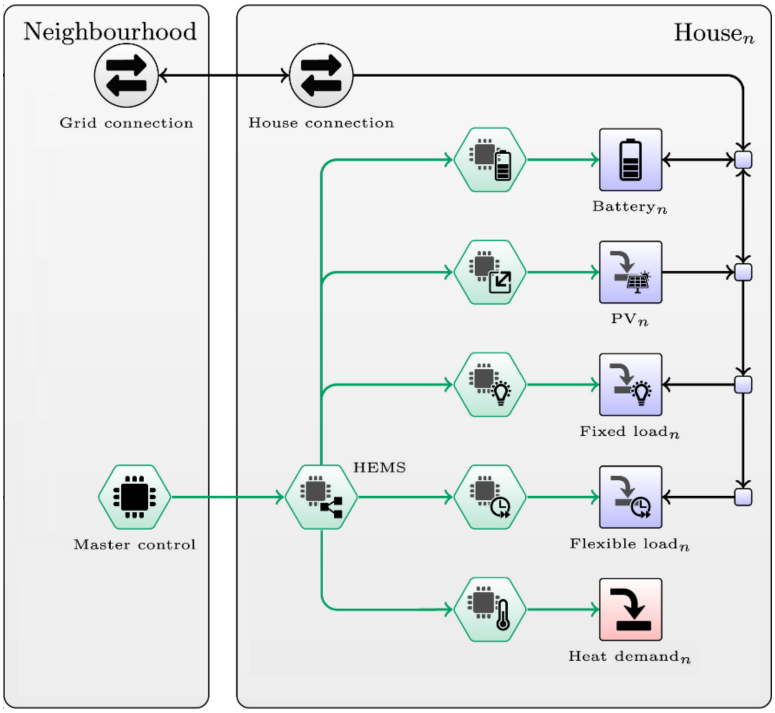

Figure 5.7: System architecture within a household with both physical power flows (black lines, rectangle shapes) and the control architecture (green arrows) with device agents (hexagons). Note that other devices as used in SUSTENANCE also fit this scheme.

To this end, based on objectives and optional input, optional operation of joined devices and/or households (in aggregation) can be achieved where also local preferences and constraints can be taken into account. Only the aggregated information as demanded, e.g., power profiles of FlexOffers have to be transmitted. Thus, the privacy sensitive data does not need to be communicated. Additionally, the local level also forms a solid basis to fall back on in case communication with the other layers fail, or would take too much time. Hence it allows to quickly respond to local adjustments or problems that can be observed from e.g., the grid state. This level therefore is also more tangible and tied to the physical system. Future envisioned markets, such as local congestion markets opened by DSO's can also be integrated in this level.

Global perspective

The other level is the global perspective where information of the local controllers is aggregated to a global controller (see Figure 5.8). The local levels already communicate their flexibility in abstract manners to ensure that sensitive data is protected. In this level, remaining flexibility can be redistributed among the local controllers if needed.

As indicated, aggregated flexibility may be more predictable on this level, such that the flexibility here can be utilized to act on global markets. Furthermore, this level has the oversight of the overall portfolio and might see additional opportunities to utilize offered flexibility to reduce costs of energy. Clear contracts on the use of such flexibility, and especially the revenue streams, are important. This also ensures that local controllers can make conscious trade-offs whether certain flexibility will be worth the potential discomfort. Note that local controllers can preserve their own flexibility by not communicating this to the higher level, keeping local levels in charge of their own assets if they desire to do so.

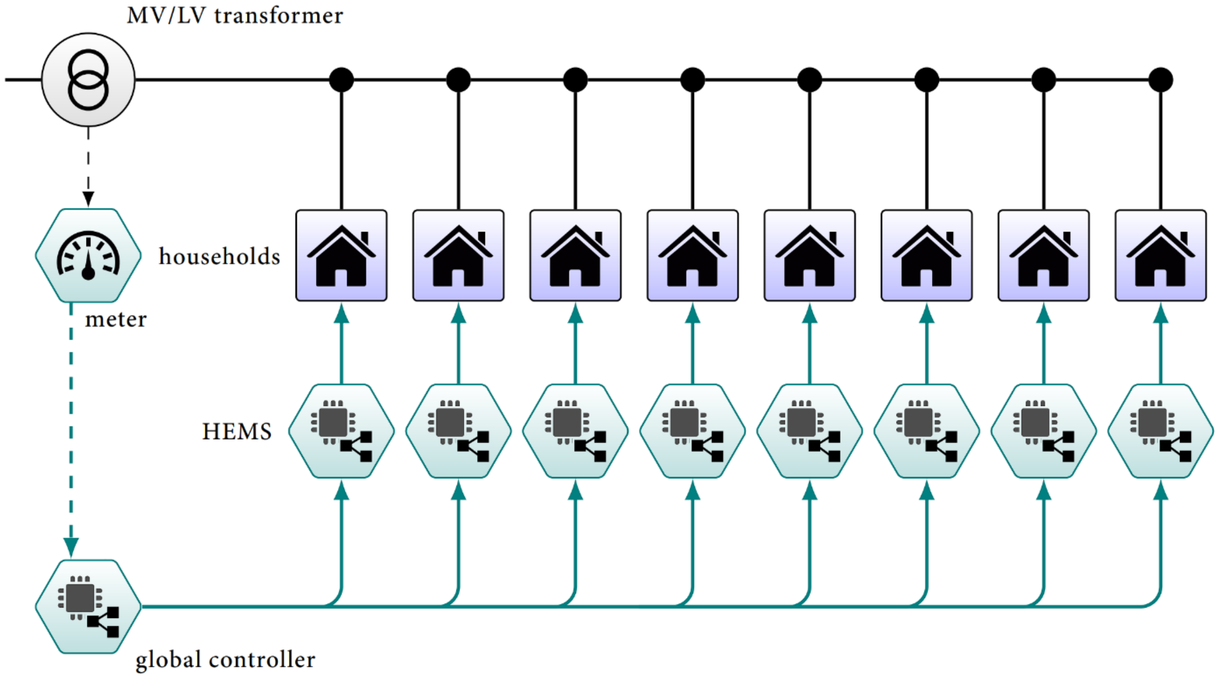

Figure 5.8: Hierarchical setup of houses with Home Energy Management Systems (HEMS) and a global coordinator aggregating and coordinating the flexibility

Therefore, this level will contain the optimization algorithms and business logic to steer a cluster of devices. Except for specific personal preferences and information (which remain local for privacy), the same data streams and interfaces with markets and service providers may be potentially integrated on this level. Optionally, centralized optimization of multiple assets may occur on this level, but it is also possible to keep this on the local level. This is a modular element that can be adjusted based on the demonstrator demands.

If more insight in effects of a decision is required, e.g. when utilizing a FlexOffer, this part could be simulated by the local controller. Hence, it can request to give an outlook on how utilizing flexibility now will affect the flexibility in the future based on models and historical data. This way, privacy sensitive data can remain local, but the global controller (e.g., an aggregator or utility) is able to get a clear picture of its position in the market, now and in the future.

Modules, Interaction and Hierarchy

Based on these two levels, we define a system of (optional) modules and blueprints that work together. These modules either run local or global, but also have dependencies in time and information from other modules. Furthermore, each module has its own responsibilities and potentially responsible party as well. These are outlined below, in chronologic order, starting from day ahead optimization. These modules are depicted in Figure 5.9 below.

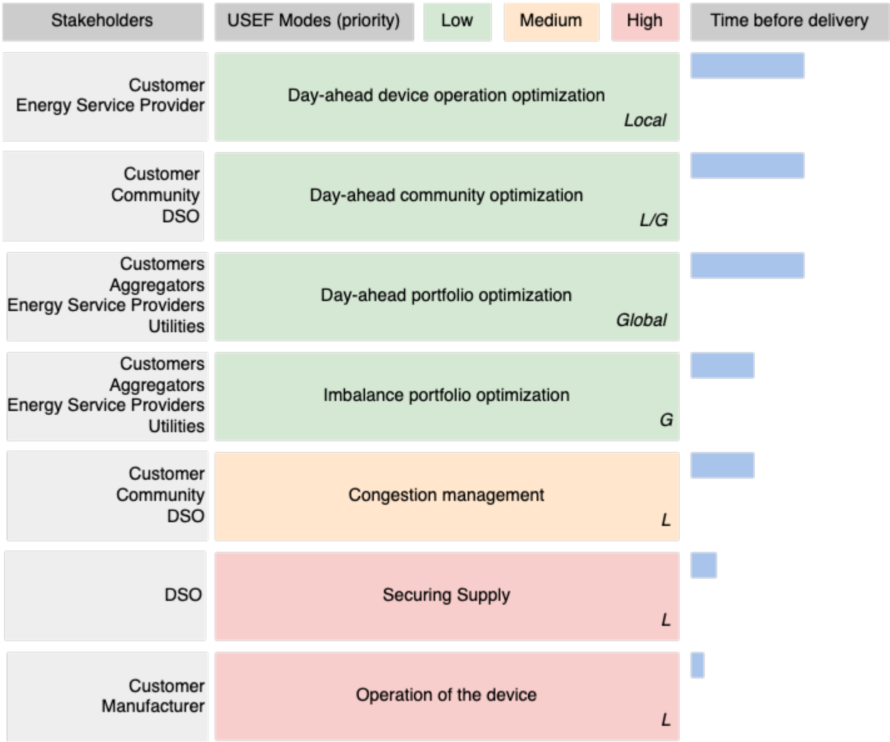

Figure 5.9: Local (L) and Global (G) modules that conceptually make up the energy management system

Day-ahead device operation optimization

- *Time:* Approximately a day ahead before or after market closing
- *Level:* Local, within premises
- *Responsibility:* Household EMS, possibly energy service provider
- *Priority:* Low, full control by customers through preferences (USEF: Green)
- *Stakeholders:* Customers, energy service provider
- *Description:* Creation of an optimal schedule for operation of electric-to-heat devices based on forecasts and historical data. This forms the baseline operation for one or more devices. Coordination with devices withing premises is possible. Possibility to interact on dynamic tariffs.

Day-ahead Community optimization

- *Time:* Approximately a day ahead before or after market closing
- *Level:* Local or Global (depending on configuration)
- *Responsibility:* Community, DSO
- *Priority:* Low, full control by customers through preferences (USEF: Green)
- *Stakeholders:* Customers, Community, DSO
- *Description:* Internal day-ahead sharing and trading of electricity within the community. At this stage, also prechecks of capacity problems with the DSO may be resolved (optional). The input here is the baseline energy usage profile from the households within the community.

Day-ahead Portfolio optimization

- *Time:* Approximately a day ahead before or after market closing
- *Level:* Global
- *Responsibility:* Utilities, Aggregators

- *Priority:* Low, full control by customers through preferences (USEF: Green)
- *Stakeholders:* Customers, Aggregators, Energy service providers/utilities
- *Description:* Left-over flexibility can be offered to utilities and aggregators to create more value of the flexibility for portfolio optimization. This flexibility is based on the initial local and/or community optimization

Imbalance Portfolio optimization

- *Time:* A few minutes before delivery
- *Level:* Global
- *Responsibility:* Utilities, Aggregators
- *Priority:* Low, full control by customers through preferences (USEF: Green)
- *Stakeholders:* Customers, Aggregators, Energy service providers/utilities
- *Description:* Flexibility (e.g., FlexOffers) can be dispatched (and updated) to balance a portfolio based on the portfolio balance. Comfort should be maintained through the offer specification if the customer desires to.

Congestion Management

- *Time:* A few minutes before delivery
- *Level:* Local
- *Responsibility:* Customers, Community, DSO
- *Priority:* Medium, up to forced intervention (USEF: Yellow-Orange)
- *Stakeholders:* Customers, Community, DSO
- *Description:* Flexibility (e.g., FlexOffers) can be dispatched (and updated) to avoid congestion problems. Based on rules and regulations this could be so forcibly, but should be done through policies that also ensure fairness. This is an intervention to the free market and would be the domain for energy modii (Task 6.1). Congestion management could occur simultaneously and goes together with Imbalance management, but this has a higher priority.

Securing supply

- *Time:* Just before delivery
- *Level:* Local
- *Responsibility:* Customers, Community, DSO
- *Priority:* High, direct control (USEF: Red)
- *Stakeholders:* DSO
- *Description:* (Near) real-time intervention based on the local grid state to ensure stability and avoid critical overloading. This may be observation based (e.g., voltage measurements) and will overrule all other setpoints and plans.

Operation of the device

- *Time:* At delivery
- *Level:* Local
- *Responsibility:* Manufacturer, Energy management system
- *Priority:* High, direct control (USEF: Red)
- *Stakeholders:* Customer, Manufacturer
- *Description:* Making the (planned) action concrete by controlling the device through an (exposed) API. The manufacturer of the device is responsible to reject/ignore actions that may lead to damage.

6 Evaluation

This Chapter provides an evaluation of the presented literature, models and control concepts by performing a simulation study. Using this study, we determine the suitability of presented work for application within the Sustenance project and the electricity-to-heat integration.

6.1 Validation of the PCM storage model

Simulation results of the PCM storage system dynamics, involving temperature of HTF and the thermal power flow, are validated with the real system's behaviour, as presented in [Gra21], for both charging and discharging processes of the storage system. The detailed calculation for a 785 litre PCM based thermal storage tank is presented in Annex A (9.3). Simulation is carried out for two different storage tank models (average model and discrete model). Simulation results from the discrete model shows a good alignment with the experimental values as compared to average model. In the discrete model, the thermal storage tank is divided into 5 equal parts horizontally, with equal volume of PCM and HTF. The temperature is considered uniform in each discrete layer.

During charging, the storage tank is charged with the flow of HTF at the rate of 0.1 kg/s (360kg/h) and a temperature of 67°C, while discharge is zero. For discharging, storage tank is discharged with the flow rate of 0.1kg/s and return temperature of 47 °C.

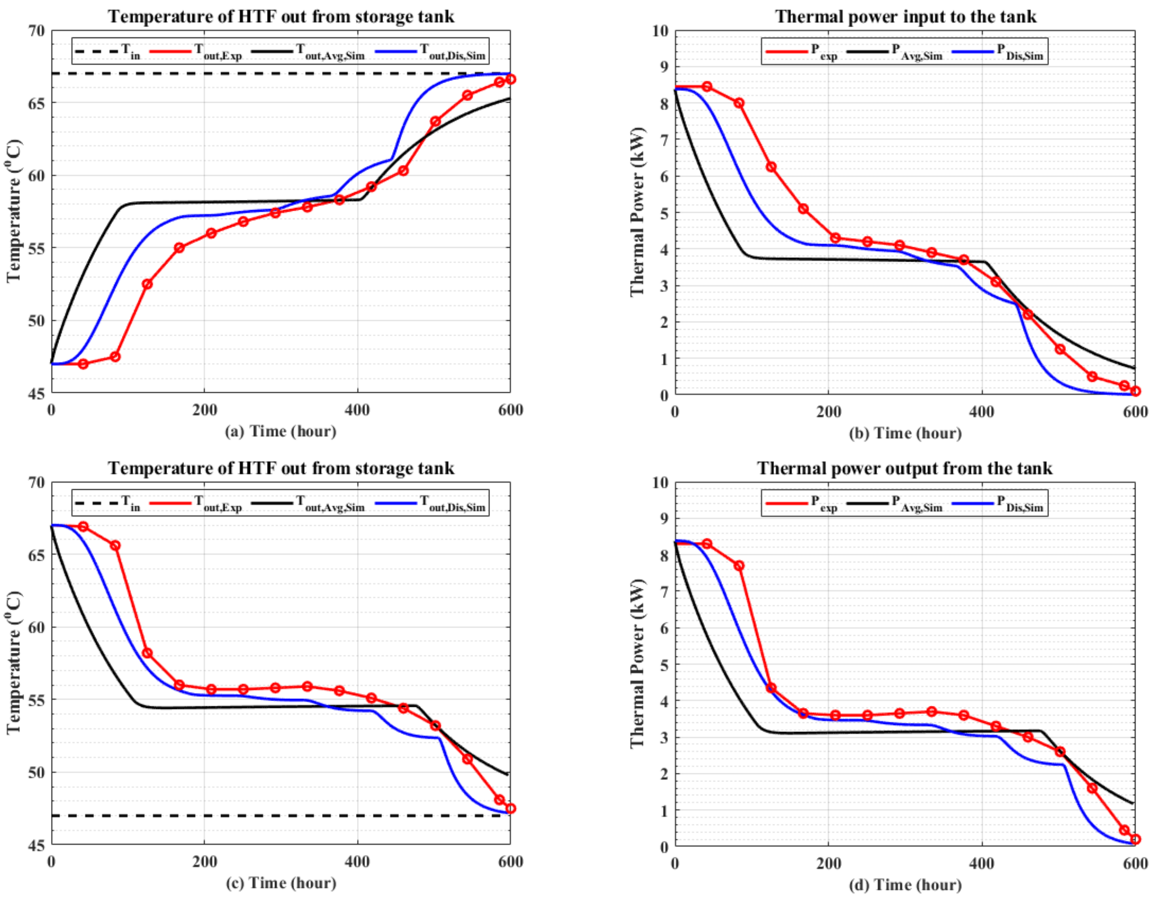

Figure 6.1: Comparison results for real system simulation model during charging and discharging using various methods

Figure 6.1 (a), (c) show the measured ($T_{out,exp}$) and simulated ($T_{out,Avg,Sim}$) temperatures for the average model and discrete model ($T_{out,Dis,Sim}$) during charging and discharging, respectively. Figure 6.1 (b), 2(d) show the thermal power measured (P_{exp}) and simulated ($P_{Avg,Sim}$) for average model and discrete model ($P_{Dis,Sim}$) during charging and discharging, respectively. Discrete model follows the system dynamics more closely than the average model.

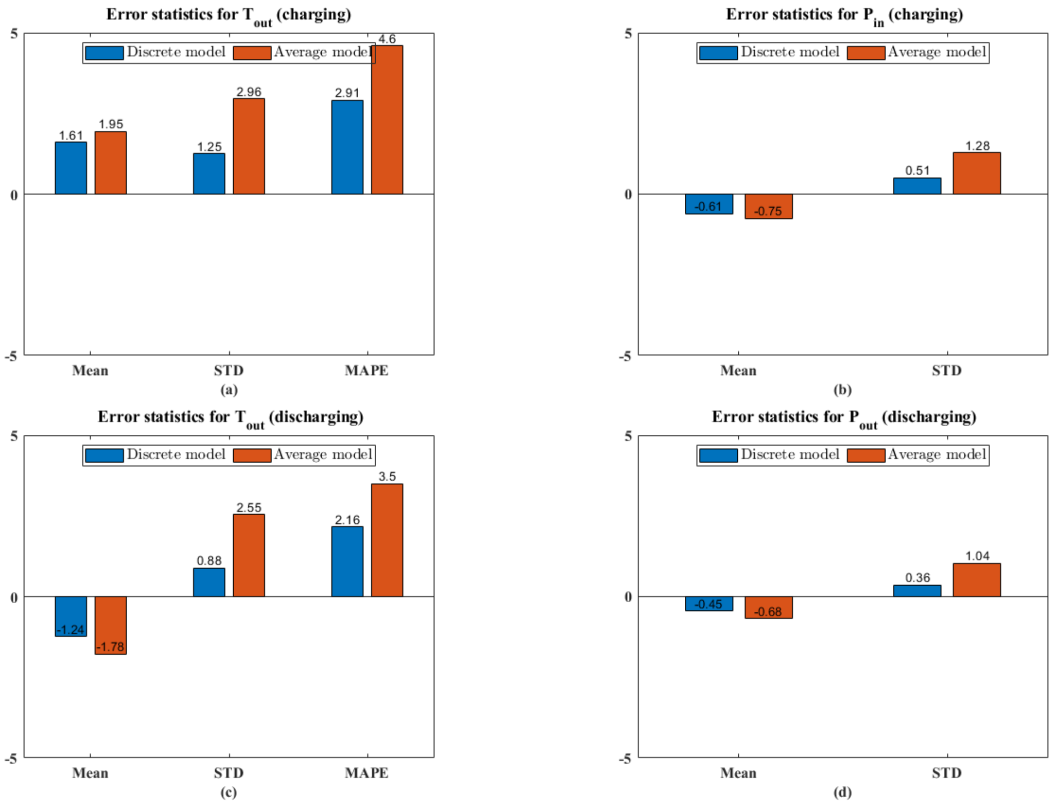

Figure 6.2: Error Statistics for temperature and thermal power based on 6.1 for (a,c) HTF temperature (b,d) Thermal power flow

Figure 6.2 shows the good alignment of simulation and actual performance of PCM based thermal storage tank, for both discrete and average model. The MAPE is less than 4% for HTF temperature and less than 2% for thermal power flow. Although the error for the discrete model is smaller than as observed for the average model, the average model is equally competitive and simple with faster computational dynamics.

6.2 Simulation studies

Model, context, and objectives

The simulation study is based on a small and representative neighbourhood of 8 households connected to a low voltage distribution grid. This size allows us to simulate the interaction between different houses in integration, whilst being small enough to be able to carefully study and evaluate the results. The details are provided below

Environment

Figure 6.3 represents a test low voltage distribution grid network with eight houses connected in a radial feeder. There are three different loads in each house, regular household load (H01-H08), EV load (EV_01-EV_08), and heat pump load (HP01-HP08). EV loads are not considered in this part of the report and would be further incorporated in future deliverables. Other load_1 and Other load_2 in the figure_RS1 represents bulk hose hold loads in other part of the distribution feeder connected within the same transformer. This grid network is further investigated for smart control of HP and analysis on terminal voltage at the point of coupling of HP as well as for line loadings.

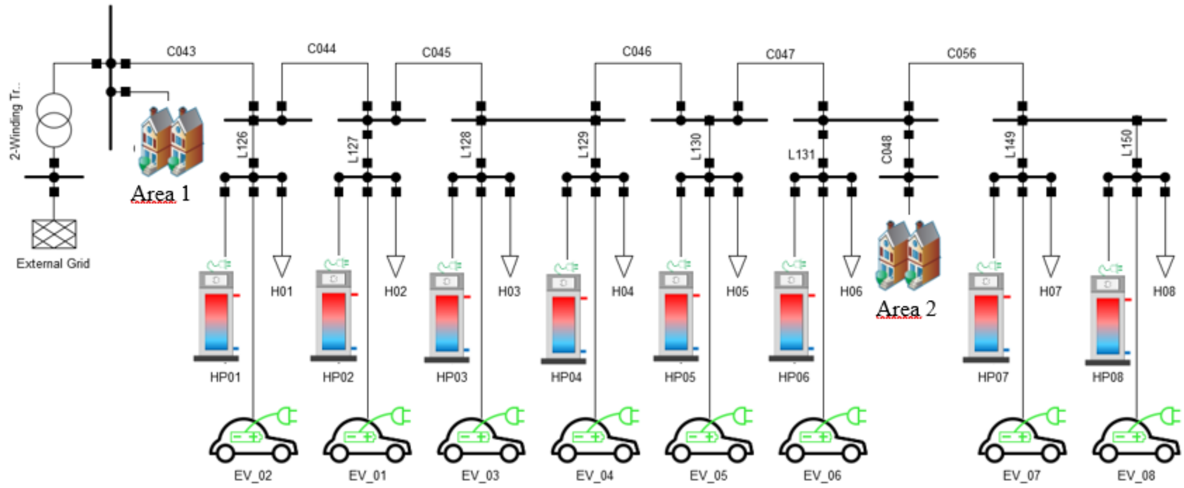

Figure 6.3: Test LV distribution grid network for with eight houses in a radial feeder

Weather data is obtained from the KNMI [KNMI] from weather station Twenthe, the Netherlands for the years 2010-2020, of which the year 2010 is used to train models and data from 2011 is used for the simulation study. This dataset contains both solar irradiation as outdoor temperature, which we need as input to calculate the total heat demand. For electricity-to-heat integration we use the day-ahead electricity market data. To be more precise, we use the 2021 electricity market data by ENTSO-E[23].

Houses

The 2R2C-model as presented in Chapter 3 is used for the thermal envelope of each of the households within the model. This model represents a floor-heating system as encountered within the Dutch and Danish use-cases and seen as the best fit system for heat pump integration. The heavily insulated semi-detached model parameters as presented by Van Leeuwen [vLe17] are used in simulation study, see the Table 6.1 below. Furthermore, 2 windows are added facing East and West.

Table 6.1: Used model parameters for the thermal envelope

Parameter	Value
R_{floor}	0.001 K/W
$R_{envelope}$	9.9985 K/W
C_{floor}	5100 Wh/K
C_{zone}	10000 Wh/K
Windows	5m^2 facing East, 5m^2 facing West

[23] https://transparency.entsoe.eu/

Human behaviour

An important factor in the heat demand is the human factor. To this end we have generated data using the Artificial Load Profile Generator (ALPG) [Hoo16]. The 8 different predefined types of household compositions by the ALPG are used to match the 8 households in the model. This allows us to simulate different types of behaviour on the heating system. The resulting data provides the necessary input as described in Chapter 3 such as, the domestic hot water usage, added heat by people and devices, ventilation, and thermostat setpoints.

Thermal devices

To supply heat, we have added a heat-pump and PCM-based thermal storage to each of the 8 households. The storage tank has a 500 L capacity with a usable storage capacity of 15 kWh. The controllable heat pump can be turned on and off only with a thermal output of 9 kW. All specifications are provided in Table 6.2 and Table 6.3 below.

Table 6.2: Parameters for PCM based thermal storage tank and HP

Parameters	Unit	Value
Volume of storage tank (V_{sto})	m^3	0.5
Ratio of height to diameter (R_a)	H/D	3.25
overall heat transfer coeff of tank (U_t)	$W/m^2\ ^oC$	0.9
Ambient temp in storage room (T_a)	^oC	10
Temp of incoming cold water (T_r)	^oC	30
Total mass of how water in the tank (m_w)	kg	346.56
thermal conductivity of pcm in solid state (k_s)	$W/m\ ^oC$	1
thermal conductivity of pcm in liquid state (k_l)	$W/m\ ^oC$	0.6
Total mass of pcm in the storage (m_{pcm})	kg	170
latent heat of fusion (L_{pcm})	J/kg	183000
Melting temp (T_l)	^oC	49.5
freezing temp (T_s)	^oC	45
Specific heat capacity liquid (C_{pl})	$J/kg\ ^oC$	3000
Specific heat capacity solid (C_{ps})	$J/kg\ ^oC$	3000
convective heat transfer coeff (h)	$W/m^2\ ^oC$	60
density of PCM (ρ_{pcm})	Kg/l	1.3
number of heat sel in the tank (N)		548

Table 6.3: Parameters of HP

Parameters	Unit	Value
Thermal rating of Heat pump	kW	9
Flow rate from HP	m^3/h	(1.2-1.5)
Flow rate from HP	l/s	0.3-4.2
flow in heating system (less than 10 l/min)	l/s	< 0.17

Control and optimization

The aforementioned model and resulting data is used as input for a dynamic physical simulation model within the DEMKit tool [Hoo19] (Figure 6.4). Subsequently, controllers are added to form a cyber-physical systems simulation model. Within this concept, all heating assets are seen as agents. The operation of the heat pumps herein is scheduled in an offline fashion using the optimization algorithm presented by Van der Klauw [Kla17]. This algorithm can deal with both on-off and modulation-based controlled heating assets. Next to this the hierarchical Profile Steering [Ger15] heuristic algorithm is added for coordination between the individual heating assets among the different households.

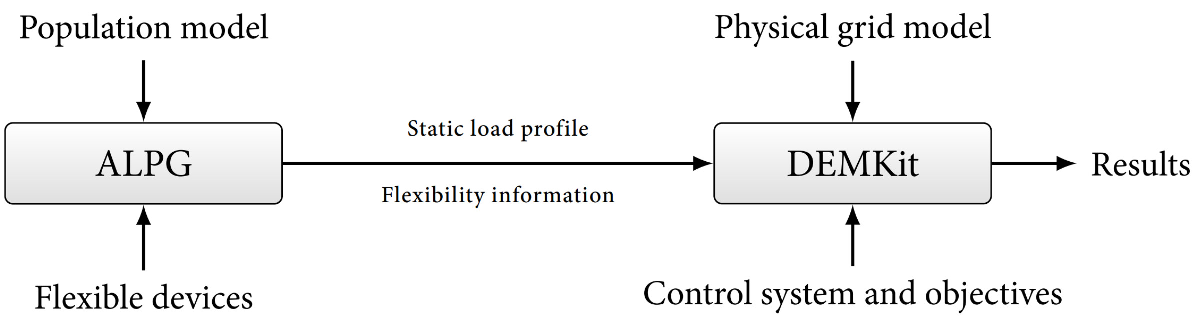

Figure 6.4: Toolchain of importing generated data into the optimization toolkit DEMKit [Hoo17]

Within this heuristic, the objective can be to minimize the Euclidean distance to a desired power profile, optimize by minimizing a specific cost function, or a linear combination of the two. The desired profile can be a flat profile with zeroes, indicating that balance is desired (i.e., utilizing local generation) and peaks (stress on the grid) should be avoided to improve the power quality. Alternatively, a vector with electricity prices (e.g., the aforementioned day-ahead prices) can be added to minimize operation costs. Note that this vector could also be the (expected) CO2 emissions by the energy mix, such that the operation can be scheduled to minimize the carbon emissions instead.

Dynamic Simulation

The resulting coordinated and optimized operation schedules are used as input for a dynamic simulation model in DigSILENT Powerfactory, which also includes the electricity grid. The use of user-defined dynamic models of the HP, control, and PCM storage, is developed using DIgSILENT Simulation Language (DSL).

Grid properties, such as the voltage at the point of coupling (POC) of the HP in the low voltage grid, loading of lines, cables and transformer, are further investigated to assess the need of grid reinforcements. The control of HP is also investigated to ensure thermal demand fulfilment for the end user while performing DR while trying to maintain electric grid voltage at POC of the HP. The HP is integrated with the electricity grid network via control system. There are two level of control architectures as shown in Figure 6.5

A first level of control is creating the optimized operation schedules (C_{sch}) based on forecasting the thermal generation and demand using Profile Steering [Ger15], algorithms by [Kla17], and utilizing the DEMKit implementation [Hoo19]. This control signal is received by second level controller that determines the demand response management of individual thermal units.

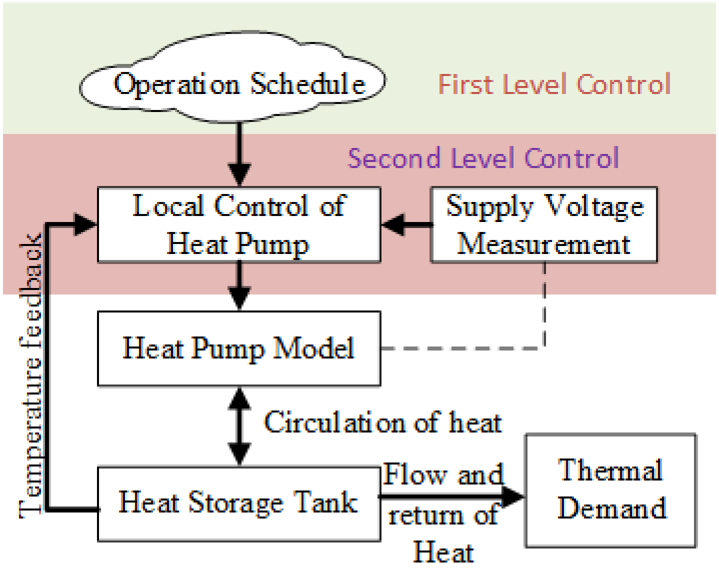

Figure 6.5: Smart control architecture for HP integration

The second level of control is locally available at the installation point of HP and thermal storage unit. This controller will manage the On/Off operation of HP with respect to state of energy of thermal storage tank, HP dynamics and supply voltage. It ensures consumer demand while supporting node voltage regulation. This two-level control ensures the reduction of forecasting errors, and communication breakdown through set of control logic presented in second level control (Figure 6.6).

The thermal storage tank can reach upper or lower limit of temperature in the storage tank while On-Off operation schedule through demand response (C_{sch}) is still high or low respectively. This error in operation of HP due to forecasting error is overcome by the support of second level control. Figure 6.6 illustrates various sub-controllers associated with second level control. Figure 6.6 (a) and (b) shows the logical operation of upper and lower limit temperature control. These sub-controllers overcome the scheduled demand response signal (C_{sch}) to determine the control action of HP operation. The upper limit controller shuts down the operation of HP when temperature of HTF in the storage (T_{ctrl}) reaches the maximum limit while (C_{sch}) is still high. Similarly, the lower limit temperature controller turns On the HP when temperature of HTF in the storage is lower than the minimum set limit while (C_{sch}) is still low. The logical operation for set (S) and reset (R) of each sub-controller module is selected to implement a hysteresis in the output (Q) of control action. Hysteresis in control action is implemented to avoid frequent On-Off operation of HP due to small deviation in set temperature logic. The hysteric in control action is illustrated using RS-Flip flop logic. The temperature difference of 5 and 15 ^{o}C in reset logic of upper and lower temperature limit controller respectively is chosen arbitrarily, so that the controller can again follow the schedule. This reset value can be set as per the need of DR flexibility.

Similarly, Figure 6.6 (c) shows the sub-controller module based on terminal voltage at the point of coupling (POC) of HP in electrical grid network. The issue of low voltage in long radial feeder of distribution grid may arise due to increase in electrical load. Shifting the operation of flexible load through the period of low voltage will be able to solve this issue [Sin19]. This shifting action is performed by the voltage limit controller. The HP is set to turn off when the terminal voltage is below the minimum set limit (V_{min}) and can be turned on again once it reaches the recovery voltage limit ($V_{recovery}$). The difference in minimum and recovery limit avoids haunting effect due to small fluctuation in voltage. However, in case of lower temperature limit or user preference (P) to operate HP, the HP will turn On despite of low voltage. This ensures end-user comfort. All three sub-controllers in Figure 6.6 (a,b,c) are combined together with logic operation illustrated in in Figure 6.6 (d) for final control signal for operation of HP (C_a). The control action is summarized in Table 6.4.

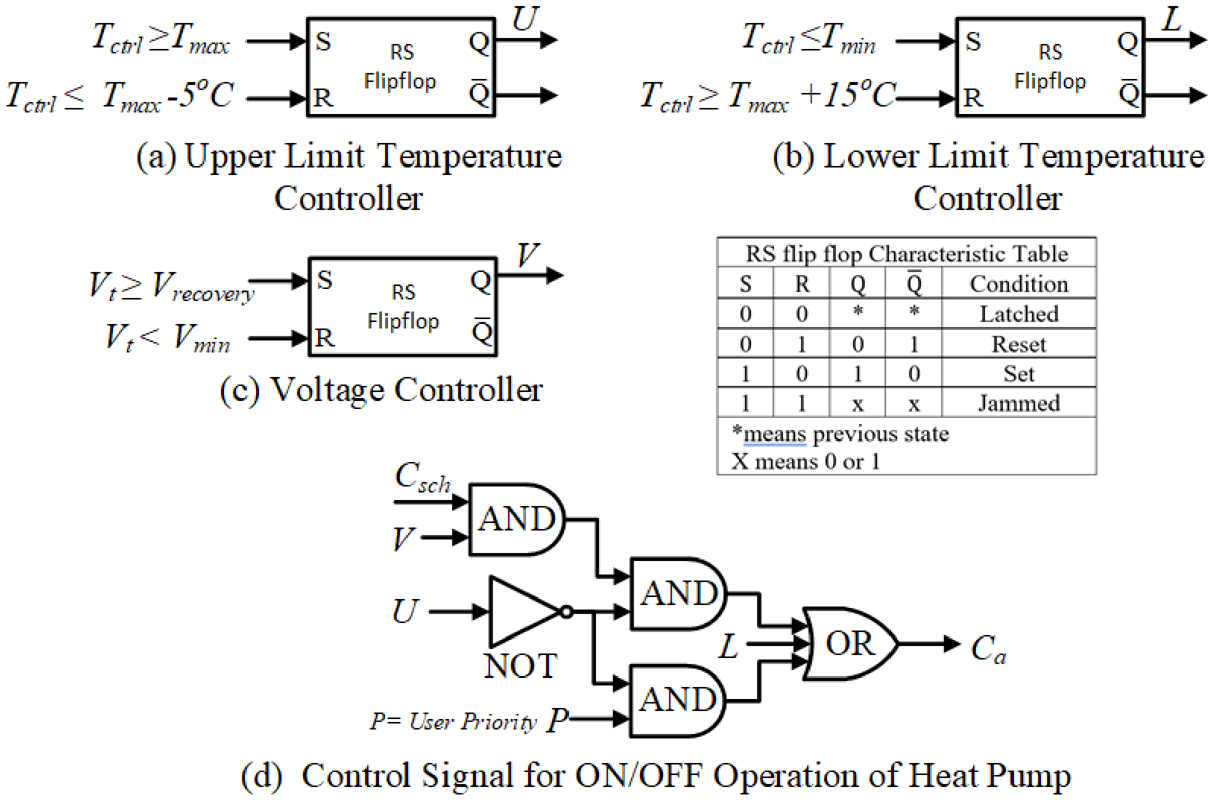

Figure 6.6: Logic diagram of secondary / local control system for HP operation

Table 6.4: Logic table of local parameters for control of the HP

U	L	V	C_{sch}	P	C_a
0	X	X	X	1	1
1	0	X	X	X	0
0	1	X	X	X	1
X	0	0	X	0	0
0	X	1	1	X	1
X means 0 or 1					
U and L cannot be in state 1 at the same time					

Simulation Results

Simulations are performed to evaluate the potential of integrating electricity-to-heat systems within energy markets. First the optimization results of day-ahead planning are presented, followed by operational DR control simulations to incorporate grid voltage measurements to ensure the operation of heat pumps does not cause problems within the local grid.

Day-ahead market optimization results

The DR control utilizes an optimized day-ahead planning as blueprint for its operational control. In this part we evaluate the results of this day ahead planning utilizing the on-off controllable heat pumps using data of one year. The optimization is performed with the objective to minimize the costs based on the 2021 Dutch day-ahead market prices for electricity provided by ENTSO-E[24]. Next to that, we also optimize towards peak shaving by minimizing the Euclidean distance of the power vector (see [Ger15]).

The results here are presented with respect to the operation of the heat pumps only. However, the models do have other loads as well which are considered in the optimization. In total, the 8 heat pumps combined consume just under 23 MWh of electricity annually in all three cases. The optimization results show a tremendous benefit in electricity costs. In the uncontrolled case, the annual cost for the 8 heat pumps combined is € 1,589.82 (without taxes), whereas in the price optimized case this is only € 1,111.17 (€ 478.65 reduction, 30% reduction). When optimizing for peak shaving, the electricity costs remain more or less the same (€ 1554.53).

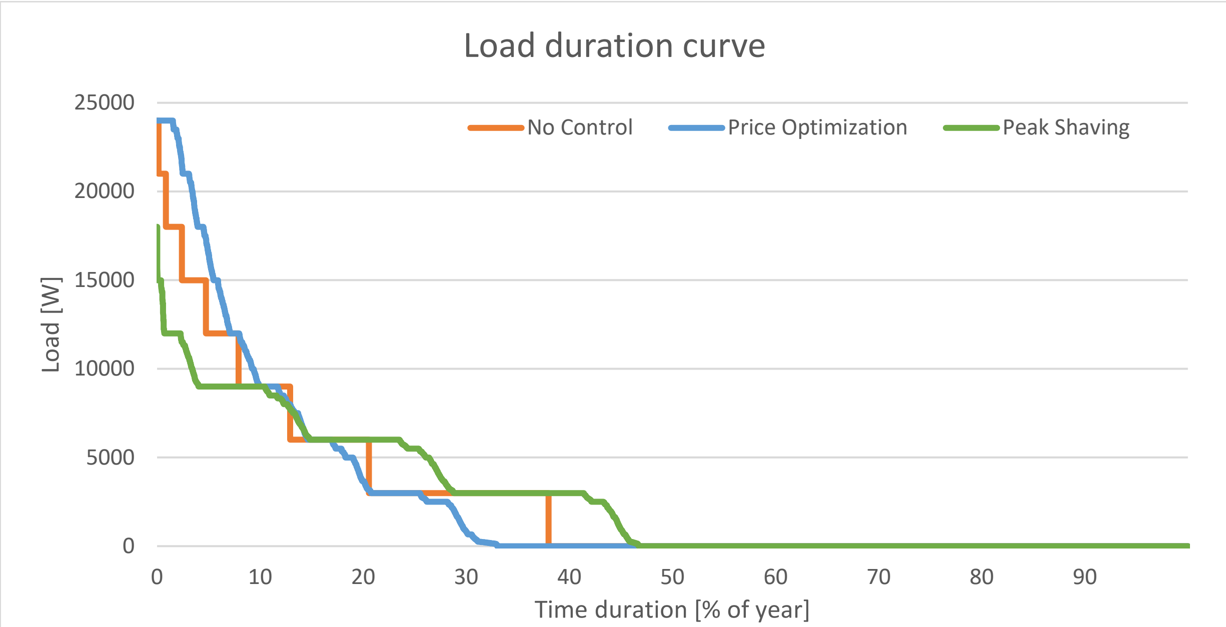

Figure 6.7: Load duration curve of the heat pump electricity demand

The load duration curve in Figure 6.7 shows that the peak shaving has a tremendous effect on lowering the stress on the grid by heat pumps. The peak load of heat pumps is reduced from 24 kW (all 8 operating) to 18 kW (maximum 6 out of 8 operating simultaneously). As expected, the price optimization tries to maximize runtimes on moments with low prices and therefore tends to operate heat pumps simultaneously. This leads to a longer duration of high load compared to the uncontrolled case.

Operational demand-response results

Results of the DR application for optimal operation of HP in individual houses based on control action discussed in section 6.1.1 are presented here. Control parameters are tabulated in Table 6.5. The simulation results of the control action with DR application for operation of HP is presented in Figure 6.8.

[24] https://transparency.entsoe.eu/

Table 6.5: Parameter of second level control

Parameter	Unit	Value
T_{max}	^oC	65
T_{min}	^oC	35
V_{min}	pu	0.95
$V_{recovery}$	pu	0.98
P	-	0

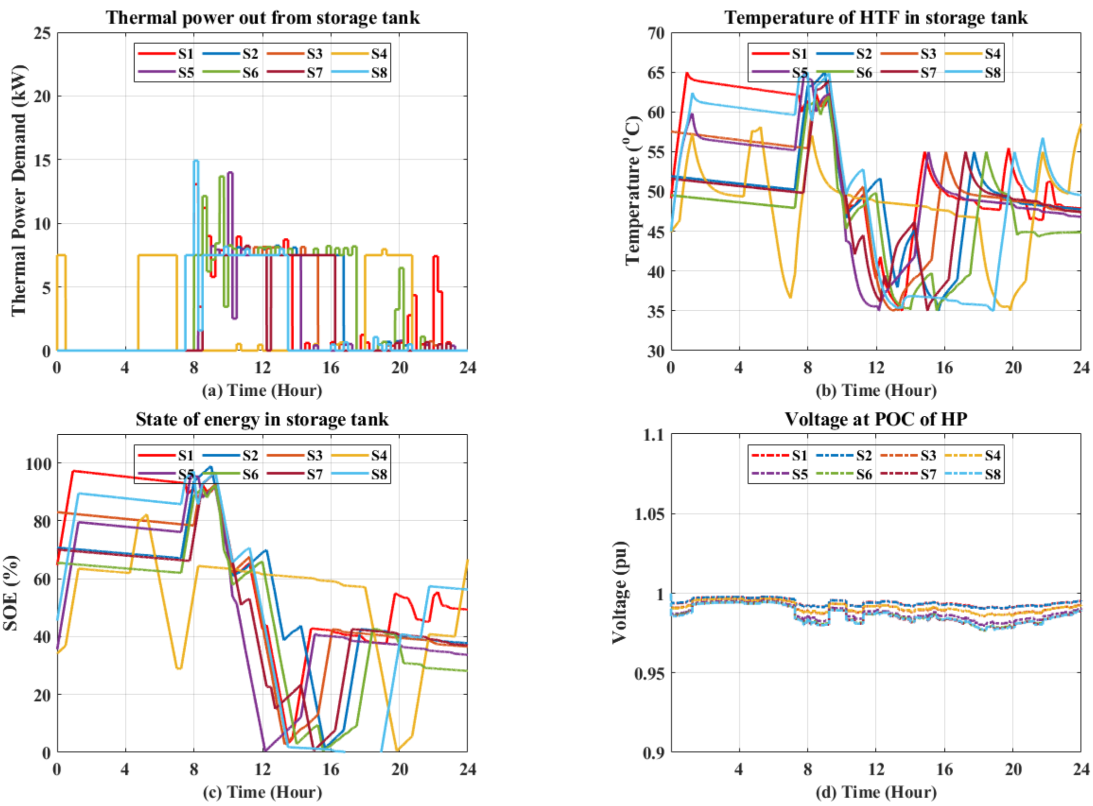

Figure 6.8: Simulated results on thermal demand, temperature of HTF, state of energy in storage tank and transformer loading based in DR application.

The thermal power delivered by the storage system (S1-S8) in houses (H01-H08) respectively is shown in Figure 6.8 (a). The temperature of the HTF delivering thermal power is shown in Figure 6.8 (b). The temperature of HTF delivering thermal power in individual houses is within the set limit, hence fulfilling the thermal demand. The SOE of individual storage tank in house is presented in Figure 6.8 (c). the SOE can go up to minimum value and the HP is turned on simultaneously to deliver thermal demand. The voltage at the POC of HP is within the permissible limit as seen from Figure 6.8 (d). The control action of second level controller for house H01 is presented in Figure 6.9 for validation. Schedule operation of HP is not accurately estimated to maintain the SOE in the thermal storage tank between 0-100% as upper limit and lower limit controller is activated (Figure 6.9 (a)). HP operation based on optimal schedule and second level control action is illustrated in Figure 6.9 (b). Actual operation of HP follows the schedule until upper and lower temperature limit is attained.

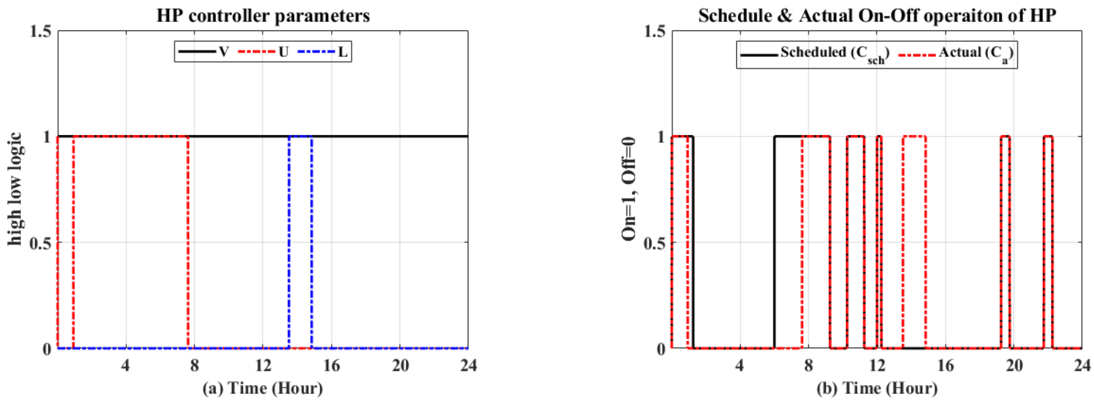

Figure 6.9: Performance of second level control.

It is observed from the simulation result that with the set limit of HTF temperature in storage tank and voltage at POC, the proposed control action can maintain thermal demand despite an error in the estimation of optimal schedule.

7 Conclusion

This deliverable investigated the integration of electricity-to-heat systems into the electricity grid. Hereby, the specific focus is to utilize offered flexibility from heating devices in aggregated form for successful integration. This chapter answers the questions set out in the Introduction:

- **How to accurately model heat demand profiles and comfort constraints on a building level and derive its flexibility on an aggregated level?**

Chapter 3 surveyed existing literature on thermal envelope models, models of heating devices and the modelling of end-user comfort when it comes to perceived heat. Various models exist that have also been validated in practice before. The separate models make for a modular approach to model various use-cases and set-up, as well as to make trade-offs in complexity and desired minimum accuracy. The latter is key to efficient control and energy management systems.

- **How to translate complex non-linear thermal models from their long-term time-scales into accurate discrete flexibility models for optimal control in short-term electricity systems?**

Non-linearity cannot be avoided when modelling. Combining knowledge of Chapters 3 and 5, we conclude that it is best to follow a 2-step approach. Herein, the first step consists of day-ahead planning where non-linearities are mostly omitted to reduce computation time. The rationale here is that also other errors stemming from e.g. weather forecasts exist, making it pointless to have better models. During operational phases, more complex models can be utilized on a local scale. Alternatively, tracer devices might be used to ease computational complexity when large clusters are to be controlled.

- **How to efficiently coordinate a heterogeneous set of thermal devices within a community?**

Chapter 5 has presented various coordination strategies. Key here is to set-up a hierarchical and modular system with clear roles and responsibilities, both in time and location. Next to this, clear interfaces for communication to allow e.g., for distributed control for scalability is essential. A framework has presented in Section 5.2 to do so.

- **What is the added value and accuracy of thermal control on an aggregated community level over existing "business-as-usual" individual control?**

From the literature review in Chapter 3 we conclude that the main added value of aggregated flexibility is the increase in predictability of the offered flexibility for heat systems. This may offer more potential for service providers to act on a wider variety of markets and therefore apply revenue stacking to increase the overall benefits. The studies in Chapter 6 also highlight the benefits for the local grid when utilizing coordinated control to enhance the supply voltage levels. Next to this it is also shown that coordination of heat production can significantly lower the load on the grid, which is especially useful to enable the transition in weak grids that are too costly to reinforce.

The presented theoretical foundation forms the basis on which electricity-to-heat devices can be integrated successfully in SUSTENANCE's demonstrators. Furthermore, through its modularity, it can adapt to other locations as well. The differences within SUSTENANCE's demonstrator sites therefore also provide a test-bed for further upscaling. It remains future work to validate the presented models and methods using measurements, observations, and learnings from the demonstrator work packages.

8 Bibliography

[ASH13] ASHRAE, Handbook-Fundamentals, Atlanta, American Society of Heating, Refridgerating and Air-conditioning Engineers (ASHRAE), 2013

[ASH55] ASHRAE, Standard 55-2017 Thermal environmental conditions for human occupancy, Atlanta, American Society of Heating, Refridgerating and Air-conditioning Engineers (ASHRAE), 2017

[Bar22] V. Barta, S. Baumgartner, S. Uhrig and R. Witzmann, "Potential of a self-sufficient control for flexible loads in low voltage grids," CIRED Porto Workshop 2022: E-mobility and power distribution systems, Hybrid Conference, Porto, Portugal, 2022, pp. 38-42, doi: 10.1049/icp.2022.0657.

[BDEW15] Bundesverband der Energie- und Wasserwirtschaft. Smart Grid Traffic Light Concept: Design of the amber phase. Technical report, March 2015

[Blo07] E. J. M. Blokker and K. Poortema, “Effect study of domestic hot water supply (in Dutch, original: “Effecten levering warm tapwater door derden”), Technical report KIWA, 2017

[Boo13] P. Booij, V. Kamphuis, O. van Pruissen, and C. Warmer. Multi-agent control for integrated heat and electricity management in residential districts. In 4th International Workshop on Agent Technologies for Energy Systems (ATES), a workshop of the 12th International Conference on Autonomous Agents and Multiagent Systems (AAMAS), Minnesota, 2013

[Bos12] M. Bosman. Planning in Smart Grids. PhD thesis, July 2012. eemcs-eprint-22062 ; http://eprints.ewi.utwente.nl/22062.

[Boy11] S. Boyd, N. Parikh, E. Chu, B. Peleato, and J. Eckstein. Distributed optimization and statistical learning via the alternating direction method of multipliers. Found. Trends Mach. Learn., 3(1):1–122, January 2011. ISSN 1935-8237. doi: 10.1561/2200000016.

[Cla12] B. J. Claessens, S. Vandael, F. Ruelens, and M. Hommelberg. Self-learning demand side management for a heterogeneous cluster of devices with binary control actions. In 2012 3rd IEEE PES Innovative Smart Grid Technologies Europe (ISGT Europe), pages 1–8, October 2012. doi: 10.1109/ISGTEurope.2012.6465679.

[Cla13] B. J. Claessens, S. Vandael, F. Ruelens, K. De Craemer, and B. Beusen. Peak shaving of a heterogeneous cluster of residential flexibility carriers using reinforcement learning. In IEEE PES ISGT Europe 2013, pages 1–5, October 2013. doi: 10.1109/ISGTEurope.2013.669525

[Dan61] G. B. Dantzig, P. Wolfe, The decomposition algorithm for linear programs, Econometrica, 29.4, The Econometric Society, 1961, pp. 767-778

[Dav22] A. David, M. Alamir and C. L. Pape-Gardeux, "Data-driven modelling for HVAC energy flexibility optimization," 2022 IEEE PES Innovative Smart Grid Technologies Conference Europe (ISGT-Europe), Novi Sad, Serbia, 2022, pp. 1-5, doi: 10.1109/ISGT-Europe54678.2022.9960426.

[Duf80] J. A. Duffie and W. A. Beckman, Solar engineering of thermals processes, New York, Wiley, 1980

[Eic06] U. Eicker, Solar Technologies for Buildings, John Wiley & Sons, 2006.

[Elm22] F. Elmaz, S. Ghane, T. Huybrechts, A. Anwar, S. Mercelis and P. Hellinckx, "Transfer Learning-based Hybrid Modeling Approach for Indoor Temperature Modeling," IECON 2022 – 48th Annual Conference of the IEEE Industrial Electronics Society, Brussels, Belgium, 2022, pp. 1-6, doi: 10.1109/IECON49645.2022.9968939.

[Erb82] D. G. Erbs, S. A. Klein, and J. A. Duffie, “Estimation of the diffuse radiation fraction for hourly, daily and monthly-average global radiation”, Solar Energy 28.4 (1982), pp. 293-302

[Ezk18] Ministerie van EZK, Regeling van de Minister van Economische Zaken en Klimaat van 25 juni 2018, nr. WJZ/18086924, houdende regels omtrent de aanwijzing van gebieden als bedoeld in artikel 10, zevende lid, onderdeel a, van de Gaswet (Regeling gebiedsaanwijzing gasaansluitplicht), Staatscourant van het Koninkrijk der Nederlanden, 36136, 27-6-2018

[Fan21] J. Fan and S. Furbo, “Thermal stratification in a hot water tank established by heat loss from the tank”, Solar Energy, 86.11 (2012), pp. 3460-3469

[Fin15] Fink, Jiří & van Leeuwen, Richard & Hurink, Johann & Smit, Gerard. (2015). Linear programming control of a group of heat pumps. Energy, Sustainability and Society. 5. 10.1186/s13705-015-0061-9.

[Fin16] Fink J, Van Leeuwen RP. Earliest Deadline Control of a Group of Heat Pumps with a Single Energy Source. Energies. 2016; 9(7):552. https://doi.org/10.3390/en9070552

[Fis17] Fischer, David & Wolf, Tobias & Triebel, Marc-André. (2017). Flexibility of heat pump pools: The use of SG-Ready from an aggregator's perspective.

[Fis17a] David Fischer, Hatef Madani, On heat pumps in smart grids: A review, Renewable and Sustainable Energy Reviews, Volume 70, 2017, Pages 342-357, ISSN 1364-0321, https://doi.org/10.1016/j.rser.2016.11.182.

[Fis18] D. Fischer, M. -A. Triebel and O. Selinger-Lutz, "A Concept for Controlling Heat Pump Pools Using the Smart Grid Ready Interface," 2018 IEEE PES Innovative Smart Grid Technologies Conference Europe (ISGT-Europe), Sarajevo, Bosnia and Herzegovina, 2018, pp. 1-6, doi: 10.1109/ISGTEurope.2018.8571870.

[Ger15] M. E. T. Gerards, H. A. Toersche, G. Hoogsteen, T. van der Klauw, J. L. Hurink, and G. J. M. Smit, "Demand side management using profile steering," In PowerTech, 2015 IEEE, Eindhoven, 6 pages, June 2015. - doi: 10.1109/PTC.2015.7232328

[Goe19] G. J. H. de Goeijen, (2019). Developing a method for the operational control of an ecovat system. [PhD Thesis - Research UT, graduation UT, University of Twente]. University of Twente. https://doi.org/10.3990/1.9789036549097

[Gra21] M. Grabo, E. Acar and Eugeny Y. Kenig, "Modeling and improvement of a packed bed latent heat storage filled with non-spherical encapsulated PCM-Elements," Renewable Energy, vol. 173, pp. 1087-1097, 2021.

[Gri15] GridWise. Transactive Energy Framework Version 1.0. [Online] Available: http://www.gridwiseac.org/pdfs/te_framework_report_pnnl-22946.pdf

[Han12] Y. M. Han R. Z. Wang, Y. J. Daim “Thermal stratification within the water tank”, Renewable and Sustainable Energy Reviews, 13.5 (2019), pp. 1014-1026

[Hom16] B. Homan, R. P. van Leeuwen, G. J. M. Smit, L. Zhu, and J. B. de Wit. Validation of a predictive model for smart control of electrical energy storage. In 2016 IEEE International Energy Conference (ENERGYCON), Leuven, Belgium, USA, July 2016. IEEE Power Electronics Society

[Hom18] B. Homan, V. M. J. J. Reijnders, G. Hoogsteen, J. L. Hurink, and Gerard J.M. Smit, "Implementation and Verification of a Realistic Battery Model in the DEMKit Simulation Software," In 2018 IEEE PES Innovative Smart Grid Technologies Europe, Sarajevo, 6 pages, October 2018. - doi: 10.1109/ISGTEurope.2018.8571691

[Hom19] B. Homan, G. Hoogsteen, S. Nebiolo, J. L. Hurink, and G. J. M. Smit, "Maximizing the degree of autarky of a 16 house neighbourhood by locally produced energy and smart control," In Sustainable Energy, Grids and Networks, vol. 20, p. 100270. October 2019, ISSN: 2352-4677. - doi: 10.1016/j.segan.2019.100270

[Hom20] B. Homan, (2020). Batteries in Smart Microgrids. [PhD Thesis - Research UT, graduation UT, University of Twente]. University of Twente. https://doi.org/10.3990/1.9789036549578

[Hoo16] G. Hoogsteen, A. Molderink, J. L. Hurink, and G. J. M. Smit, "Generation of flexible domestic load profiles to evaluate demand side management approaches," In 2016 IEEE International Energy Conference (ENERGYCON), Leuven, page 6 pages, April 2016. - doi: 10.1109/ENERGYCON.2016.7513873

[Hoo17] G. Hoogsteen, (2017). A Cyber-Physical Systems Perspective on Decentralized Energy Management (1 ed.). [PhD Thesis - Research UT, graduation UT, University of Twente]. University of Twente. https://doi.org/10.3990/1.9789036544320

[Hoo17a] G. Hoogsteen, A. Molderink, J. L. Hurink, and G. J. M. Smit, “Asynchronous event driven distributed energy management using profile steering," In 2017 IEEE Manchester PowerTech, 6 pages, June 2017. - doi: 10.1109/PTC.2017.7980986

[Hoo18] G. Hoogsteen, M. E. T. Gerards, J. L. Hurink, "On the scalability of decentralized energy management using profile steering," In 2018 IEEE PES Innovative Smart Grid Technologies Europe, Sarajevo, 6 pages, October 2018. - doi: 10.1109/ISGTEurope.2018.8571823

[Hoo19] G. Hoogsteen, J. L. Hurink, and G. J. M. Smit, “DEMKit: a Decentralized energy management simulation and demonstration toolkit,” In 2019 IEEE PES Innovative Smart Grid Technologies Europe, Bucharest, 5 pages, October 2019. - doi: 10.1109/ISGTEurope.2019.8905439

[Hoo20] G. Hoogsteen, M. E. T. Gerards, and J. L. Hurink, “Optimization of Multi-Energy Systems Using the Profile Steering Coordination Framework,” In 2020 IEEE PES Innovative Smart Grid Technologies Europe, The Hague, 5 pages, October 2020. - doi: 10.1109/ISGT-Europe47291.2020.9248766

[Hoo22] G. Hoogsteen, A. Pappu, B. Ahmadi, J. L. Hurink, E. W. Schaefer, C. Gercek, and R. P. van Leeuwen, "On the Effects of Active Energy Community Participation in the Energy System," in 2022 IEEE PES Innovative Smart Grid Technologies Conference Europe, Novi Sad, 5 pages, October 2022. - doi: 10.1109/ISGT-Europe54678.2022.9960552

[Hus17] A. Hussain, V. Bui, H. Kim, Y. Im, and J. Lee. Optimal Energy Management of Combined Cooling, Heat and Power in Different Demand Type Buildings Considering Seasonal Demand Variations. Energies, 10:789, 2017.

[Iac17] S. Iacovella, F. Ruelens, P. Vingerhoets, B. J. Claessens, and G. Deconinck. Cluster control of heterogeneous thermostatically controlled loads using tracer devices. IEEE Transactions on Smart Grid, 8(2):528–536, March 2017. ISSN 1949-3053. doi: 10.1109/TSG.2015.2483506.

[ISO7730] ISO 7730:2005. Ergonomics of the thermal environment — Analytical determination and interpretation of thermal comfort using calculation of the PMV and PPD indices and local thermal comfort criteria

[Jet22] R. Jetten, Kamerbrief besluit infrastructuur collectieve warmtevoorziening in publieke handen, 2022, Online: https://www.rijksoverheid.nl/documenten/kamerstukken/2022/10/21/wet-collectieve-warmtevoorziening-besluit-infrastructuur-in-publieke-handen

[Kla16] T. van der Klauw, G. Hoogsteen, M. E. T. Gerards, J. L. Hurink, X. Feng, R. E. Hebner, “Assessing the potential of residential HVAC systems for demand-side management,” In 2016 IEEE PES Innovative Smart Grid Technologies Conference, Minneapolis, 6 pages September 2016. - doi: 10.1109/ISGT.2016.7781193

[Kla17] T. van der Klauw, (2017). Decentralized Energy Management with Profile Steering: Resource Allocation Problems in Energy Management. [PhD Thesis - Research UT, graduation UT, University of Twente]. University of Twente. https://doi.org/10.3990/1.9789036543019

[Kli19] Klimaatakkoord, https://www.klimaatakkoord.nl/documenten/publicaties/2019/06/28/klimaatakkoord, 2019

[KNMI] KNMI. Uurgegevens van het weer in Nederland. Available online: http://www.knmi.nl/nederland-nu/klimatologie/uurgegevens.

[Kok13] K. Kok. The PowerMatcher: smart coordination for the smart electricity grid. PhD thesis, Vrije Universiteit Amsterdam, July 2013.

[Lee18] W. Lee, K. Kim, J. Park, J. Kim and Y. Kim, "Forecasting Solar Power Using Long-Short Term Memory and Convolutional Neural Networks," in IEEE Access, vol. 6, pp. 73068-73080, 2018, doi: 10.1109/ACCESS.2018.2883330.

[Len22] Lennard Visser, Tarek AlSkaif, Wilfried van Sark, Operational day-ahead solar power forecasting for aggregated PV systems with a varying spatial distribution, Renewable Energy, Volume 183, 2022, Pages 267-282, ISSN 0960-1481, https://doi.org/10.1016/j.renene.2021.10.102.

[Let12] Letschert, Virginie, Desroches, Louis-Benoit, Ke, Jing, and McNeil, Michael. Estimate of Technical Potential for Minimum Efficiency Performance Standards in 13 Major World Economies. United States: N. p., 2012. Web. doi:10.2172/1223013.

[Mad95] H. Madsen, J. Holst, Estimation of continuous-time models for the heat dynamics of a building, Energy and Buildings, 1995, pp. 67-79

[Mbu20] B. V. Mbuwir, C. Manna, F. Spiessens and G. Deconinck, "Benchmarking reinforcement learning algorithms for demand response applications," 2020 IEEE PES Innovative Smart Grid Technologies Europe (ISGT-Europe), The Hague, Netherlands, 2020, pp. 289-293, doi: 10.1109/ISGT-Europe47291.2020.9248800.

[Nij22] B. Nijenhuis, L. Winschermann, N. Bañol Arias, G. Hoogsteen, and J. L. Hurink, "Protecting the Distribution Grid while Maximizing EV Energy Flexibility with Transparency and Active User Engagement," In CIRED Porto Workshop 2022: E-mobility and power distribution systems, Porto, 5 pages, June 2022. - doi: 10.1049/icp.2022.0696

[OADR17] OpenADR Alliance. OpenADR 2.0 Specifications, 2017

[Ped18] T. B. Pedersen, L. Šikšnys and B. Neupane, "Modeling and Managing Energy Flexibility Using FlexOffers," 2018 IEEE International Conference on Communications, Control, and Computing Technologies for Smart Grids (SmartGridComm), Aalborg, Denmark, 2018, pp. 1-7, doi: 10.1109/SmartGridComm.2018.8587605.

[Pfl13] N. Pflugradt, J. Teuscher, B. Platzer, and W. Schufft. Analysing low-voltage grids using a behaviour based load profile generator. In International Conference on Renewable Energies and Power Quality, volume 11, page 5, 2013.

[Pha13] Phadke, Amol, Abhyankar, Nikit, Shah, Nihar, and Lawrence Berkeley National Lab., CA. Avoiding 100 new power plants by increasing efficiency of room air conditioners in India: opportunities and challenges. United States: N. p., 2013. Web.

[Put18] Y. Putter, Distributed Control Design of District Heating Networks, Master’s thesis, TU Delft, 2018

[Rid14] F. de Rider and M. Coomans, “Grey-box model and identification procedure for domestic thermal storage vessels”, Applied Thermal Engineering, 67.1 (201) pp. 14-158

[Rij20] Reijnders, V. M., van der Laan, M. D., & Dijkstra, R. (2020). Energy communities: A Dutch case study. In Behind and Beyond the Meter (pp. 137-155). Academic Press.

[Ros01] M. A. Rosen, “The exergy of stratified thermal energy storage”, Solar Energy, 71.3 (2001), pp. 173-185

[Sae22] M. H. Saeed, H. Syed Kazmi and G. Deconinck, "Bottom-up quantification of energy flexibility in cluster of residential heat pump systems," 2022 IEEE PES Innovative Smart Grid Technologies Conference Europe (ISGT-Europe), Novi Sad, Serbia, 2022, pp. 1-5, doi: 10.1109/ISGT-Europe54678.2022.9960599.

[Sau17] Kumar Saurav and Vikas Chandan. 2017. Gray-Box Approach for Thermal Modelling of Buildings for Applications in District Heating and Cooling Networks. In Proceedings of the Eighth International Conference on Future Energy Systems (e-Energy '17). Association for Computing Machinery, New York, NY, USA, 347–352. https://doi.org/10.1145/3077839.3084078

[Sch17] M. H. H. Schoot Uiterkamp, G. Hoogsteen, M. E. T. Gerards, J. L. Hurink, and G. J. M. Smit, “Multi-commodity support in profile steering," In 2017 IEEE PES Innovative Smart Grid Technologies Europe, Turin, 6 pages, September 2017. - doi: 10.1109/ISGTEurope.2017.8260190

[Sim22] J. Simeunović, B. Schubnel, P. -J. Alet and R. E. Carrillo, "Spatio-Temporal Graph Neural Networks for Multi-Site PV Power Forecasting," in IEEE Transactions on Sustainable Energy, vol. 13, no. 2, pp. 1210-1220, April 2022, doi: 10.1109/TSTE.2021.3125200.

[Sin17] R. Sinha, B. B. Jensen, J. R. Pillai, C. Bojesen and B. Moller-Jensen, “Modelling of hot water storage tank for electric grid integration and demand response control,” in 2017 52nd International Universities Power Engineering Conference (UPEC), 2017.

[Sin19] R. Sinha, Flexible Control for Local Heating and Transportation Units in Low Voltage Distribution, Aalborg, Denmark: Aalborg Universitetsforlag. Ph.d.-serien for Det Ingeniør- og Naturvidenskabelige Fakultet, Aalborg, 2019.

[Sin20] R. Sinha, B. Bak-Jensen, J. Radhakrishna Pillai and H. Zareipour, “Flexibility from Electric Boiler and Thermal Storage for Multi Energy System Interaction,” Energies , vol. 13, 2020.

[Sing22] Singla, P., Duhan, M. & Saroha, S. A comprehensive review and analysis of solar forecasting techniques. Front. Energy 16, 187–223 (2022). https://doi.org/10.1007/s11708-021-0722-7

[Som17] O. De Somer, A. Soares, K. Vanthournout, F. Spiessens, T. Kuijpers and K. Vossen, "Using reinforcement learning for demand response of domestic hot water buffers: A real-life demonstration," 2017 IEEE PES Innovative Smart Grid Technologies Conference Europe (ISGT-Europe), Turin, Italy, 2017, pp. 1-7, doi: 10.1109/ISGTEurope.2017.8260152.

[Son78] R. Sonderegger, Diagnostic tests determining the thermal response of a house, ASHRAE Meeting, Atlanta, 1978

[Spi21] G. van Spil, “Device optimization using machine learning with hybrid heat pumps”, Master’s thesis, University of Twente, 2021

[Toe16] H. A. Toersche. Effective and efficient coordination of flexibility in smart grids. PhD thesis, University of Twente, October 2016.

[Uri13] Urieli, D., & Stone, P. (2013, May). A learning agent for heat-pump thermostat control. In Proceedings of the 2013 international conference on Autonomous agents and multi-agent systems (pp. 1093-1100).

[USEF21] Universal Smart Energy Framework. Usef: The framework explained 2021. [Online] Available: https://www.usef.energy

[Vay14] M. G. Vayá, G. Andersson, and S. Boyd. Decentralized control of plug-in electric vehicles under driving uncertainty. In IEEE PES Innovative Smart Grid Technologies, Europe, pages 1–6, October 2014. doi: 10.1109/ISGTEurope.2014.7028989.

[vLe17] R. P. van Leeuwen, (2017). Towards 100% renewable energy supply for urban areas and the role of smart control. [PhD Thesis - Research UT, graduation UT, University of Twente]. University of Twente. https://doi.org/10.3990/1.9789036543460

[Zha19] Zhiang Zhang, Adrian Chong, Yuqi Pan, Chenlu Zhang, Khee Poh Lam, Whole building energy model for HVAC optimal control: A practical framework based on deep reinforcement learning, Energy and Buildings, Volume 199, 2019, Pages 472-490, ISSN 0378-7788, https://doi.org/10.1016/j.enbuild.2019.07.029.

9 Annex A

Average Temperature Model

Considering the uniform temperature of the heat transfer fluid (HTF) inside the tank, the average HTF temperature in the storage tank can be calculated from eq.(10). The first term on the RHS is for charging, second for discharging, the third for energy stored in PCM and the fourth is loss from the storage tank.

$$\frac{C_f dT_{avg}}{dt} = C_w \dot{m}_s (T_s - T_{avg}) - C_w \dot{m}_d (T_{avg} - T_r) - \dot{Q}_{PCM} - \dot{Q}_{loss} \quad \text{eq.(8)}$$

$$= C_w \dot{m}_s (T_s - T_{avg}) - C_w \dot{m}_d (T_{avg} - T_r) - U_{pcm} A_{pcm} (T_{avg} - T_{pcm}) - U_t A_{st} (T_{avg} - T_a)$$

A_{pcm} = effective heat transfer surface area (Conductive exchange) of the PCM [m^2]
A_{st}= surface area to the thermal storage tank responsible for thermal loss [m^2]
$C_f = m_w C_w$ = Thermal capacitance of HTF [J/K]
C_w = specific heat capacity of HTF (water) [J/kg.K]
$C_w \dot{m}_s (T_s - T_{avg})$= Net rate of energy transport for charging storage tank
$C_w \dot{m}_d (T_{avg} - T_r)$ = Net rage of energy flow during discharging of tank
$\dot{m}_d$ = flow rate of heat transfer fluid for discharging storage tank [kg/s]
$\dot{m}_s$ = flow rate of heat transfer fluid from source for charging storage tank [kg/s]
m_w = mass of water in the tank (kg)
$\dot{Q}_{PCM}$= net rate of energy transport for charging/discharging PCM storage
T_a= ambient temperature [K]
T_{avg} = average temperature of HTF in storage tank [K]
T_{pcm} = average temperature of PCM in storage tank [K]
T_r = Temperature of return HTF from heat sink [K]
U_{pcm}= overall heat transfer coefficient of PCM [$W/m^2.K$]
$U_{pcm} A_{pcm} (T_{avg} - T_{pcm})$ = Net rate of energy exchanged between the HTF and the PCM capsule
U_t= overall heat transfer coefficient of thermal storage tank[$W/m^2.K$]
$U_t A_{st} (T_{avg} - T_a)$= Net rate of energy exchanged between the HTF and the ambient.

Calculation of energy transfer between PCM and HTF:

Mapping the shape of PCM into a rectangular block: To simplify the problem of effective heat transfer area among various geometry of PCM, an assumption is made as follows. The mapping is visualized as in Figure A.1 for cylinder and spherical PCM as an example.

- The total number of PCM (N) in a tank is lumped into one single unit of rectangular block.
- The mapped rectangular PCM block has same volume equal to N number of PCM material in the tank.
- The upper surface area of mapped rectangular PCM block is only responsible for transfer of heat between HTF and PCM.
- The upper surface area of the mapped rectangular block is equal to the total conducting surface area of the of the actual PCM geometry, as in eq.(11) for cylindrical PCM unit.

- Then the thickness of mapped PCM rectangular block is calculated as eq.(12), considering cylindrical PCM unit.
- The total heat energy absorbed by the PCM is stored at the bottom of the rectangular block (i.e, the energy density is concentrated only at bottom layer, instead of distribution around the material.).
- Similar mapping technique can be applied for any geometrical shape of PCM

$$A_{pcm} = N \times A_1 \qquad \text{eq.(9)}$$

$$x_{pcm} = x_1 = \frac{N \times V_1}{N \times A_1} = \frac{V_1}{N_1} \qquad \text{eq.(10)}$$

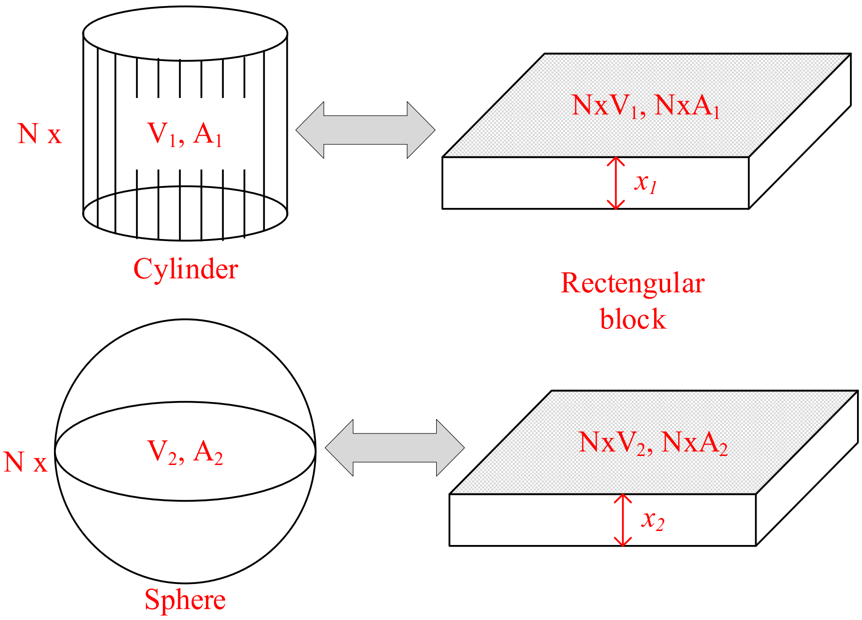

Figure A.1: Mapping of PCM geometry to rectangular block

Let us neglect the thermal internal of PCM capsule wall (i.e, all the energy that is transferred to the PCM wall from the HTF through convection ($\dot{Q}_{conv}$) is simultaneously transferred to the associated PCM control volume through conduction ($\dot{Q}_{cond}$). The conductive and convective Heat Transfer to PCM Capsule from HTF can be calculated from eq.(13) and eq.(14).

$$\dot{Q}_{conv} = h_{pcm}A_{pcm}\left(T_{avg} - T_w\right) \qquad \text{eq.(11)}$$

$$\dot{Q}_{cond} = \frac{k_{pcm}A_{pcm}\left(T_w - T_{pcm}\right)}{x_{pcm}} \qquad \text{eq.(12)}$$

A_{pcm} = Effective surface area of PCM for heat exchange
β= melting fraction as in **eq.(23)**
h_{pcm}= convective heat transfer coefficient of PCM wall [W/m^2.K]

k_{pcm}= PCM conductivity [W/mK] [has different value for solid (k_s), liquid (k_l) and phase change $(k_l - k_s)\beta$)]
$\dot{Q}_{cond}$= rate of heat transfer by conduction through PCM wall and PCM.
$\dot{Q}_{conv}$= rate of heat transfer is by convection from HTF to surface of PCM
T_l= temperature at start of liquidification of PCM[K]
T_s= Temperature at the start of solidification of PCM [K]
T_w= temperature of the PCM at the surface of contact between HTF and PCM [K]
x_{pcm}= thickness of the PCM [m]

PCM conductivity during a phase change is calculated as a linear interpolation between liquid and solid-state value eq.(15) according to the enthalpy of each PCM control volume [2]

$$k_{pcm} = (k_l - k_s)\beta + k_s \qquad \text{eq.(13)}$$

The phase change of PCM occurs within a particular range of temperature due to mixture of different materials in PCM. PCM starts to solidify at temperature T_s during release of thermal energy (or discharging). However, it starts to melt at temperature T_l during absorption of thermal energy (or charging).

Considering same amount of heat passes through each section during steady state as shown in eq.(16) and solving eq.(13) eq.(14), and eq.(16), we can derive eq.(17) and eq.(18),

$$\dot{Q}_{PCM} = \dot{Q}_{conv} = \dot{Q}_{cond} \qquad \text{eq.(14)}$$

$$\Rightarrow \quad \dot{Q}_{PCM} = U_{pcm}A_{pcm}\left(T_{avg} - T_{pcm}\right) \qquad \text{eq.(15)}$$

$$U_{pcm} = \frac{1}{\frac{1}{h_{pcm}} + \frac{x_{pcm}}{k_{pcm}}} \qquad \text{eq.(16)}$$

U_{pcm} = overall heat transfer coefficient of PCM[W/m^2.K]

Calculation of PCM temperature (T_{pcm}):

Energy is stored in PCM as a sensible heat and latent heat. During energy stored as sensible heat, the temperature of PCM rises, whereas during latent heat temperature remains constant. The rate of energy stored in PCM can be defined by eq.(19). The overall heat transfer coefficient during sensible heat area, as defined in eq.(18), changes based on conductivity defined in eq.(15).

$$\dot{Q}_{PCM} = \dot{Q}_{PCM,s} + \dot{Q}_{PCM,l} \qquad \text{eq.(17)}$$

$\dot{Q}_{PCM,s}$ = net rate of energy transport for charging/discharging PCM storage as sensible heat
$\dot{Q}_{PCM,l}$ = net rate of energy transport for charging/discharging PCM storage as latent heat

The temperature variation of PCM is defined with eq.(20), for sensible heat storage and during latent heat storage, temperature remains constant.

$$m_{pcm}C_{pcm}\frac{dT_{pcm}}{dt} = U_{pcm}A_{pcm}\left(T_{avg} - T_{pcm}\right) \times S \qquad \text{eq.(18)}$$

Where,

$$S = \begin{matrix} 0 & for, & T_{pcm} = T_l & and\ charging \\ 0 & for, & T_{pcm} = T_s & and\ discharging \\ 1 & elsewhere & & \end{matrix} \qquad \text{eq.(19)}$$

$$C_{pcm} = C_{pcm} = (C_{pl} - C_{ps})\beta + C_{ps} \qquad \text{eq.(20)}$$

C_{pcm}= specific heat of PCM [J/Kg.K] different for solid and liquid phase
C_{pl}= specific heat of PCM in liquid phase [J/Kg.K]
C_{ps}= specific heat of PCM in solid phase [J/Kg.K]
m_{pcm}= total mass of PCM in the storage tank [kg]
S= control function to determine temperature rise during sensible heat storage.
T_{pcm} = average temperature of PCM in storage tank [K]
U_{pcm} = overall heat transfer coefficient of PCM[W/m^2.K]

The specific heat capacity of PCM is described in eq.(22) for different phases. During phase change process, C_{pcm} is very high. This high value of C_{pcm} causes slow rise in temperature. However, it is assumed that temperature of PCM remains constant during the phase change process, and thus C_{pcm} is not considered during the period of phase change. However, if the flow of thermal energy in PCM is reversed during the middle of phase change process, the new value of C_{pcm} is calculated as linear interpolation between liquid and solid-state as in in eq.(22).

To determine the amount of latent heat storage in the tank, melting fraction is considered. Melting fraction is defined as ratio of total heat energy stored as latent heat to the total latent heat capacity of the material eq.(23).

$$\beta = \begin{matrix} 0 & for, & T_{pcm} < T_s \\ \dfrac{\int_{t1}^{t2} U_{pcm}A_{pcm}\left(T_{avg} - T_{pcm}\right)dt}{L_{pcm}m_{pcm}} & for, & T_{pcm} = T_l\ and\ charging \\ \dfrac{\int_{t1}^{t2} U_{pcm}A_{pcm}\left(T_{avg} - T_{pcm}\right)dt}{L_{pcm}m_{pcm}} & for, & T_{pcm} = T_s\ and\ discharging \\ 1 & for, & T_{pcm} > T_l \end{matrix} \qquad \text{eq.(21)}$$

β= melting fraction
L_{pcm}= Latent heat of fusion of PCM [J/kg]
m_{pcm}= total mass of PCM [Kg]

Discretized PCM Storage Tank

The storage tank is divided into n number of horizontal layers with the equal mass of HTF and PCM material in it. The energy flow from each layer and between the stratified layer, as well as losses to the environment from the tank is well presented in Figure A.2 (a,b). The exchange of thermal energy from PCM is only with the HTF in each stratified layer. The modelling of discretized layers for the HTF is based on [Sin20].

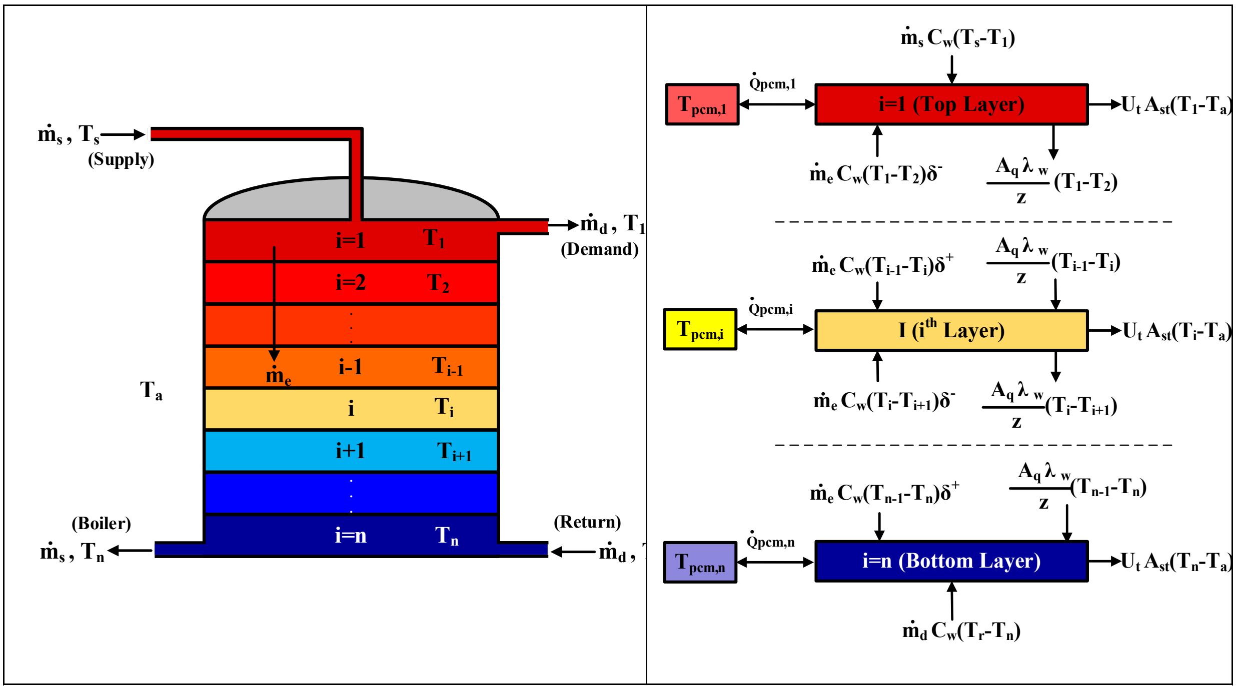

(a)	(b)

Figure A.2: (a)Stratified PCM based thermal storage tank; (b) Stratified PCM based thermal storage tank with n layers and flow variables [Sin20]

T_i = temperature of HTF in i^{th}layer , $(i = 1,2,3 \ldots..n)$[K]
$T_{pcm,i}$ = temperature of PCM in i^{th}layer , $(i = 1,2,3 \ldots..n)$[K]
$\dot{m}_e = \dot{m}_s - \dot{m}_d$= mass flow rate of water between the stratified layers [kg/s]
A_q= horizontal area of each stratified layer [m^2]
C_w = specific heat capacity of HTF (water) [J/kg.K]
λ_w = effective vertical heat conductivity of water (1–1.5)[W/mK] [Eic06]
δ^+ , δ^- = logic parameter (0,1) to define the direction of flow of water inside the storage tank from top to bottom and bottom to top respectively
U_t= overall heat transfer coefficient of thermal storage tank[W/m^2.K]

The heat exchange between PCM and HTF in each layer is added based on eq.(24) derived from eq.(20), where the subscript (i) denotes i^{th} layer of discretization in the storage tank. The complete energy flow in the stratified PCM storage tank is shown in Figure A.2 (b).

$$m_{pcm,i}C_{pcm,i}\frac{dT_{pcm,i}}{dt} = U_{pcm,i}A_{pcm,i}\left(T_i - T_{pcm,i}\right) \times S_i \qquad \text{eq.(22)}$$

$$S_i = \begin{array}{lll} 0 & for, \quad T_{pcm,i} = T_l & and\ during\ charging \\ 0 & for, \quad T_{pcm,i} = T_s & and\ during\ discharging \\ 1 & elsewhere & \end{array} \qquad \text{eq.(23)}$$

$$C_{pcm,i} = \begin{array}{lll} C_{ps} & for, & T_{pcm,i} < T_s \\ - & for, & T_s \le T_{pcm,i} \le T_l \\ C_{pl} & for, & T_{pcm,i} > T_l \end{array} \qquad \text{eq.(24)}$$

$$U_{pcm,i} = \frac{1}{\frac{1}{h_{pcm}} + \frac{x_{pcm}}{k_{pcm,i}}} \quad \text{eq.(25)}$$

$$k_{pcm,i} = (k_l - k_s)\beta_i + k_s \quad \text{eq.(26)}$$

$$\beta_i = \begin{cases} 0 & for, \quad T_{pcm,i} < T_s \\ \dfrac{\int_{t1}^{t2} U_{pcm,i}A_{pcm,i}\left(T_i - T_{pcm,i}\right)dt}{L_{pcm}m_{pcm,i}} & for, \quad T_{pcm,i} = T_l \; and\; charging \\ \dfrac{\int_{t1}^{t2} U_{pcm,i}A_{pcm,i}\left(T_i - T_{pcm,i}\right)dt}{L_{pcm}m_{pcm,i}} & for, \quad T_{pcm,i} = T_s \; and\; discharging \\ 1 & for, \quad T_{pcm,i} > T_l \end{cases} \quad \text{eq.(27)}$$

$A_{pcm,i} = \frac{A_{pcm}}{n}$, where n is the number of stratified layers

$m_{pcm,i} = \frac{m_{pcm}}{n}$, where n is the number of stratified layers

The temperature of the HTF in each discrete layer is calculated using eq.(30) [Sin19]

$$\begin{aligned} m_i C_w \frac{dT_i}{dt} = \; & \dot{m}_s C_w (T_s - T_i)\delta_{(i=1)} + \dot{m}_d C_w (T_r - n)\delta_{(i=n)} + \dot{m}_e C_w (T_{i-1} - T_i)\delta^+ \delta_{(i\neq 1)} \\ & + \dot{m}_e C_w (T_i - T_{i+1})\delta^- \delta_{(i\neq n)} - U_t A_{sn}(T_i - T_a) \\ & + \frac{A_q \lambda_w}{z}\left[(T_{i-1} - T_i)\delta_{(i\neq 1)} - (T_i - T_{i+1})\delta_{(i\neq n)}\right] \\ & - U_{pcm,i}A_{pcm,i}\left(T_i - T_{pcm,i}\right) \end{aligned} \quad \text{eq.(28)}$$

A_{sn}= surface area of the side wall of each discrete layer [m^2]
A_q= Horizontal surface area of the storage tank [m^2]
$\dot{m}_e = (\dot{m}_s - \dot{m}_d)$: effective flow rate of HTF inside the tank [kg/s]
m_i= mass of HTF in each discrete layer [kg]
T_i= Temperature of HTF in each discrete layer [kg]
z= Thickness of each discrete layer [m]
$\delta^+ = 1 \; if \; \dot{m}_e > 0, else \; 0$
$\delta^- = 1 \; if \; \dot{m}_e < 0, else \; 0$
$\delta_{(X)} = 1$ for all the conditions defined by term X is true, else 0.
λ_w= effective vertical heat conductivity of water (1–1.5 W/mK] [Eic06]

Calculation of PCM tank parameters for simulation.

The experimental data is taken from [Sin17].

- Volume of storage tank: $V_{sto} = 785 \; lit$
- Ratio of height to diameter of the tank: $R_a = \frac{1.45}{0.734} = 2$

- Capsules formed a packed bed with a porosity: $\varepsilon = 0.57 = \frac{void\ volume}{Total\ volume} = \frac{volume\ of\ water\ (HTF)}{Total\ volume}$
  $\therefore$ volume of water in the storage tank: $V_{htf} = 0.57 \times 785 = 447.5\ lit$
- Total number of pcm capsule: $N = 950$
- Volume of each capsule: $V_{ind} = 290$ ml
- Total volume of pcm: $V_{pcm} = 950 \times 0.29 = 275.5$ liter=0.2755 m^3
- Density of PCM [kg/m3]: ρ_{pcm}= 1280
- Total mass of pcm: $m_{pcm} = \rho_{pcm} \times V_{pcm} = 1280 \times 0.2755 = 353\ kg$
- Volume of plastic wall = 785-447.5-275.5 = 62 lit
- Area of PCM for heat transfer [m^2]: $A_{pcm} = N \times 4\pi R^2 = 950 \times 4\pi 0.08^2 = 76.403\ m^2$ (individual capsule has surface area equivalent sphere of radius 80mm) [Gra21]
- thickness of the PCM [m]: $x_{pcm} = \frac{V_{pcm}}{A_{pcm}} = \frac{0.2755}{76.403} = 0.00361$ m=3.61mm
- Solidification temperature: $T_s = 57.5$ °C
- Melting temperature: $T_l = 56$ °C
- Specific Heat capacity of PCM capsule [J/(kgK)]: $C_{pcm} = \begin{matrix} C_{ps} & = & 3000 \\ - & - & - \\ C_{pl} & = & 3000 \end{matrix}$
- Heat conductivity pf PCM [W/(mK)]: $k_{pcm} = \begin{matrix} k_s = & 1 \\ k_l = & 0.6 \end{matrix}$
- Heat storage capacity (50-65°C)= HL_{pcm} =240kJ/kg
- Latent heat of fusion [kJ/kg]: L_{pcm} = HL_{pcm}-$mC_{pcm}\Delta T$ = 240000-1x3000x15 = 195000 J/kg
- Flow rate for charging [kg/s]: $\dot{m}_s = 360\ \frac{kg}{h} = 0.1 \frac{kg}{s}$
- convective heat transfer coefficient of PCM wall (h_{pcm}) [W/m^2.K]= 100

<u>For Stratified layer tank</u>

- Number of stratified layer in the tank: $n = 5$
- Mass of HTF and PCM are equally divided into each layer of storage tank
- Effective vertical heat conductivity of water: $\lambda_w = 0.644$ [W/mK] [Eic06]